AFFDL-TR-70-129

A DISCRETE, STOCHASTIC, OPTIMAL CONTROL MODEL OF THE HUMAN OPERATOR IN A CLOSED-LOOP TRACKING TASK

HARVEY M. PASKIN, MAJOR, USAF

FOREWORD

This report was originally prepared by Major Harvey M. Paskin as a thesis in partial fulfillment of the requirements for a Doctor of Philosophy in Aerospace Engineering from the Air Force Institute of Technology, Wright-Patterson Air Force Base, Ohio. Major Paskin's thesis advisor was Lt Col Russell A. Hannen and the remainder of his thesis committee were Dr. Mathew Kabrisky and Capt Carroll Day.

The research was accomplished while the author was assigned to the Control Criteria Branch, Flight Control Division, Air Force Flight Dynamics Laboratory, Wright-Patterson Air Force Base, Ohio. The research was initiated under Project 8219, "Stability and Control Investigations," and Task 821910, "Pilot-Vehicle System Integration and Evaluation."

The research was conducted during the period October 1968 through March 1970. This report was submitted by the author 9 September 1970.

The author gratefully acknowledges the efforts of those people who contributed to the successful conclusion of this investigation. These include Lt Col R. A. Hannen, Mr. P. Pietrzak, and Capt E. J. Rathswohl. Mr. R. O. Anderson deserves special credit for his encouragement, suggestions, and critical evaluation of this work.

This technical report has been reviewed and is approved.

C. B. WESTBROOK
Chief, Control Criteria Branch
Flight Control Division
Air Force Flight Dynamics Laboratory

ABSTRACT

A discrete stochastic optimal control model of the human operator is developed for the single-loop compensatory and pursuit tracking situations. The model generates signals corresponding to those in the physical closed-loop tracking situation. There is one primary model parameter which is varied to match model-experimental normalized tracking error at a bandwidth of $\omega_B = 1.0$ rad/sec for an input which approximates a rectangular spectra. With this parameter fixed, the model then predicts normalized tracking error and power spectra of control loop signals across a range of input bandwidths of 0.5 to 2.0 rad/sec. The model is applied to simple first- and second-order controlled elements in both compensatory and pursuit display situations.

A comparison between model and experimental normalized tracking error and power spectral density data confirms the model capability of matching and predicting operator performance with sufficient correlation to warrant its application as a tool in manual vehicular control system design. Furthermore, the success of the model substantially confirms the hypothesis that the human operator behaves in some optimal manner when performing in a closed-loop tracking task.

TABLE OF CONTENTS

SECTION		PAGE
I	INTRODUCTION	1
	1. Background	1
	2. Types of Manual Control Systems	2
	3. Existing Models	2
	4. Purpose of Investigation	5
II	THE DISCRETE STOCHASTIC OPTIMAL CONTROL MODEL	7
	1. The Concept of Optimal Control Models	7
	2. Description	8
	a. Input Forcing Function	8
	b. Controlled Element (Plant)	9
	c. Manipulator	10
	3. Plant and Observation Equations	10
	4. Remnant	16
	5. Optimal Control Model	18
III	DIGITAL SIMULATION OF THE OPTIMAL CONTROL MODEL	26
	1. Description of System-Model Parameters	26
	2. Selection of Model Parameters	27
IV	EXPERIMENTS	29
	1. Experimental Objectives	29
	2. Equipment	29
	3. Training	30
	4. Experimental Runs	30
V	EXPERIMENTAL RESULTS AND DISCUSSION	33
	1. Model Matching to the Experimental Data	33
	a. Observation Noise	34
	b. Motor Noise	39
	c. Control Weighting	46
	2. Experimental Results	46
	a. Normalized Tracking Error	46
	b. Power Spectral Densities	55

TABLE OF CONTENTS (CONTD)

SECTION		PAGE
	c. Pursuit Display	56
	d. Compensatory Display	76
	3. Pursuit-Compensatory Comparisons	84
VI	CONCLUSIONS AND RECOMMENDATIONS	85
	1. Conclusions	85
	2. Recommendations	86
APPENDIX I	Computation of Φ (T), $\underline{A}$, and $\underline{B}$	87
APPENDIX II	Digital Simulation Program for Optimal Control Model	93
APPENDIX III	The Power Spectral Density Data Reduction	104
BIBLIOGRAPHY		107

ILLUSTRATIONS

FIGURE		PAGE
1.	Functional Block Diagram of Single-Loop Tracking Situations	3
2.	Compensatory and Pursuit Displays	4
3.	Schematic Representation of the Discrete Optimal Control Model	20
4.	Experimental Equipment Layout	29
5.	Operator and Scope Arrangement	31
6.	Typical Learning Curve	32
7.	Observation Noise Effect $Y_C = K/s^2$	37
8.	Observation Noise Effect $Y_C = K/s-1$	38
9.	Motor Noise Effect $Y_C = K/s^2$	41
10.	Motor Noise Effect $Y_C = K/s+1$	42
11.	Motor Noise Effect $Y_C = K/s-1$	43
12.	Motor Noise Effect $Y_C = K/s$	44
13.	Power Spectral Density Asymptotes	45
14.	Input Power Spectral Density	47
15.	Output Power Spectral Density	47
16.	Error Power Spectral Density	48
17.	Control Power Spectral Density	48
18.	NTE vs ω_B $Y_C = K/s-1$	52
19.	NTE vs ω_B $Y_C = K/s+1$	52
20.	NTE vs ω_B $Y_C = K/s$	53
21.	NTE vs ω_B $Y_C = K/s^2$	54
22-28.	Power Spectral Densities $Y_C = K/s$ Pursuit	57-63
29-32.	Power Spectral Densities $Y_C = K/s+1$ Pursuit	64-67
33-36.	Power Spectral Densities $Y_C = K/s-1$ Pursuit	68-71
37-40.	Power Spectral Densities $Y_C = K/s^2$ Pursuit	72-75

ILLUSTRATIONS (CONTD)

FIGURE		PAGE
41.	Theoretical Control Power Spectra	77
42.	Power Spectral Densities Y_C = K/s Compensatory	78
43-45.	Power Spectral Densities Y_C = K/s+1 Compensatory	79-81
46.	Power Spectral Densities Y_C = K/s-1 Compensatory	82
47.	Power Spectral Densities Y_C = K/s^2 Compensatory	83
48.	Comparison of Forcing Function Power Spectra	105

TABLES

TABLE		PAGE
I	Effects of Observation Noise	36
II	Effect of Motor Noise	40
III	Experimental NTE Data	49
IV	Experimental vs Model NTE Data	50
V	Power Spectral Density	106

SYMBOLS

a	plant time constant
b	plant gain
$e = x - i$	system error
$i = x_2$	forcing function input
k	noise filter gain
s	Laplace transform variable
t	time
u	control input
$x = x_3$	system output
x_1	intermediate noise
x_4	system velocity
A $\underline{A}$	matrix
B $\underline{B}$	vector
G(n)	feedback gain matrix
J	cost function
K(n)	estimation gain matrix
N	number of samples
Q	convariance matrix of plant noise vector
R	convariance matrix of observation noise vector
$R(\tau)$	autocorrelation function
S	control weighting
T	sampling period
V	state weighting matrix
$\underline{V}$	observation noise vector
W $\underline{W}$	plant noise vector
X	state vector

SYMBOLS (CONTD)

$\bar{X}$	conditional expectation of X
Y	observation vector
ω_B	forcing function bandwidth or noise filter time constant
ω	frequency (rad/sec)
σ_I^2	variance of forcing function input
σ_E^2	variance of system error
σ_u^2	variance of control input
σ_q^2	motor noise variance
$\sigma_{v_i}^2$	observation noise variance i = 1, 2, 3, 4
Φ	state transition matrix
$\phi(\omega)$	power spectral density (PSD)
$E\left[z\middle\|y\right]$	expected value of z conditioned on knowing y
$E\left[z\right]$	expected value of z
z^n	$\left\{z(n),\ z(n-1),\ \ldots\ ,\ z(0)\right\}$
NTE	normalized tracking error = σ_E^2 / σ_I^2
$Y_C(s)$	controlled element transfer function
db	decibels - $10 \log_{10}(\ )$
nT	time increments n = 0, 1, 2, ... , N

SECTION I

INTRODUCTION

1. BACKGROUND

In the early 1950s, designers of manual vehicular control systems (pilot-aircraft, operator-automobile, gunner-gun platform, etc.) began to determine the feasibility of describing the control characteristics of the human operator in such a manner that the results could be incorporated with the concepts of servomechanism design theory. With such a knowledge of human-operator characteristics, the designers could design the remaining system components about these characteristics to approach or equal some predetermined performance level.

The human operator's control characteristics should be studied only under carefully defined control situations if universal results are to be obtained. The control situations which have received the most attention are those in which the human operator is involved in a closed-loop control task such as stabilizing a vehicle subject to random disturbances or tracking a random appearing input signal by controlling the vehicle.

As recognized by McRuer (Reference 22:3)[1], a unique control characteristic of the operator cannot be expected, since a description of the operator will depend on at least the following factors:

a. The dynamic characteristics of the vehicle being controlled.

b. The particular disturbance or input signal; such as its predictability and frequency content.

c. The actual individual reaction times, thresholds, etc., of the operator during a particular control situation.

d. The motivation, attention, training, and psychological condition of the operator at the time of the experiment.

The human-operator modeling concept has been to assume that the operator is well motivated, attentive, well trained, and that psychological conditions do not affect the operator characteristics. The models have been developed with parameters which can be varied to account for factors a, b, and c above. After a description of the types of manual control systems considered for modeling purposes, reference will be made to some of the more successful models.

[1] Indicates the item and page numbers in the Bibliography.

2. TYPES OF MANUAL CONTROL SYSTEMS

The control situations that have received the most attention are the single-loop compensatory and pursuit tracking tasks where a random signal appears either as a vehicle disturbance to be stabilized by the operator or as an input signal to be tracked by the operator-vehicle combination. The single-loop compensatory and pursuit tracking situations are described by functional block diagrams in Figure 1. Since only the tracking (not stabilizing) situation is considered in this investigation, the figure represents the tracking task. Here, a stationary random forcing function i (t) is applied to the system input. The operator has control of a manipulator whose output u (t) acts on the vehicle (controlled element) to produce the system output x (t).

The primary difference between compensatory and pursuit tracking is the nature of the display presented to the operator (Figure 2). In the compensatory display, the operator is presented with an indicator showing only the difference or error e (t) between the forcing function input i (t) and the system output x (t). The operator's task is to minimize the error by trying to keep the error indicator superimposed on the stationary zero-error reference. In the pursuit display, the operator sees both the forcing function input and the system output. Again the operator's task is to minimize the error existing between the location of the input bar (target) and the output bar (follower) by pursuing the target with the follower.

3. EXISTING MODELS

Reference 9 presents an inclusive bibliography pertaining to modeling the human operator as an element in a control system tracking loop. Works of special note are denoted by two asterisks, and of the 65 modeling papers only two are so denoted. The first is the quasi-linear describing function model (Reference 19) and the second is the sampled-data model originated by Bekey (Reference 3). Modeling work has, for the most part, persisted in the quasi-linear describing function approach with some exceptions (References 8 and 12). One notable exception has been an optimal control approach to modeling developed by Kleinman et al (Reference 16). The assumptions and details used in deriving each of the referenced models will not be discussed here since they are readily available in the literature. A few comments will be made, however, on the general concepts of operator modeling which have been basic to all the modeling work undertaken and on some of the problems encountered.

The general approach to modeling the human operator has been to match the experimentally obtained output response of the operator with a response generated by a model which has been subjected to a similar input. The forcing function most commonly used is

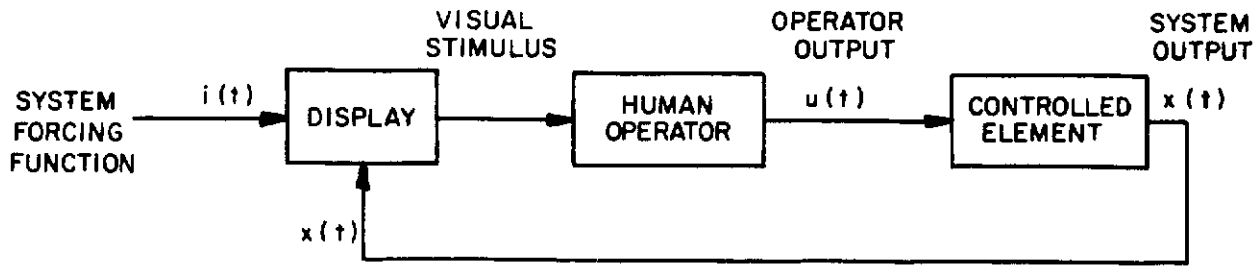

a. Functional Block Diagram of a Pursuit Control System

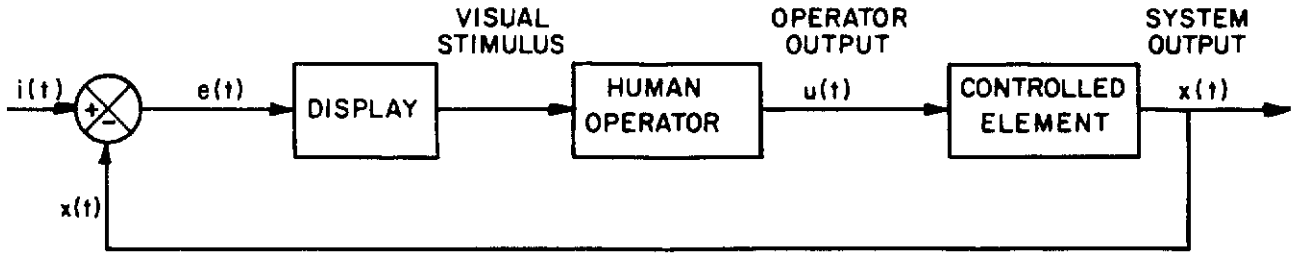

b. Functional Block Diagram of a Compensatory Control System

Figure 1. Functional Block Diagram of Single-Loop Tracking Situations

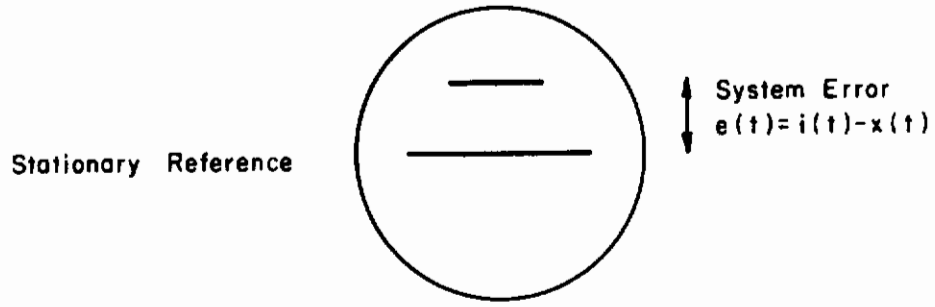

a. Compensatory Display

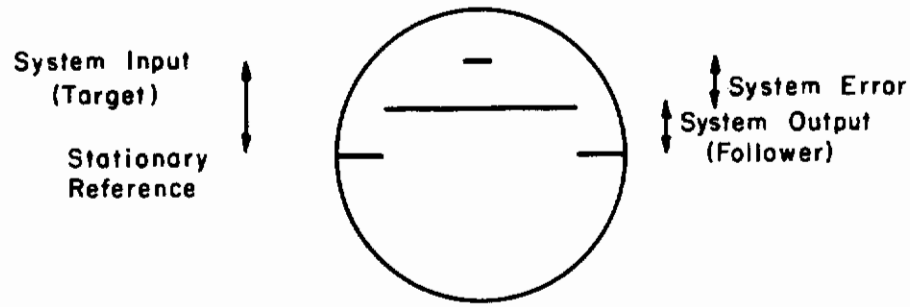

b. Pursuit Display

Figure 2. Compensatory and Pursuit Displays

a stationary random appearing time signal so the operator cannot predict future input data and must operate in a continuous feedback tracking mode. The models are usually defined mathematically by some linear operation on the input stimulus, and the output response match is normally made in the frequency domain. The portion of the operator output not linearly correlated with the input is called "remnant." Most constituents of the model are chosen to represent some observed or assumed physical or physiological operator characteristic such as time delay, neuromuscular behavior, and indifference thresholds. These model parameters are then varied to obtain a "best fit" to the experimental tracking data. The number of model parameters normally determines how well the model output can be made to match the actual operator data, the better fits requiring more parameters.

Because of this curve fitting approach, many models have no practical use since the model is essentially a match for a particular control situation and there is no way of predicting whether the model will apply if the controlled element, type of display, or frequency range of the input is changed. A good model should respond to these changing situations. The quasi-linear describing function model (Reference 19) and the optimal control model (Reference 16) have been the most successful models developed using this criterion. Both models have been applied to various controlled elements over a wide range of input frequencies, but both have been limited to compensatory tracking tasks.

Many investigators have found conflicting data (References 1, 7 and 29) concerning what information the operator actually uses when controlling a pursuit display. Hence there is no single well-defined operator input-output relation, and the concept of a single transfer function for the operator is no longer considered possible. There have been a few attempts to use the describing functions in pursuit tracking (References 1 and 29), but none have developed a successful model. Kreifeldt (Reference 17) proposes a sample-data pursuit tracking model, but the model is essentially a four parameter curve fit to data obtained for a pure gain controlled element.

In Reference 21 the authors devote a chapter to listing deficiencies in the existing quasi-linear models. One deficiency which has long been cited is the requirement for engineering "artistry" if the model is to be applied effectively (i. e. verbal adjustment rules). The authors suggest the inverse optimal control and direct optimal control approaches as possible methods of alleviating this problem. As a result of their investigations in these areas, the authors found that the performance criterion which yielded an optimal controller which matched human operator data was different for each type of controlled element. Furthermore, they found that if it is assumed that the operator-control system satisfies the criterion

$$J = \min E \left[e^2 + Su^2 \right]$$

where S is a constant, e is the difference between the desired response and the actual system response, and u is the operator output, then there is a consistent trend towards small negative values of S when actual test data are analyzed. Negative values of S in performance criteria are a little disquieting when applying optimal control theory because stability via Lyapunov's Second Method is no longer assured.

4. PURPOSE OF INVESTIGATION

The object of this investigation is to develop a model of the operator-vehicle control loop which will predict operator performance, reproduce the essential control characteristics of

the operator, be applicable over a wide range of forcing function bandwidths and controlled elements, and apply to both pursuit and compensatory tracking tasks. The approach taken here is novel in the sense that there is no attempt made to derive an input-output operator transfer function or impulse response. Rather, the tracking loop dynamics are written in state equation form, and an optimal controller is synthesized to minimize a specified cost function. The synthesis is accomplished using linear discrete, stochastic, optimal control theory. The resultant optimal control model is construed to represent the total human operator-display-controlled element tracking system.

SECTION II

THE DISCRETE STOCHASTIC OPTIMAL CONTROL MODEL

1. THE CONCEPT OF OPTIMAL CONTROL MODELS

The concept that the human operator acts in some optimal manner has been considered by many authors. McRuer et al (Reference 19) recognized the notion of optimality and one of the parameter adjustment rules for the describing function model states that "... parameters are adjusted so that ... closed-loop low frequency performance in operating on the forcing function is optimum in some sense analogous to that of minimum mean-squared tracking error." With the advent of modern optimal control theory, there has been some effort to relate the performance of the human operator to that of an optimal controller performing the same task (References 6, 21 and 30). The most successful of these modeling efforts has been the work of Kleinman et al (Reference 16).

Kleinman et al have developed a continuous, stochastic, optimal control model of the human operator in a compensatory tracking task. The model includes the psychophysical limitations inherent in the human operator such as time delay, neuromuscular dynamics, and remnant. The model attempts to relate its constituent parts to the physical processes attributed to the human operator while performing the closed-loop tracking task. Consequently, there are many adjustable parameters in the model. In addition, the concept of attempting to relate model parameters to physiological activities requires that the mathematical construct of the physical plant dynamics be accomplished very selectively. This is so because of the underlying hypothesis of the model is that the visual stimuli presented to the operator (the observation vector) can be derived by a linear transformation of the state vector in the model control equation. Then the operator "acts like" a Kalman filter and estimates all the components of the state vector. Many of these state vector components may be quantities which the human operator would never consider during the control task, and so the validity of a model-physiological parameter match may be questionable.

The works of Kleinman et al, Roig, and others have reinforced the hypothesis that the well trained human operator behaves in some optimal manner and have motivated the development of the discrete, stochastic, optimal control model to be described. As mentioned in Section I, the model to be developed will be construed to represent the total closed-loop tracking situation, human operator included. It is to be considered as a mathematical construct which will simulate the performance of the required tracking task in a "similar manner" and with "comparable results." In a "similar manner" means that the power

spectra of the signals in the model conform to the power spectra of the corresponding signals in the physical control situation in terms of bandwidth and cutoff characteristics. With "comparable results" means that the normalized tracking error (σ^2_E/σ^2_I) of the model will agree with the tracking error obtained experimentally within the 1 sigma limits of human operator tracking performance.

2. DESCRIPTION

The physical situation to be modeled is the closed-loop tracking situation described by the functional block diagrams in Figure 1. No distinction will be made between pursuit and compensatory tracking tasks. This approach can be taken since there is no attempt made to relate the physical situation to the model structure other than by defining the element to be controlled, the signal to be tracked, and the quantity to be minimized.

The operator is presented a display as in Figure 2 and is given a manipulator with which he can control the output of a controlled element (plant) described by a linear, constant coefficient, differential equation of the form

$$\dot{X} = AX + Bu \tag{1}$$

Equation 1 is a vector-differential equation describing the response of the controlled element to a scalar input command u(t) generated by the human operator through the manipulator. The operator is generally instructed to control the plant output so as to minimize the mean-squared error between the displayed input signal and the displayed output signal (pursuit case) or to minimize the mean-squared value of the displayed error (compensatory case).

The hypothesis of this dissertation is that a discrete, stochastic, optimal control system can be synthesized which will generate a control signal u that will stimulate the plant to respond in such a manner that the normalized tracking error agrees with human operator performance. In addition, the power spectral densities of the signals in the model will conform to the corresponding signals in the physical tracking loop. The first step in developing the model is to establish the differential equations relevant to the physical tracking situation.

a. Input Forcing Function

The forcing function chosen for this tracking task is a wide-sense stationary stochastic process with a Gaussian amplitude distribution and zero mean whose autocorrelation function is

$$R_{ii}(\tau) = \frac{k^4 \exp(-\omega_B|\tau|)}{4\omega_B^2}\left[|\tau| + 1/\omega_B\right] \tag{2}$$

and whose power spectral density is

$$\phi_{ii}(\omega) = \frac{K^4}{\omega^4 + 2\omega_B^2\,\omega^2 + \omega_B^4} \tag{3}$$

This process was chosen because it is representative of the kinds of inputs which an operator might be required to track in an air-to-air gunnery of aircraft pursuit situation and also because it has application to closed-loop compensatory tracking situations where the operator is required to stabilize the vehicle when subjected to the input as a plant disturbance. The model is not limited, however, to this forcing function, and only the differential equations which generate the desired input need be changed.

Sample functions for the process described above can be obtained by operating linearly on a Gaussian amplitude white-noise process with two first-order filters, each of which is governed by the following differential equation:

$$\dot{z} + \omega_B z = kw \tag{4}$$

where k = constant

ω_B = bandwidth frequency (rad/sec)

Thus, if w(t) denotes a sample function from a Gaussian amplitude white-noise process, a sample function of the desired input $x_2(t)$ is generated as follows:

$$\dot{x}_1(t) = -\omega_B x_1(t) + kw(t) \tag{5}$$

$$\dot{x}_2(t) = -\omega_B x_2(t) + kx_1(t) \tag{6}$$

where $x_1(t)$ is an "intermediate noise."

b. Controlled Element (Plant)

In an actual tracking situation, the operator would normally have control over a complex vehicle whose input-output characteristics are described by a set of differential equations. These equations might be linear, nonlinear, or even time-varying. As a first step in system analysis, most designers will linearize the equations about some operating point and will try to eliminate time varying effects. When transformed into the frequency domain (Laplace transform), the resulting set of differential equations will have dominant poles and zeros which determine the gross behavior of the vehicle, gross behavior being defined by descriptions such as first-order, second-order, stable, and conditionally stable. In accord with this design practice, the controlled elements considered in this dissertation are limited to simple plants whose linear input-output differential equations represent first- and second-order conditions.

These conditions can be synthesized by two differential equations. They are

$$\dot{x} = ax + bu \tag{7}$$

and

$$\ddot{x} = bu \tag{8}$$

where

a = plant time constant

b = plant gain

u = plant input

x = plant output

The second-order condition is described in Equation 8 and first-order stable, unstable, and neutrally stable conditions are described in Equation 7 with the plant time constant 'a' being negative, positive, and zero, respectively. The Laplace transforms of the impulse responses for the linear systems above are, respectively

$$Y_C = \frac{b}{s-a} \tag{9}$$

$$Y_C = \frac{b}{s^2} \tag{10}$$

c. Manipulator

The manipulator, or control stick, used in the experiments conducted in this investigation was an AC powered stiff-stick transducer. This type of manipulator was chosen because it has an essentially linear voltage output versus applied force, and, hence, unwanted nonlinear control stick characteristics are eliminated. Thus the manipulator transfer characteristic is merely a gain, and no manipulator dynamics are included in the model. If a manipulator whose transfer characteristics can be described by a linear differential equation is used, this equation can be combined with the plant equations and the result considered as an augmented plant.

3. PLANT AND OBSERVATION EQUATIONS

Now that the differential equations which describe the operation of the control loop without the operator have been established, they will be combined to form one linear vector-differential equation of the form

$$\dot{X} = AX + Bu + W \tag{11}$$

Let $X = (x_1, x_2, \ldots, x_n)$ denote a "state" vector (column) of dimension n with components $x_1, x_2, \ldots, x_n$. Let A denote an nxn matrix and B a column vector of dimension n. Let u

denote the scalar control applied to the plant input. Let $W = (w_1, w_2, \ldots, w_n)$ denote a "plant noise" vector (column) of dimension n with components $w_1, w_2, \ldots, w_n$. Select a particular plant equation, Equation 7 or 8, and combine the plant equation with Equations 5 and 6 as follows:

$$\dot{x}_1(t) = -\omega_B x_1(t) + k w_1(t) \tag{12}$$

$$\dot{x}_2(t) = -\omega_B x_2(t) + k x_1(t) \tag{13}$$

$$\dot{x}_3(t) = a x_3(t) + b u(t) \qquad \text{Using Equation 7} \tag{14}$$

$$\left.\begin{aligned} \dot{x}_3(t) &= x_4(t) \\ \dot{x}_4(t) &= b u(t) \end{aligned}\right\} \qquad \text{Using Equation 8} \tag{15, 16}$$

The decomposition of Equation 8 into two first-order linear differential equations is known as reducing a linear differential equation to "normal form" (Reference 31:29), and the same approach can be used to decompose plant equations of higher order.

To distinguish between the choice of a first-order plant and a second-order plant, the choices will be categorized as Cases I and II, respectively. Thus the combined vector-differential equation is

$$\dot{X} = AX + Bu + W \tag{17}$$

where

Case I

x_1 = intermediate noise

x_2 = desired noise input

x_3 = system output

$$A = \begin{bmatrix} -\omega_B & 0 & 0 \\ k & -\omega_B & 0 \\ 0 & 0 & a \end{bmatrix} \tag{18}$$

$$B = \begin{bmatrix} 0 \\ 0 \\ b \end{bmatrix} \tag{19}$$

$$W = \begin{bmatrix} kw_1 \\ 0 \\ 0 \end{bmatrix} \tag{20}$$

Case II: x_1 = intermediate noise

x_2 = desired noise input

x_3 = system output

x_4 = system velocity

$$A = \begin{bmatrix} -\omega_B & 0 & 0 & 0 \\ k & -\omega_B & 0 & 0 \\ 0 & 0 & 0 & 1 \\ 0 & 0 & 0 & 0 \end{bmatrix} \tag{21}$$

$$B = \begin{bmatrix} 0 \\ 0 \\ 0 \\ b \end{bmatrix} \tag{22}$$

$$W = \begin{bmatrix} kw_1 \\ 0 \\ 0 \\ 0 \end{bmatrix} \tag{23}$$

This completes the first step in developing the model. Note that no special effort is made to formulate the state equations so the states represent some physical quantity observable or derivable by the human operator. The states are chosen as a logical consequence of writing the differential equations in "normal form."

The next step in the modeling procedure is to add the observation equation and then to put these equations in discrete form.

Define the observation equation as

$$Y(t) = X(t) + \underline{V}(t) \tag{24}$$

where $Y = (y_1, y_2, \ldots, y_3)$ is an "observation" vector (column) of dimension n with components $y_1, y_2, \ldots, y_n$ and $\underline{V} = (\underline{v}_1, \underline{v}_2, \ldots, \underline{v}_n)$ is an "observation noise" vector (column) of dimension n with components$(\underline{v}_1, \underline{v}_2, \ldots, \underline{v}_n)$.

If the A matrix and B vector in Equation 17 are constant, then Equations 17 and 24 represent a time invariant linear system, and the complete solution for X(t) and Y(t) for such a system is given by (Reference 10:376)

$$X(t) = \Phi(t-\tau)X(\tau) + \int_{\tau}^{t} \Phi(t-\xi)\left[Bu(\xi) + W(\xi)\right] d\xi \tag{25}$$

$$Y(t) = X(t) + \underline{V}(t) \tag{26}$$

where

t = observation time

τ = time $u(t)$ was applied

$\Phi(t) = \exp(At)$ = state transition matrix

The state transition matrix can be calculated in several different ways, some of which are the Cayley-Hamilton technique, Sylvester's Theorem, and the infinite series method (Reference 10).

For computational purposes, it is desirable to develop a model which can be simulated on a digital computer. Consequently, Equations 25 and 26 will be converted to a discrete form to which discrete, linear stochastic, optimal control theory can be applied and which can be simulated on a digital computer.

Consider the situation where the control signal u(t) and the plant noise vector W(t) are sampled every T seconds and applied to a zero-order hold network which maintains the

value of u(t) and W(t) at the sampling instant for a time T, i.e.,

$$\underline{u}(t) = u(t) \qquad nT \le t < (n+1)T \qquad n = 0, 1, 2, \ldots, N$$

$$\underline{W}(t) = W(t) \qquad nT \le t < (n+1)T \qquad n = 0, 1, 2, \ldots, N$$

It is shown (Reference 31:126) that the response of a continuous time system to a sampled input of the form above at the sampling instants (t = 0, T, 2T, ...) is

$$X\left[(n+1)T\right] = \Phi(T)\,X(nT) + \int_0^T \Phi(\xi)\,d\xi\left[Bu(nT) + W(nT)\right] \tag{27}$$

Denote:

$$\underline{A} = \Phi(T) \tag{28}$$

$$B = \int_0^T \Phi(\xi)\,d\xi B \tag{29}$$

$$X\left[(n+1)T\right] = X(n+1)$$

$$X(nT) = X(n)$$

$$Y(nT) = Y(n)$$

$$\underline{V}(nT) = \underline{V}(n)$$

$$W(nT) = W(n)$$

$$u(nT) = u(n)$$

$$\underline{W}(n) = \int_0^T \Phi(\xi)\,d\xi W(n) \tag{30}$$

Then, the value of the output state vector of a continuous time system at the sampling instants t = 0, T, 2T, ..., nT, ... is given by

$$X(n+1) = \underline{A}X(n) + \underline{B}u(n) + \underline{W}(n) \tag{31}$$

$$Y(n) = X(n) + \underline{V}(n) \tag{32}$$

The calculation of $\Phi(T)$, $\underline{A}$, $\underline{B}$, and $\underline{W}(n)$ for Case I is shown in Appendix I. The results are similar for Case II.

Case I: $\alpha \neq 0$

$$\underline{A} = \begin{bmatrix} \exp(-\omega_B T) & 0 & 0 \\ kT\exp(-\omega_B T) & \exp(-\omega_B T) & 0 \\ 0 & 0 & \exp(\alpha T) \end{bmatrix} \tag{33}$$

$$\underline{B} = \begin{bmatrix} 0 \\ 0 \\ b\left[\exp(aT)-1\right]/a \end{bmatrix} \tag{34}$$

$$\underline{W}(n) = \begin{bmatrix} \frac{k}{\omega_B}\left[-\exp(-\omega_B T)\right] w_1(n) \\ \frac{k^2}{\omega_B^2}\left[1-\exp(-\omega_B T)(1+\omega_B T)\right] w_1(n) \\ 0 \end{bmatrix} \tag{35}$$

$$a = 0$$

$$\underline{A} = \begin{bmatrix} \exp(-\omega_B T) & 0 & 0 \\ kT\exp(-\omega_B T) & \exp(-\omega_B T) & 0 \\ 0 & 0 & 1 \end{bmatrix} \tag{36}$$

$$\underline{B} = \begin{bmatrix} 0 \\ 0 \\ bT \end{bmatrix} \tag{37}$$

$\underline{W}(n)$: Same as Equation 35

For Case II

$$\underline{A} = \begin{bmatrix} \exp(-\omega_B T) & 0 & 0 & 0 \\ kT\exp(-\omega_B T) & \exp(-\omega_B T) & 0 & 0 \\ 0 & 0 & 1 & T \\ 0 & 0 & 0 & 1 \end{bmatrix} \tag{38}$$

$$\underline{B} = \begin{bmatrix} 0 \\ 0 \\ bT^2/2 \\ bT \end{bmatrix} \tag{39}$$

$$\underline{W}(n) = \begin{bmatrix} \frac{k}{\omega_B}\left[1-\exp(-\omega_B T)\right] w_1(n) \\ \frac{k^2}{\omega_B^2}\left[1-\exp(-\omega_B T)(1+\omega_B T)\right] w_1(n) \\ 0 \\ 0 \end{bmatrix} \tag{40}$$

Note that Equations 36 and 37 reduce to Equations 33 and 34 as 'a' approaches zero. Thus Cases I and II are represented by Equations 33, 34, 35, 38, 39, and 40.

Now that the discrete plant and observation equations have been developed, a means of considering operator remnant will be incorporated into the model.

4. REMNANT

Attempts to model the human operator by matching experimental data with a linear model have shown that there is always some portion of the operator's output which is not linearly correlated with the input. A comprehensive discussion about the possible sources of remnant is included in Reference 22:37. The essence of the discussion is that the remnant could result from the following sources:

a. Operator response to other than the desired input.

b. Nonlinear operation by the operator on the desired input.

c. Injection of "noise" into the tracking loop.

d. Time varying behavior by the operator.

The status of remnant data as it pertains to the quasi-linear describing function model of the human operator in compensatory tracking tasks is summarized in Reference 19:188. Reference 29 includes an analysis of the remnant data found in pursuit-plus-disturbance tracking, and the author concludes that the remnant for the compensatory and pursuit-plus-disturbance tracking is identical for tasks that have the same input spectra and controlled element dynamics.

In Reference 18, the authors propose a model for human operator remnant in which the remnant is assumed to arise from an observation noise vector whose components are linearly independent white-noise processes. The power spectral density level of each component of the vector is assumed to be proportional to the observed variable. That is

$$V(t) = \begin{bmatrix} N_1 \sigma^2_{x_1} & v_1(t) \\ N_2 \sigma^2_{x_2} & v_2(t) \\ \vdots & \\ N_r \sigma^2_{x_r} & v_r(t) \end{bmatrix} \tag{41}$$

where

$V(t)$ = observation noise vector

$v_i(t)$ = white-noise process such that $E[v_i\ v_j] = 0$

$i \neq j,\ i,\ j \leq r$

$\sigma^2_{x_i}$ = variance of the observed variable

N_i = "noise constant"

The validity of the model was tested by comparing predicted remnant results with observed remnant data obtained from a variety of single-loop compensatory control experiments. The basic model was substantially validated and makes this concept of remnant representation attractive for use in optimal control models of human operator behavior. Thus the "observation vector" $\underline{V}$ in Equations 24 will be interpreted as a noise vector whose components are linearly independent, Gaussian amplitude, white-noise processes. The power spectral density level of each component will be proportional to the variance of that noise component.

In addition to the concept of remnant as an observation noise, compensatory control experiments have shown that under certain circumstances (Reference 13:12) the human operator will generate control output even though there is no external forcing function input. As mentioned (Reference 19:189), there is also evidence of a pulsing behavior in control of second-order controlled elements, and this pulsing behavior of the operator's output contributes an additional source of remnant. These portions of the remnant are described as "noise injection" in the quasi-linear model. To account for this observed behavior, a Gaussian amplitude white-noise process $w_2(t)$ will be added to the control output $u(t)$, and this is the control which will be applied to the controlled element. Thus if the control signal is re-defined to be

$$u'(t) = u(t) + w_2(t) \tag{42}$$

the discretized equations for Cases I and II are modified as follows:

Case I

$\underline{A}$ unchanged

$\underline{B}$ unchanged

$$\underline{W}(n) = \begin{bmatrix} \frac{k}{\omega_B}\left[1-\exp(-\omega_B T)\right] w_1(n) \\ \frac{k^2}{\omega_B^2}\left[1-\exp(-\omega_B T)(1+\omega_B T)\right] w_1(n) \\ \frac{b}{a}\left[\exp(aT)-1\right] w_2(n) \end{bmatrix} \tag{43}$$

Case II

$\underline{A}$ unchanged

$\underline{B}$ unchanged

$$\underline{W}(n) = \begin{bmatrix} \frac{k}{\omega_B}\left[1-\exp(-\omega_B T)\right] w_1(n) \\ \frac{k^2}{\omega_B^2}\left[1-\exp(-\omega_B T)(1+\omega_B T)\right] w_1(n) \\ \frac{bT^2}{2} w_2(n) \\ bT w_2(n) \end{bmatrix} \tag{44}$$

The "observation" and "motor" noises have been incorporated into the model to investigate their effect on model performance and as parameters which can be varied to obtain correlation between model and human operator performance. There will be no attempt made to associate the effects of these parameters with human physiological behavior.

5. OPTIMAL CONTROL MODEL

The plant and observation equations

$$X(n+1) = \underline{A}X(n) + \underline{B}u(n) + \underline{W}(n)$$

$$Y(n) = X(n) + \underline{V}(n)$$

are represented schematically in Figure 3. Note that a box labeled "optimal controller" has been included in this figure. The optimal controller is the mathematical construct from which the control u(n) is derived on the basis of the observed output Y(n). Thus Figure 3 is the schematic representation of the proposed discrete optimal control model of the human operator in a closed-loop tracking task. The form of the optimal controller is now described.

The theory of discrete optimal control has been developed and documented by Kalman (Reference 14), Meditch (Reference 24), Aoki (Reference 2), Meier (Reference 25), and others. The specific case where the plant and observation equations are linear and the cost function is quadratic is derived in detail by Meier (Reference 25:19). The problem is defined as follows

Given:

a. Linear plant and observation equations

$$X(n+1) = \underline{A}X(n) + \underline{B}u(n) + \underline{W}(n) \tag{45}$$

$$Y(n) = X(n) + \underline{V}(n) \tag{46}$$

b. Quadratic cost function

$$J = E\left[\sum_{n=0}^{N} X(n)^T V X(n) + S u(n)^2 \mid Y^N, u^{N-1}\right] \tag{47}$$

c. Gaussian probability distributions

$$p(X_0) = c_1 \exp\left[(X(0) - \bar{X}(0))^T M^{-1} (X(0) - \bar{X}(0))\right] \tag{48}$$

$$p\left[\underline{W}(n)\right] = c_2 \exp\left[\underline{W}(n)^T Q^{-1} \underline{W}(n)\right]$$

$$p\left[\underline{V}(n)\right] = c_3 \exp\left[\underline{V}(n)^T R^{-1} \underline{V}(n)\right]$$

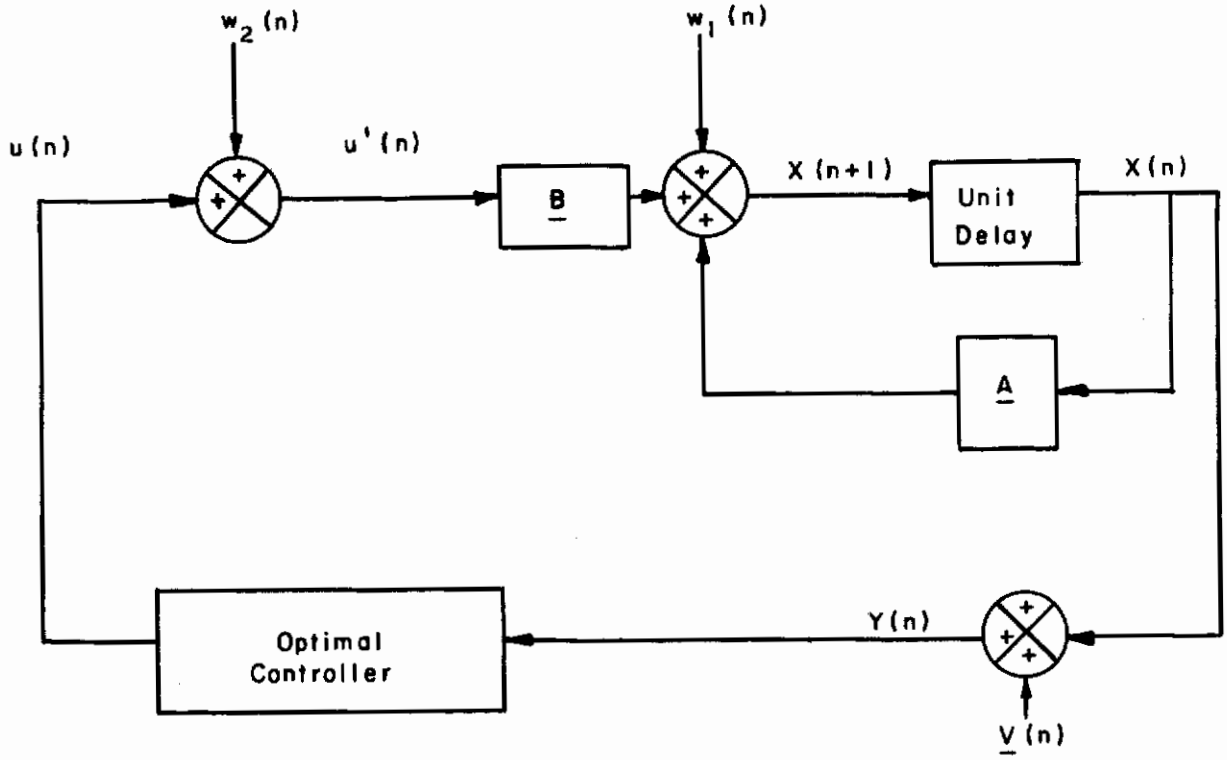

Figure 3. Schematic Representation of the Discrete Optimal Control Model

where

c_1 , c_2 , c_3 = constants

M = covariance matrix of X(0)

Q = covariance matrix of plant noise vector

R = covariance matrix of observation noise vector

$\bar{X}(0)$ = a priori mean of X(0)

d. $\underline{w}_i(n)$ and $\underline{v}_i(n)$ are independent and X(0) is independent of both $\underline{W}(n)$ and $\underline{V}(n)$ for all n.

e. $u(n) \in \Omega(n)$ where $\Omega(n)$ is the class of admissible controls.

Find: The admissible combined controller and estimator that minimizes J where

a. A combined controller and estimator is defined as any algorithm which at time n generates u(n) as a function of the present and all past observations.

b. An admissible controller and estimator is defined as any controller and estimator which, when used in the closed-loop system shown in Figure 3, yields an admissible u(n).

For the linear case, Meier (Reference 25) proves that the combined optimal estimation and control problem can be divided into two parts: control, which is the selection of the optimum input to the plant as a function of the conditional probability density of the state of the plant; and estimation, which is the computation of the conditional probability density. The control equation is generated by an application of dynamic programming, and the estimation equation is generated by an application of Baye's Rule. The results are

$$u(n) = -G(n)\,\bar{X}(n) \tag{49}$$

$$\bar{X}(n+1) = \underline{A}X(n) + \underline{B}u(n) + K(n)\left[Y(n+1) - (\underline{A}X(n) + \underline{B}u(n))\right] \tag{50}$$

where

$$\bar{X}(n) = E\left[X(n) \mid Y^n, u^{n-1}\right] = \text{conditional mean of } X(n)$$

$$\text{given } Y^n = \left\{Y(n), Y(n-1), \ldots, Y(0)\right\} \text{ and}$$

$$u^{n-1} = \left\{u(n-1), u(n-2), \ldots, u(0)\right\} \tag{51}$$

$$G(n) = \left[\underline{B}^T P(n+1)\,\underline{B} + S\right]^{-1} \underline{B}^T P(n+1)\,\underline{A} \qquad 0 \le n < N \tag{52}$$

$$P(n) = V + A^T P(n+1)\left[\underline{A} - \underline{B}G(n)\right] \qquad 0 \le n \le N \tag{53}$$

$$P(N) = V \tag{54}$$

$$K(n+1) = \underline{P}(n)\left[\underline{P}(n) + R(n+1)\right]^{-1} \qquad 0 \le n < N \tag{55}$$

$$\underline{P}(n+1) = Q + \underline{A}\left[I - K(n+1)\right]\underline{P}(n)\,\underline{A}^T \qquad 0 \le n < N \tag{56}$$

$$\underline{P}(0) = \text{Cov}\left[X(0)\right] = M \tag{57}$$

The optimal controller and estimator can be simulated with Equations 45 through 57. To simulate the optimal controller and estimator for the human operator model, a cost function must be defined. In both Cases I and II, the control u(n) is a scalar, and hence

the weighting on the control in Equation 47 is the scalar value S. The matrix V is formed such that

$$X(n)^T V X(n) = (\text{System Input} - \text{System Output})^2$$

Thus for Case I

$$V = \begin{bmatrix} 0 & 0 & 0 \\ 0 & 1 & -1 \\ 0 & -1 & 1 \end{bmatrix} \tag{58}$$

and for Case II

$$V = \begin{bmatrix} 0 & 0 & 0 & 0 \\ 0 & 1 & -1 & 0 \\ 0 & -1 & 1 & 0 \\ 0 & 0 & 0 & 0 \end{bmatrix} \tag{59}$$

The convariance matrices of the plant and observation noise vectors are formed as follows:

Let: Q = covariance matrix of plant noise vector.

Assume: $E\left[\underline{W}(n)\right] = 0$ and $E\left[w_i(n) w_j(n)\right] = 0,\ i \neq j$

Then: $Q = E\left[\underline{W}(n)\underline{W}(n)^T\right]$ and $q_{ij} = E\left[\underline{w}_i(n)\underline{w}_j(n)\right] = q_{ji}$

Case I

$$Q = \begin{bmatrix} q_{11} & q_{12} & 0 \\ q_{21} & q_{22} & 0 \\ 0 & 0 & q_{33} \end{bmatrix}$$

where

$$q_{11} = E\left[\underline{w}_1(n)^2\right] \tag{60}$$

$$= \frac{k^2}{\omega_B^2}\left[1-\exp(-\omega_B T)\right]^2 E\left[w_1(n)^2\right]$$

$$q_{12} = q_{21} = E\left[\underline{w}_1(n)\,\underline{w}_2(n)\right]$$

$$= \frac{k^3}{\omega_B^3}\left[1-\exp(-\omega_B T)\right]\left[1-\exp(-\omega_B T)(1+\omega_B T)\right]\cdot E\left[w_1(n)^2\right] \tag{61}$$

$$q_{22} = E\left[\underline{w}_2(n)^2\right]$$

$$= \frac{k^4}{\omega_B^4}\left[1-\exp(-\omega_B T)(1+\omega_B T)\right]^2 E\left[w_1(n)^2\right] \tag{62}$$

$$q_{33} = E\left[\underline{w}_3(n)^2\right]$$

$$= \frac{b^2}{a^2}\left[\exp(aT)-1\right]^2 E\left[w_2(n)^2\right] \tag{63}$$

$$q_{13} = q_{31} = E\left[\underline{w}_1(n)\,\underline{w}_3(n)\right] = 0 \text{ by assumption} \tag{64}$$

$$q_{23} = q_{32} = E\left[\underline{w}_2(n)\,\underline{w}_3(n)\right] = 0 \text{ by assumption} \tag{65}$$

Case II

$$Q = \begin{bmatrix} q_{11} & q_{12} & 0 & 0 \\ q_{21} & q_{22} & 0 & 0 \\ 0 & 0 & q_{33} & q_{34} \\ 0 & 0 & q_{43} & q_{44} \end{bmatrix}$$

where

q_{11} is given by Equation 60

$q_{12} = q_{21}$ is given by Equation 61

$$q_{13} = q_{31} = E\left[\underline{w}_1(n)\,\underline{w}_3(n)\right] = 0 \text{ by assumption} \tag{66}$$

$$q_{14} = q_{41} = E\left[\underline{w}_1(n)\,\underline{w}_4(n)\right] = 0 \text{ by assumption} \tag{67}$$

q_{22} is given by Equation 62

$$q_{23} = q_{32} = E\left[\underline{w}_2(n)\,\underline{w}_3(n)\right] = 0 \text{ by assumption} \tag{68}$$

$$q_{24} = q_{42} = E\left[\underline{w}_2(n)\,\underline{w}_4(n)\right] = 0 \text{ by assumption} \tag{69}$$

$$q_{33} = E\left[\underline{w}_3(n)^2\right] = b^2T^4E\left[w_2(n)^2\right] \tag{70}$$

$$q_{34} = q_{43} = E\left[\underline{w}_3(n)\,\underline{w}_4(n)\right] = b^2T^3E\left[w_2(n)^2\right] \tag{71}$$

$$q_{44} = E\left[\underline{w}_4(n)^2\right] = b^2T^2E\left[w_2(n)^2\right] \tag{72}$$

Let: R = convariance matrix of the observation noise vector.

Assume : $E\left[\underline{V}(n)\right] = 0$ and $E\left[\underline{v}_i(n)\,\underline{v}_j(n)\right] = 0,\ i \neq j$

Then : $R = E\left[\underline{V}(n)\,\underline{V}(n)^T\right]$ and $r_{ij} = E\left[\underline{v}_i(n)\,\underline{v}_j(n)\right] = r_{ji}$

The a priori expected value of X(0) is taken to be zero, and the convariance matrix M of X(0) is taken to be Q, i.e.,

$$M = Q \tag{73}$$

$$X(0) = 0 \tag{74}$$

Equations 45 through 74 are all that are required to simulate the closed-loop tracking situation and as such represent the discrete, stochastic, optimal control model of the human operator in a closed-loop tracking task. These equations are in a format which can readily be programmed for simulation on a digital computer.

SECTION III

DIGITAL SIMULATION OF THE OPTIMAL CONTROL MODEL

The discrete, stochastic, optimal control model is simulated on an IBM 7094 digital computer using FORTRAN IV language. The computer program generates N values of i (n), x (n), e (n), and u (n) where

$x_2(n) = i(n)$ = digitized value of system input at $t = nT$

$x_3(n) = x(n)$ = digitized value of system output at $t = nT$

$e(n) = i(n) - x(n)$

$u(n)$ = digitized value of control input at $t = nT$

The power spectra of these signals are computed and the spectra are plotted versus frequency. The variances of the input and error are calculated and the normalized tracking error defined as

$$NTE = \sigma_E^2 / \sigma_I^2 \tag{75}$$

is computed

The computer routines for generating the data are included in Appendix II.

1. DESCRIPTION OF SYSTEM-MODEL PARAMETERS

The parameters in the model are tabulated below. These parameters are classed as either system parameters or model parameters. The system parameters are those which are specificed by the dynamics of the tracking task to be modeled. The model parameters are those which can be varied to change the model characteristics.

System Parameters:

a = plant time constant (for first order plant)

ω_B = forcing function bandwidth

σ_I^2 = variance of input forcing function

b = plant gain

Model Parameters:

T = sampling period

S = control weighting in cost function

$\sigma_q^2 = E\left[\underline{w}_2 (n)^2\right]$ = motor noise variance

$\sigma_{v_i}^2 = E\left[\underline{v}_i (n)^2\right]$ = variance of i^{th} component of $\underline{V}(n)$, i = 1, 2, 3, 4

N = number of samples

2. SELECTION OF MODEL PARAMETERS

As mentioned in Section II, a sample function for the input stochastic process can be generated by operating on Gaussian amplitude white noise with two first-order filters. The digital simulation of this process requires a sequence of N "random" numbers whose statistics approximate those of theoretical white noise. A random number generator called RANDNM is used in conjunction with the digital simulation. The routine is based on a modified table look-up technique (Reference 23). A detailed study by Bowser and Schubert (Reference 5) presents the results of a digital simulation of Gaussian amplitude white noise being operated on by one first-order filter. The principal result is a plot of dispersion versus $\omega_B NT$. The percent dispersion is defined as

$$\frac{\sigma_e^2}{\sigma_y^2} \times 100 = \text{percent dispersion}$$

where σ_y^2 is defined by the desired autocorrelation function

$$R_{yy}(\tau) = \sigma_y^2 \exp(-\omega_B|\tau|)$$

and σ_e^2 is defined as the variance of the difference between the autocorrelation function defined over a doubly infinite domain (assuming ergodicity) and the one defined over the finite sample length of the random variable.

The value of N is chosen to obtain the minimum percent dispersion of the first-order noise simulation without exceeding the memory capacity of the IBM 7094. For all of the model simulations in this development, the value of N is fixed at 4000.

The value of T is chosen to obtain a power spectral density plot within the frequency range of interest. As noted in Appendix III, the maximum frequency at which the power spectral density can be computed is determined by the equation

$$\omega_{max} = \pi/T \text{ rad/sec}$$

A value of T = 0.1 sec is chosen to provide power spectral density plots up to ω_{max} = 10 rad/sec. All data of interest in manual control tracking tasks fall well below this value of ω_{max}. Thus a value of NT = (4000) (0.1) or NT = 400 is used in this development and the

resulting values of percent dispersion versus $\omega_B NT$ all fall below 10% for the values of ω_B under consideration.

The remaining model parameters are the noise variances and the control weighting. The noise variance σ^2_{w1}, which represents the variance of the Gaussian amplitude white-noise process is taken to be unity and the gain factor k in the noise filter equation is chosen as

$$k = \sqrt{2\sigma_I} (\omega_B)^{3/4}$$

so that $R_{ii}(0) = \sigma^2_I$ can be entered as a system parameter. The choice of the control weighting and the motor and observation noise variances will be discussed in Section V, Experimental Results and Discussion.

SECTION IV

EXPERIMENTS

1. EXPERIMENTAL OBJECTIVES

The experiments conducted during this investigation were undertaken to "validate" the proposed model and to expand the limited data base of human operator tracking data in the pursuit mode. To "validate" the proposed model is to show that the normalized tracking errors and power spectra obtained experimentally agree with the same quantities predicted by the model.

2. EQUIPMENT

A block diagram of the experiment equipment layout is shown in Figure 4.

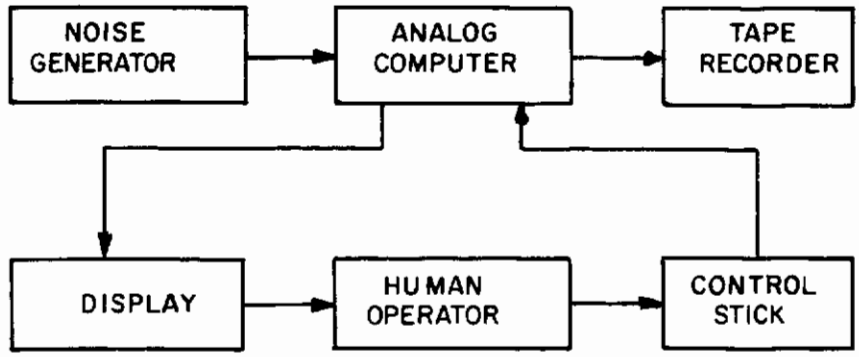

Figure 4. Experimental Equipment Layout

The Gaussian amplitude white-noise process, with which the input forcing function is generated, is obtained from an Eigenco Incorporated, low-frequency, noise generator, Model 310A.

The analog computer used is an Applied Dynamics Inc. Model AD-64PB. The computer is used to simulate the control element dynamics, generate the forcing function input, compute mean and mean-square values, sum signals, and make signals available for display and recording.

The tape recorder is a Sangamo Model 4700 FM 1/2-inch tape recorder and is used to record the analog signals from which the power spectra are computed.

The display is a Dumont dual-beam cathode-ray oscillograph, Type 322. Both channels are calibrated to have the same linear gain over the portion of the face utilized (±3 cm). Two moving purple markers are used; a long bar (2 cm) representing the system output, and a

short bar (1/4 cm) representing the target. In addition there is a reference indicator as shown in Figure 2b.

The control stick used is a Measurement Systems, Inc., Model 435 AC-powered stiff-stick transducer. The transducer has no damping, back lash, or dead zone and produces an essentially linear output voltage proportional to the applied force (0.1 volt/lb).

Figure 5 shows an operator and the scope display arrangement.

3. TRAINING

The experiments will be categorized first by controlled element and then by ω_B, the forcing function bandwidth frequency. Four frequencies ($\omega_B = 0.5,\ 1.0,\ 1.5,\ 2.0$ rad/sec) were used for each controlled element considered. Subjects were trained on each controlled element at each bandwidth frequency until their learning curves of normalized tracking error stabilized to a mean value with a "reasonable" 1-sigma standard deviation. The term "reasonable" is used here because the dispersion about the mean increases with ω_B, and hence the suitable 1-sigma values vary. A typical learning curve is shown in Figure 6. The learning curves normally stabilized after about 20 runs. Each run lasted 90 seconds and runs were made in groups of two or three at each frequency both during the training and during the data experiments. Lines between data points in Figure 6 indicate successive data runs.

4. EXPERIMENTAL RUNS

The experimental data runs were planned to meet the experimental objectives stated earlier. Specifically, the runs were designed to obtain human operator performance data in terms of normalized tracking error and power spectral density plots as a function of controlled element, forcing function bandwidth, and type of display. Two types of displays were investigated; the pursuit and compensatory (Figure 2). Four types of controlled elements were considered. In the Laplace transform domain, they are represented by their impulse responses as follows:

$$Y_c = K/s$$

$$Y_c = K/s+1$$

$$Y_c = K/s-1$$

$$Y_c = K/s^2$$

Four forcing function bandwidth frequencies were investigated. They are $\omega_B = 0.5,\ 1.0,\ 1.5,\ 2.0$ rad/sec.

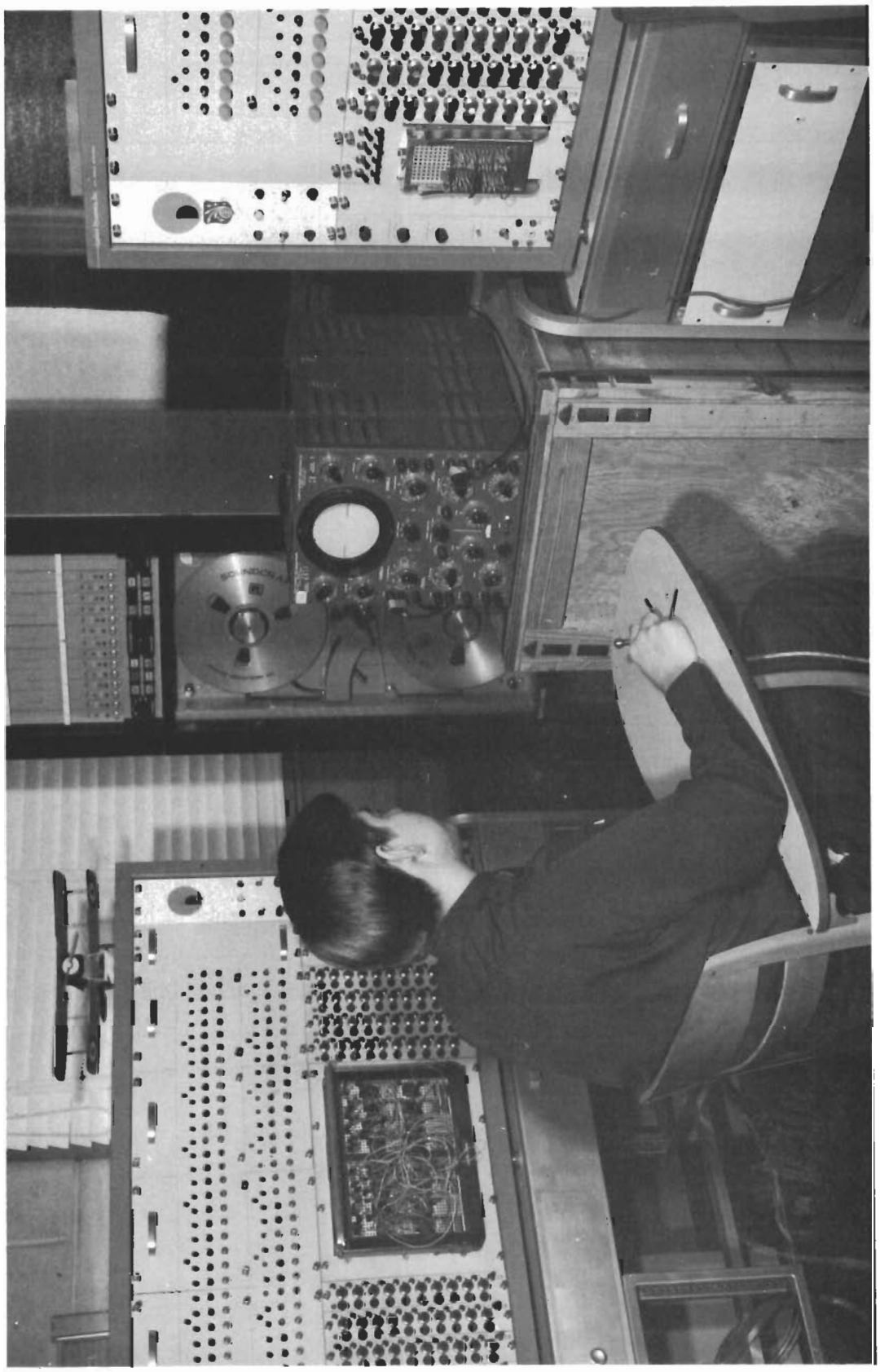

Figure 5. Operator and Scope Arrangement

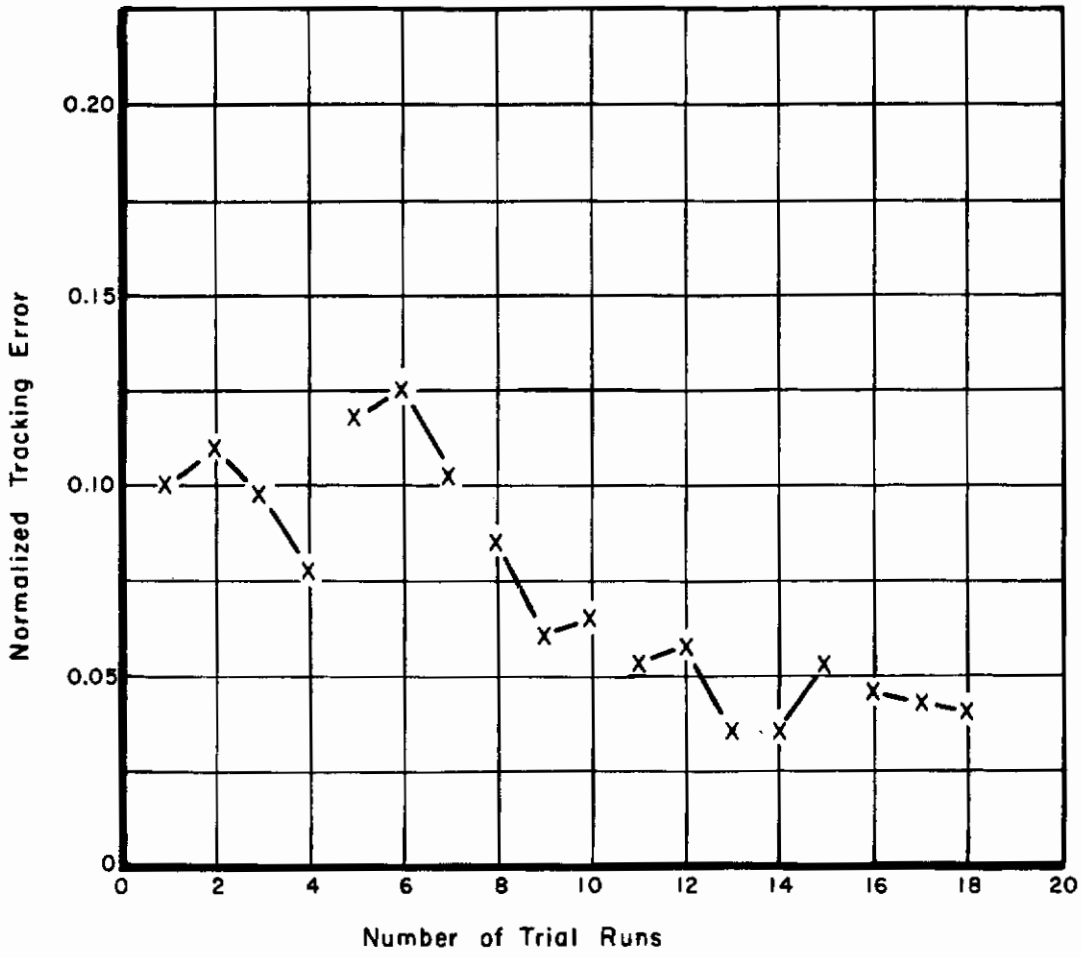

Figure 6. Typical Learning Curve

For the pursuit display situation, normalized tracking error (NTE) and power spectral density (PSD) plots were obtained for each of the four controlled elements at each of the four forcing function bandwidths. For the compensatory display, NTE data were obtained for each of the four controlled elements at each of the four forcing function bandwidths, and PSD plots were obtained for the $Y_c = K/s+1$ plant at $\omega_B = 0.5$, 1.0, and 2.0 rad/sec. PSD plots for the remaining three controlled elements were obtained at $\omega_B = 1.0$ rad/sec only.

Four subjects were used during the experiments. Two were rated Air Force officers (pilots), one had a private pilot's license, and the last was a nonrated Air Force Officer.

SECTION V

EXPERIMENTAL RESULTS AND DISCUSSION

1. MODEL MATCHING TO THE EXPERIMENTAL DATA

Since the experimental data and model output will be shown comparatively in most of the following tables and figures, it is appropriate at this point to discuss how the remaining model parameters (control weighting, observation noise variances, and motor noise variance) are chosen. For all the controlled elements considered, a forcing function bandwidth of $\omega_B = 1.0$ rad/sec was chosen as the data point at which to match the model to the data and at which to evaluate the effects of model parameter variations. This value of ω_B was chosen on the basis of an analysis of the tracking data presented by McRuer, et al (Reference 19).

Assume that the root-mean-squared (rms) value of the input is chosen so the display remains active within some central area of the scope face; then for a given controlled element, the difficulty of the tracking task is determined by the bandwidth (ω_B) of the forcing function input. For very low ω_B (< 0.5 rad/sec), the input signal moves so slowly that the operator does not respond to minor deviations from the desired condition of zero error. Such behavior has been characterized by an "indifference threshold" effect in the describing function model (Reference 19:16). Conversely, as ω_B becomes large (> 2.0 rad/sec), the task difficulty increases significantly and the operator tends to devote more attention to minimizing the error. This behavior has been well documented, and McRuer (Reference 19:159) presents curves of effective time delay versus ω_B for various controlled elements. These curves indicate a decrease in effective time delay (a parameter in the describing function model) as the forcing function bandwidth increases. A decrease in effective time delay is related to a corresponding decrease in normalized tracking error (Reference 19:180), and, hence, as the bandwidth increases the operator behavior departs from what the linear model would predict. McRuer attributes this decrease in effective time delay with increasing forcing function bandwidth to the human operator neuromuscular system.

The above discussion indicates that the human operator may not operate in a linear manner across the range of forcing function bandwidths considered. Thus a mid-point frequency ($\omega_B = 1.0$ rad/sec) is chosen as the data point at which the human operator performance will be closest to any linear representation of the operator and hence the point at which the model parameters will be adjusted to match operator performance.

a. Observation Noise

As can be seen from Equations 53 and 55, the convariance matrix of the observation noise does not influence the a priori calculation of the gain matrix G(n) but appears as an additive term in the recursion formula for the estimation matrix K(n). Thus the effect of the observation noise variances is to influence the a priori calculation of the estimation matrices K(n) which in turn affect the on-line calculation of the conditional mean of the state vector X(n) through Equation 50. When the estimation of the state is degraded by increasing the observation noise variances, the control u(n) is affected through Equation 49, and the extent to which the performance of the system is degraded can be measured by computing the NTE. The effects of observation noise variances can also be determined by examining the PSD plots of the various signals in the control loop.

The state equations for both the first- and second-order controlled-element tracking situations have been formulated so that the first two state equations simulate the desired forcing input. In order to generate a faithful reproduction of the desired input PSD (Equation 13), the observation noise variances for the first two components of the observation noise vector are chosen to be 1×10^{-6}. This number is chosen so the variance of the additive Gaussian amplitude white-noise process is 6 orders of magnitude less than the variance of the forcing function input and hence has no appreciable effect on the desired PSD. See Appendix III for a comparison of the theoretical and simulated PSD for the desired forcing function input.

Thus the variable observation noise parameters will be restricted to the variance of the additive observation noise on the controlled element position in Cases I and II and to the variance of the additive observation noise on the controlled element velocity in Case II.

As an aid in investigating the effects of these observation noise variances, an auxiliary computation routine was temporarily added to the digital simulation program. The purpose of the routine is to get a quantitative measure of the effects of observation noises on the estimation of the conditional mean of the state vector. The rationale for the routine calculations is as follows. Let the actual value of a state vector component at time nT be denoted by $x_A(n)$ and the estimated value (conditional mean) be denoted by $x_E(n)$. If the estimation is exact, then

$$x_E(n) = x_A(n)$$

otherwise

$$x_E(n) = cx_A(n) \qquad c \neq 1$$

To measure the performance of the estimator, the following calculation is performed for each component of the state vector at each sampling instant nT, $0 \leq n \leq NT$:

$$c' = \left| \frac{x_E(n) - x_A(n)}{x_A(n)} \right| = \left| \frac{cx_A(n) - x_A(n)}{x_A(n)} \right|$$

Thus

$$c' = |c-1|$$

is a measure of how good the state estimation is, for if the estimation is perfect, $c = 1$ and $c' = 0$. If $x_E(n) = 0.5\, x_A(n)$ or $x_E(n) = 1.5\, x_A(n)$, then $c' = 0.5$, etc. As the estimation error increases, so does c'. A reference value of c' is chosen and compared with the actual values of c' calculated at each sampling instant for each state vector component. A cumulative total of the number of times the actual value of c' exceeds the reference value is kept for each component of the state vector. Finally the percentage of total samples that exceeded the reference value of c' is computed for each component.

A reference value of $c' = 0.5$ was used throughout the model analysis. For all the cases where the variance of the observation noise process was 6 orders of magnitude less than the variance of the input, the percentage of samples that exceeded the reference value of c' was less than 1% for all components of the state vector. To measure the effects of observation noise, the motor noise variance was chosen so it was 6 orders of magnitude less than the variance of the forcing function input and the value of the control weighting S was fixed. The system parameters were fixed for the particular controlled element being considered. Two model simulation runs were made: a reference run with the variances of the observation noises 6 orders of magnitude less than the variance of the forcing function input and the second with the variances of the observation noises equal to the variance of the forcing function input. The effects of the observation noises on the NTE and the performance of the estimator are tabulated in Table I. The effects of the observation noises on the PSD of the tracking loop signals are shown in Figures 7 and 8. The normalization $\phi_{ii}(0)$ in the PSD plots is really $\phi_{ii}(0.1 \text{ rad/sec})$ and is an approximation to $\phi_{ii}(0)$.

It can be seen from Table I that the effect of adding observation noise was most severe in the second-order and unstable first-order controlled elements. As a matter of fact, the addition of observation noise above the reference level had little or no effect on the K/s+1 and K/s controlled elements. The variance of the control signals (σ_u^2) and the normalized tracking errors for these controlled elements were unchanged, and the PSD plots for the

TABLE I

EFFECTS OF OBSERVATION NOISE

Controlled Element	Observation Noise	NTE	Percent of Samples where C' > 0.5				
			Intermediate Noise Input x_1	Forcing Function x_2	Plant Output x_3	Plant Velocity x_4	σ_u^2
K/s^2	NO	.099	0.2	0	0.2	0.2	3.05
	YES	.12	0.2	0	19.9	0.7	3.05
$K/s+1$	NO	.04	0.1	0	0.1		1.23
	YES	.04	0.1	0	0.1		1.23
$K/s-1$	NO	.047	0.1	0	0.3		1.17
	YES	2.66	0.1	0	74.5		12.0
K/s	NO	.04	0.1	0	0.1		.512
	YES	.04	0.1	0	0.5		.512

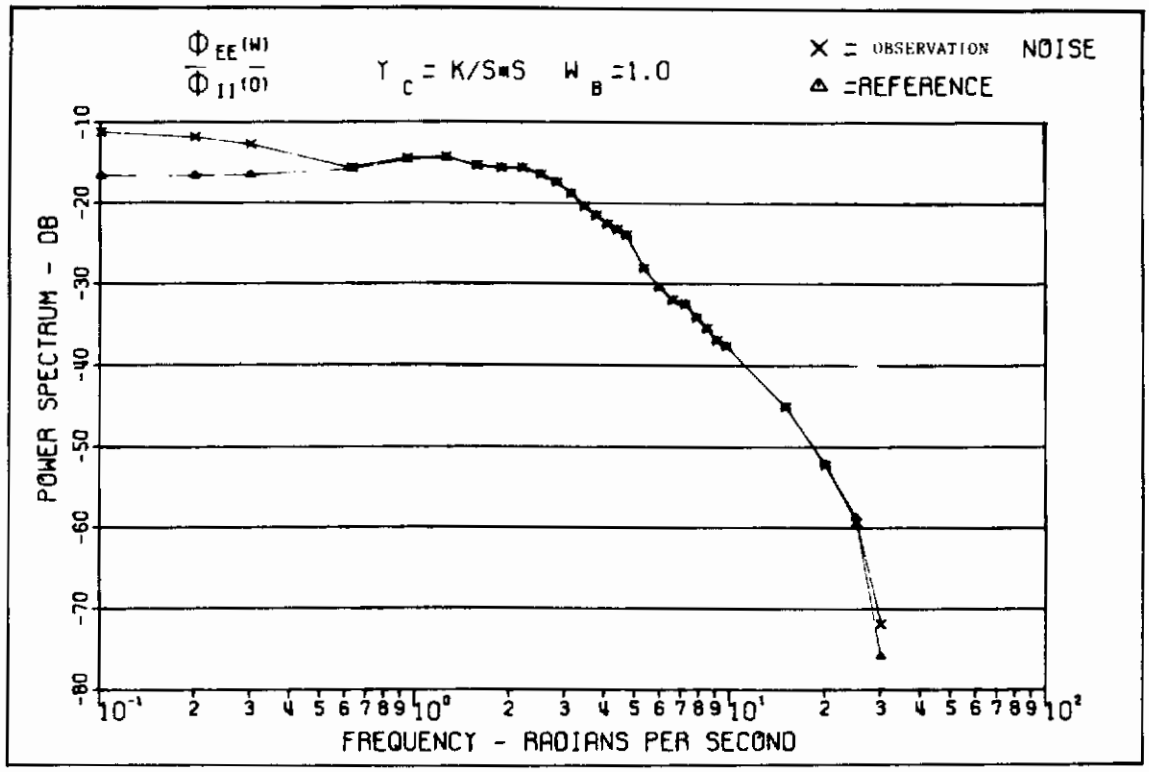

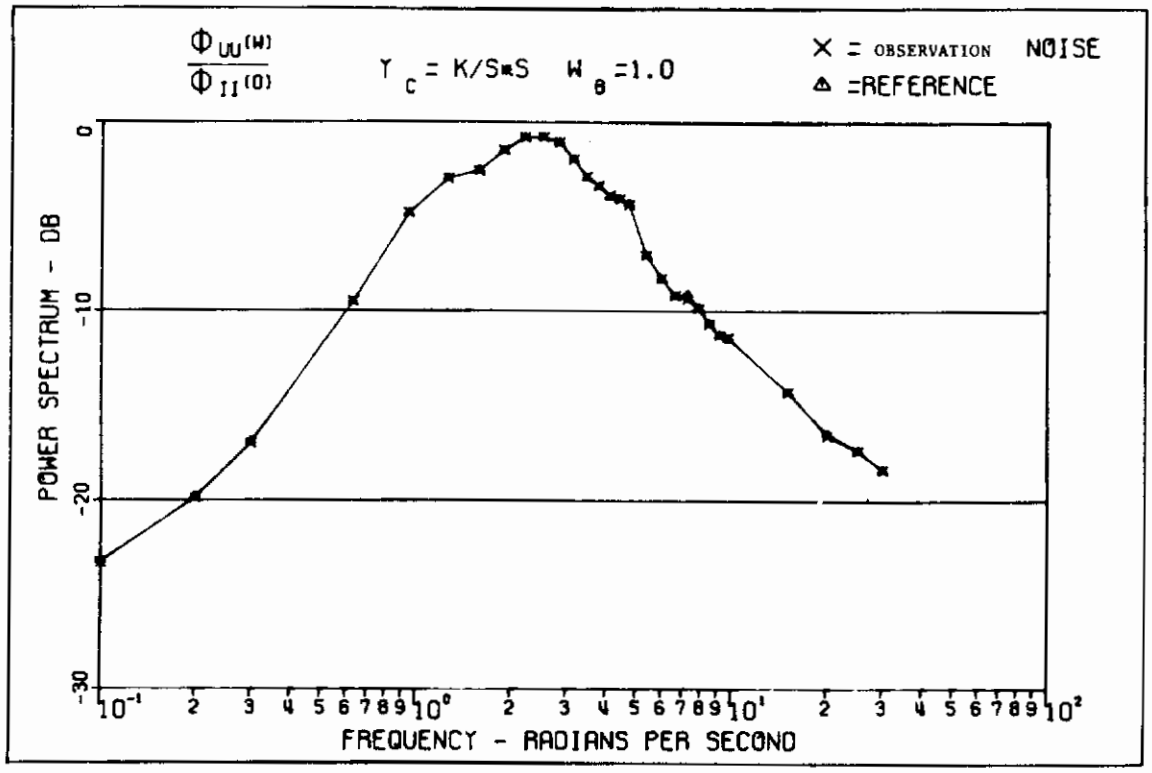

Figure 7. Observation Noise Effect $Y_C = K/s^2$

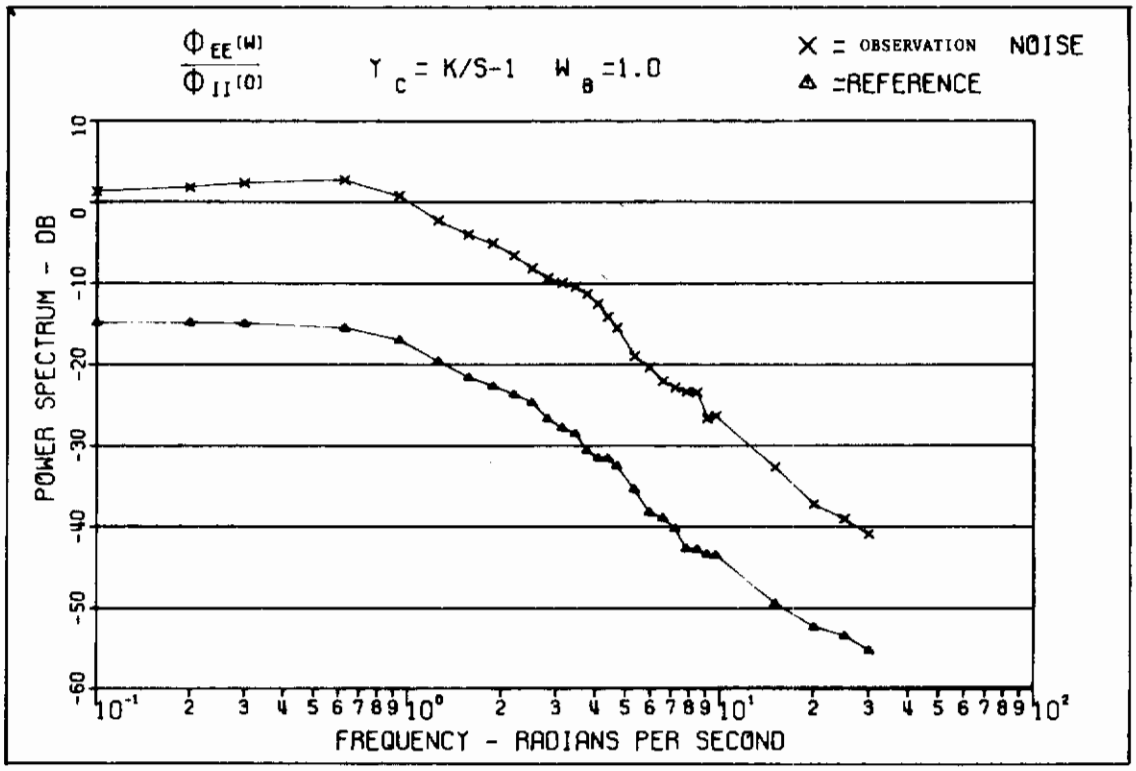

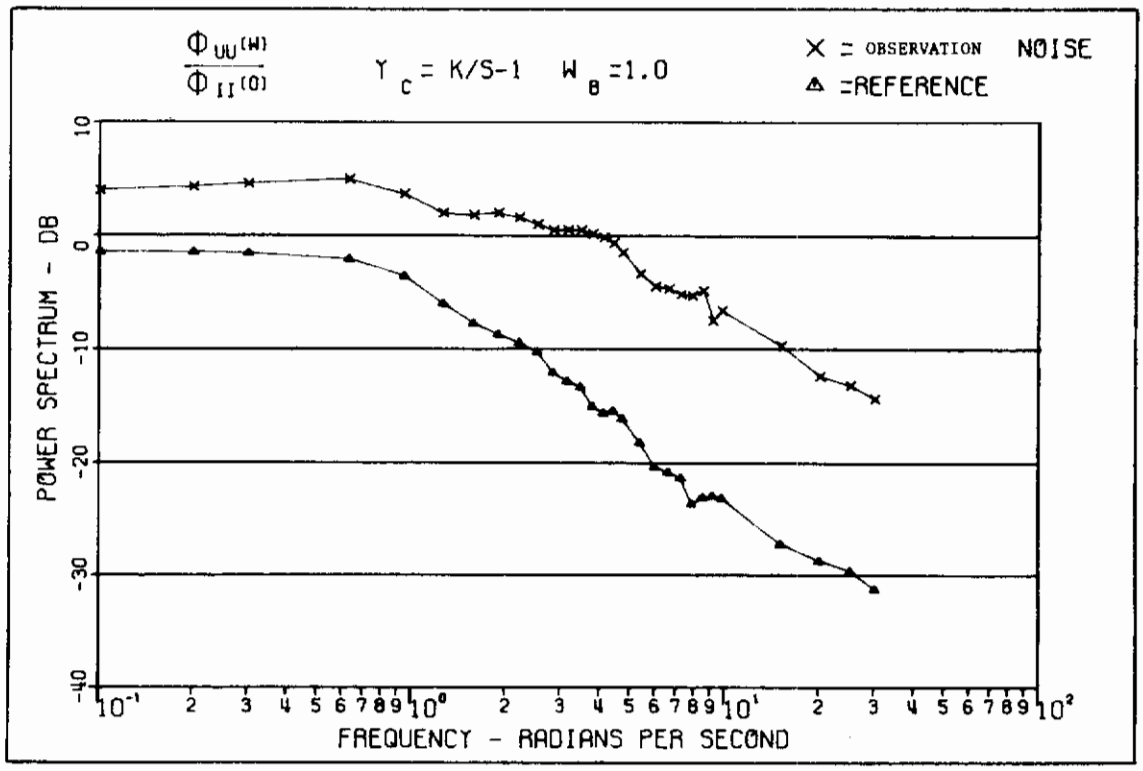

Figure 8. Observation Noise Effect Y_C = K/s-1

noise versus reference cases were identical and hence not included here. For the K/s^2 case, the variance of the control signal was unchanged, and hence the PSD of the control signal ($\phi_{uu}(\omega)$) is unchanged (Figure 7). The NTE for the noise case, however, was greater than the reference because of the degradation of plant output estimation and the effect is an increase in the error PSD at low frequencies (Figure 7). For the K/s-1 case there was a significant increase in control signal variance and hence a rise in the PSD of the control signal (Figure 8). Similarly, the increase in NTE for this case resulted in a higher level of the error PSD (Figure 8).

Although only one deviation from the reference was investigated, the results of the analysis indicate that observation noise effects do not change the basic shape of the PSD plots although there can be significant changes in control signal variances and normalized tracking errors. Significant increases in control signal variances correspond to increases in NTE, and these cause upward shifts in the error and control PSD plots relative to the reference levels. As mentioned in Section V1a, any change in control signal variance because of observation noise is caused by the increase in variance of the conditional mean of the state vector and not by the multiplicative gain matrix G in Equation 49. Because observation noise effects do not change the basic shape of the tracking loop PSDs, it was decided not to try to develop a rationale for picking observation noise variances based on controlled element or forcing function bandwidth. Instead the observation noise variances were fixed at the reference value of 1×10^{-6}.

b. Motor Noise

The covariance matrix of the plant (motor) noise vector does not influence the a priori calculation of the gain matrix G(n). It appears as an additive term in the recursion formula for P(n), Equation 53, which in turn is used in the recursion formula for the estimation matrix K(n+1), Equation 55. To determine the effects of motor noise, a reference situation was established with the motor noise variance (σ_q^2) set at 1×10^{-6}. Again, this number was chosen so the variance of the additive Gaussian white-noise process is 6 orders of magnitude less than that of the forcing function input. The system parameters were fixed for the controlled element being considered, the control weighting was fixed as before, and the observation noise variances were also set at 1×10^{-6}. The motor noise condition was established by choosing σ_q^2 such that the variance of the additive motor noise process was equal to the variance of the forcing function input.

As was to be expected, with the condition of essentially no observation noise, the motor noise had no effect on the state estimation. For all controlled elements, the percentage of

samples that exceeded a reference value of $c' = 0.5$ was less than 1% for all components of the state vector for both the reference and the motor noise situations. As Table II indicates, however, there were significant changes in NTE and control signal variances. The corresponding effects of the motor noise on the power spectra are shown in Figures 9 through 12. As the figures indicate, the increases in NTE are reflected by upward shifts of the error power spectra. The effect of the motor noise on the control spectra for each controlled element can be predicted by noting that the motor noise is additive only to the state equation describing the dynamics of the controlled element, and not to the equations which generate the forcing function input.

TABLE II

EFFECT OF MOTOR NOISE

Controlled Element	Motor Noise	NTE	σ_u^2
K/s^2	NO	0.11	3.05
	YES	0.15	5.86
$K/s+1$	NO	0.040	1.23
	YES	0.23	1.91
$K/s-1$	NO	0.047	1.17
	YES	0.29	3.96
K/s	NO	0.040	0.51
	YES	0.31	1.61

The control signal u(n) is a linear combination of the estimated components of the state vector, and, with motor noise in the system, the plant output is the sum of a component due to the control u and a component due to the additive noise w_2. The control PSD is also a sum of the spectra and cross-spectra of the terms in the linear summation for u(n), and hence the control PSD with the motor noise will differ from the reference by the contribution of the motor noise to the plant output. Figure 13 shows the power spectra which result from operating on Gaussian amplitude white noise with each of the controlled elements considered. As Figure 13 indicates, there is a high gain at low frequencies (< 0.1 rad/sec) for the K/s and K/s^2 controlled elements. This explains the emphasized upward shift of the control

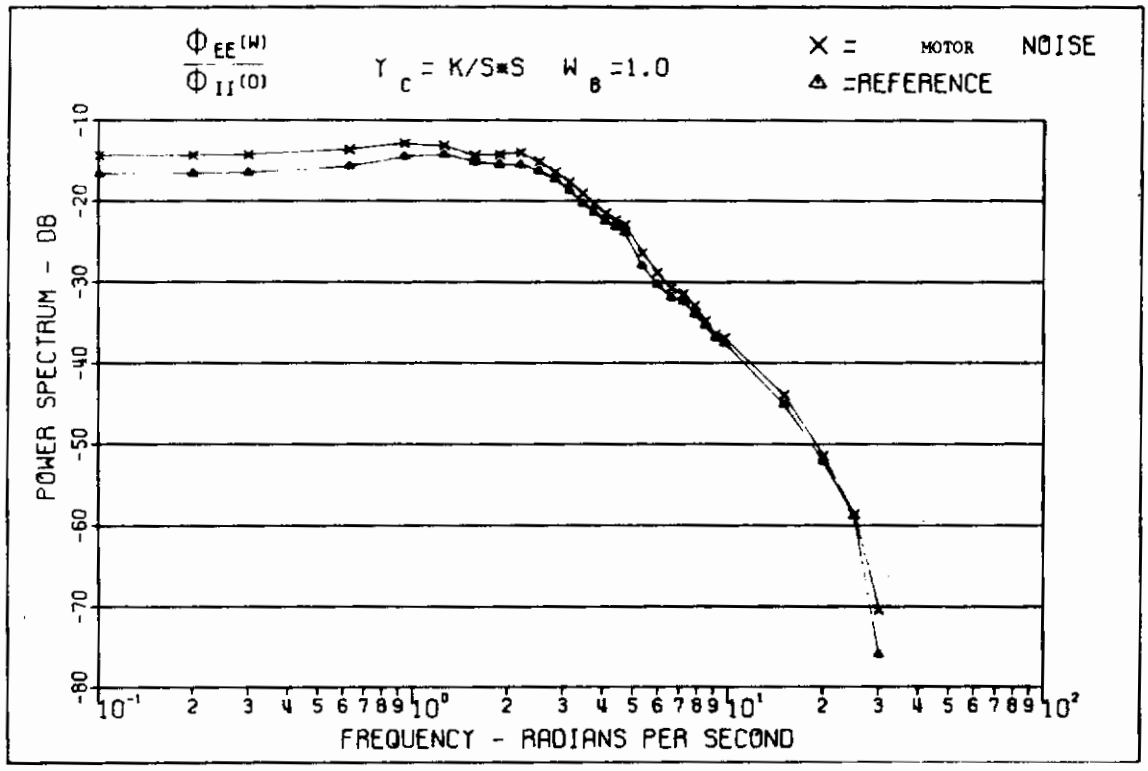

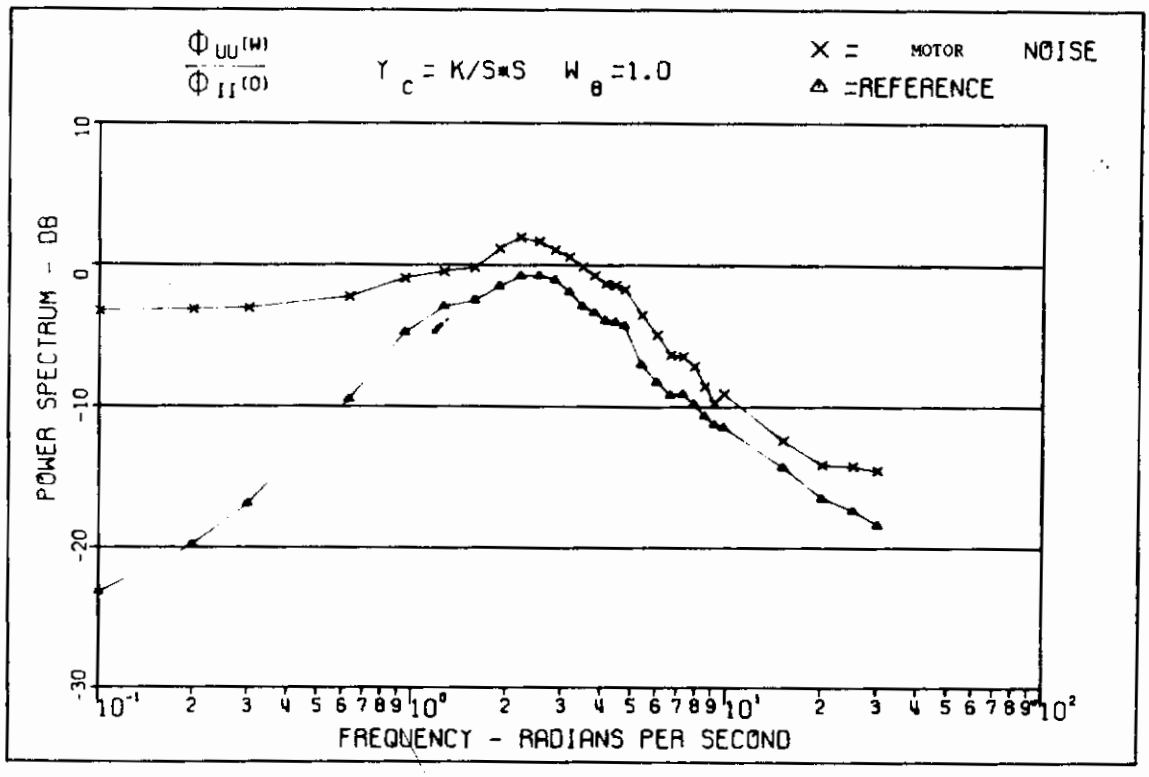

Figure 9. Motor Noise Effect $Y_C = K/s^2$

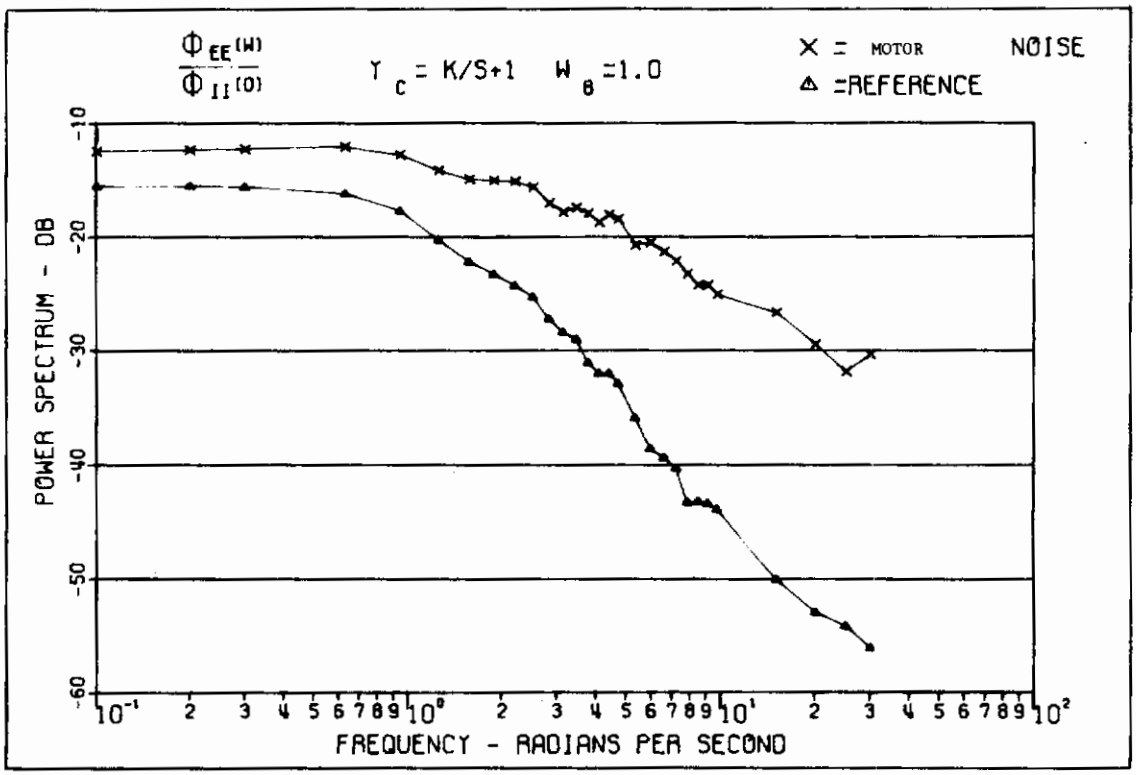

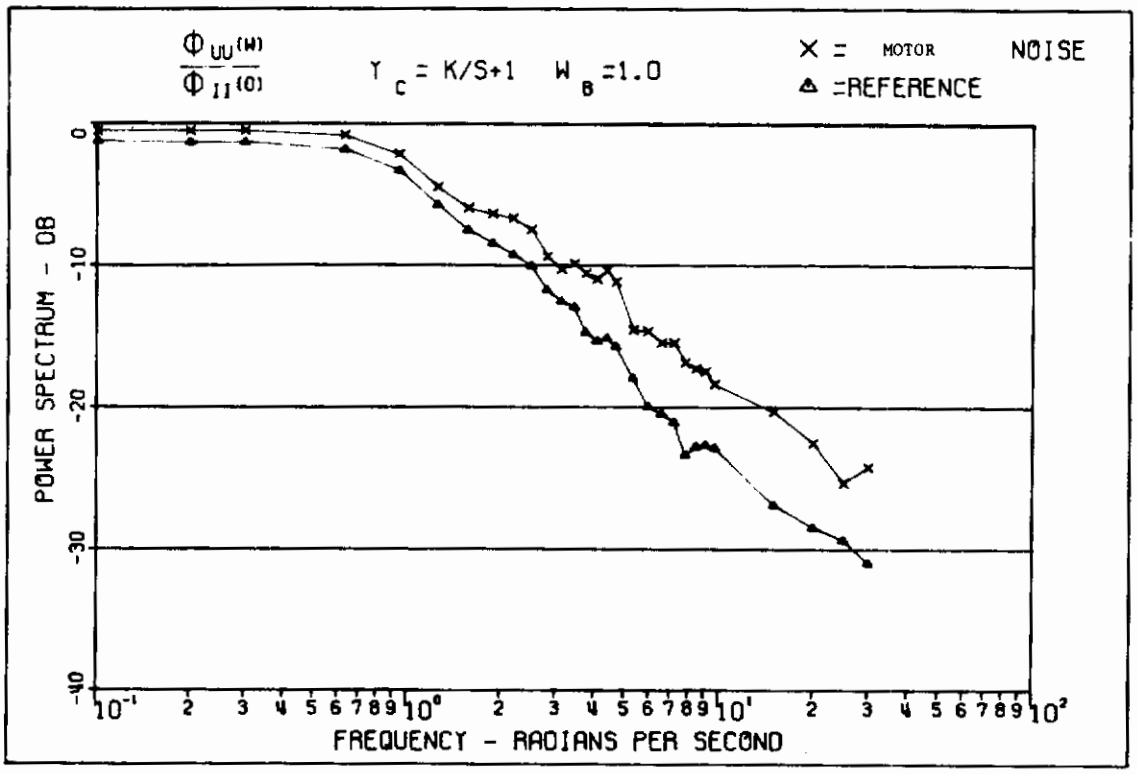

Figure 10. Motor Noise Effect Y_C = K/s+1

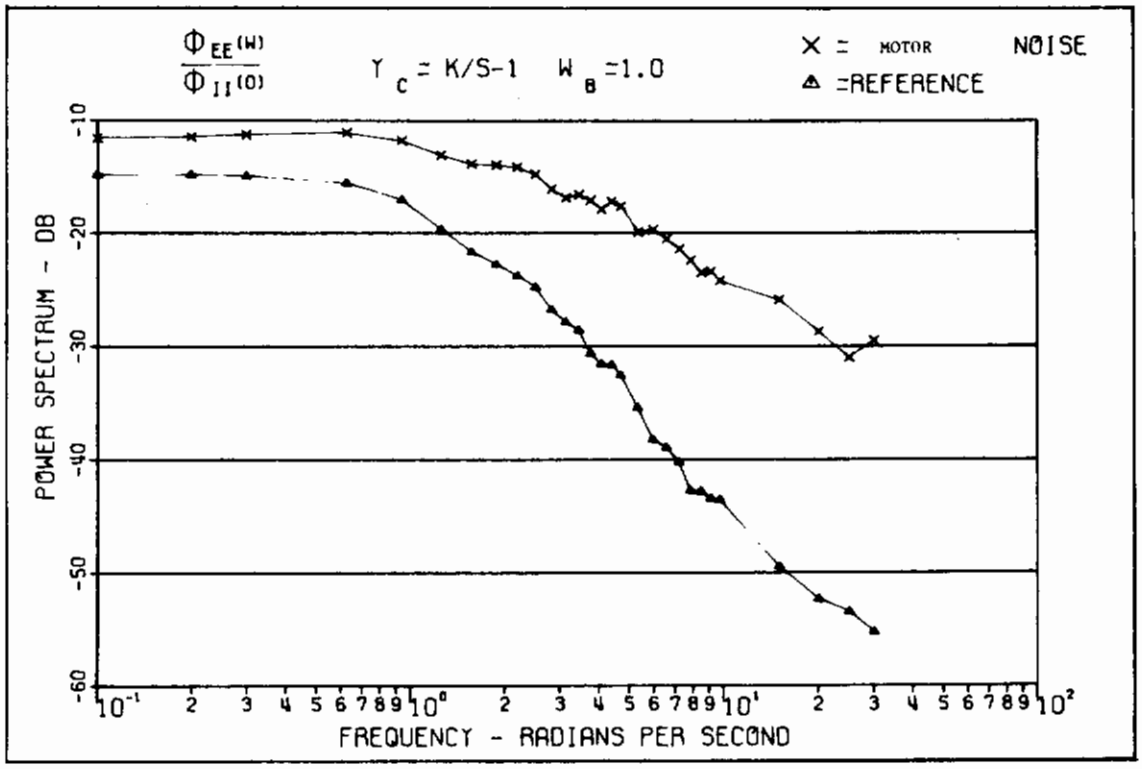

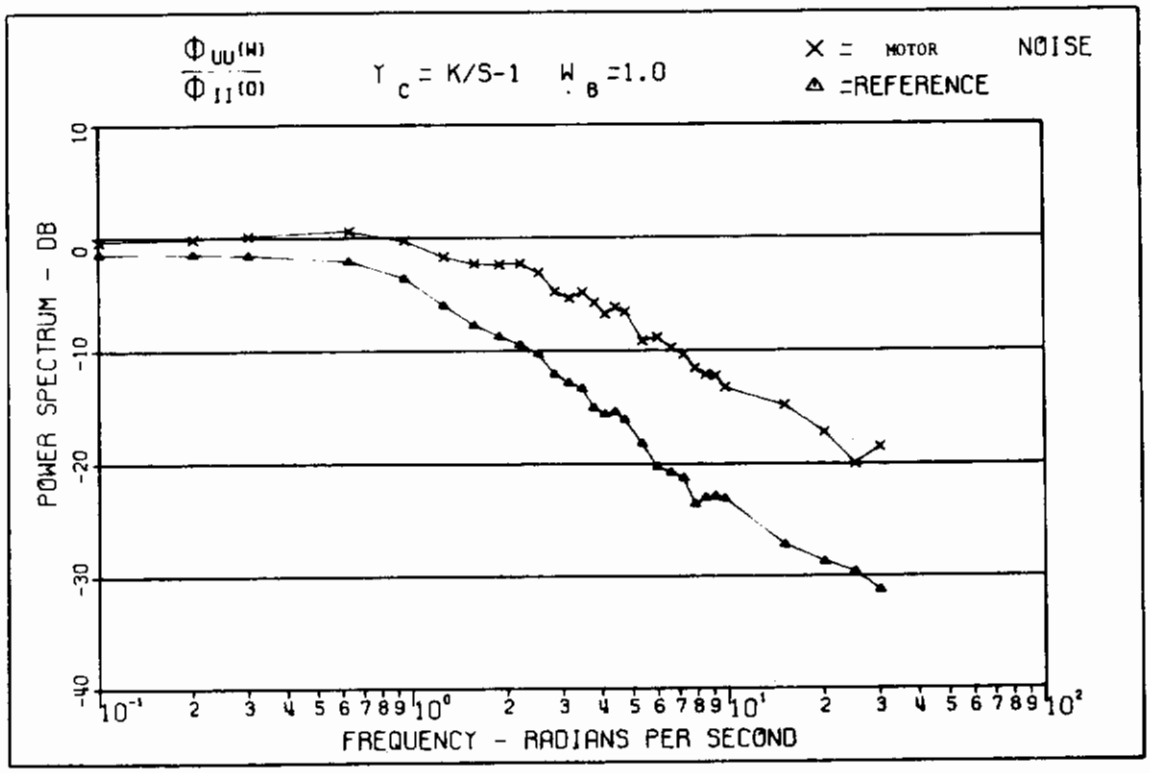

Figure 11. Motor Noise Effect Y_C = K/s-1

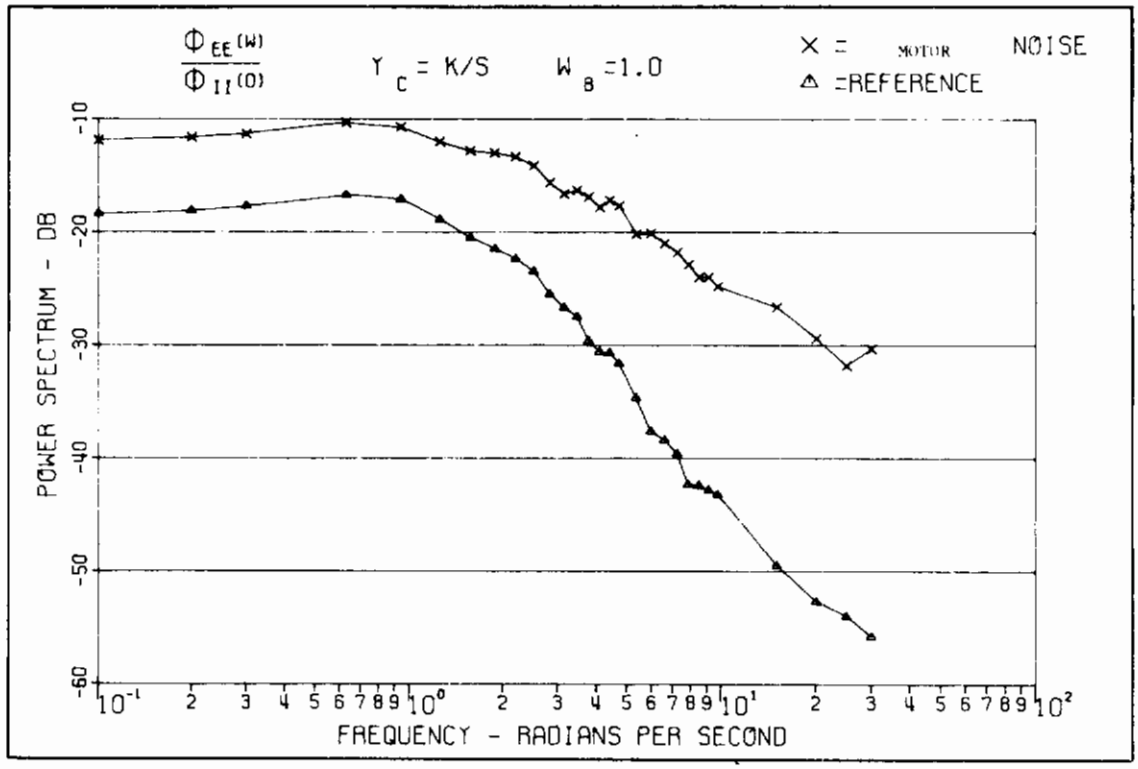

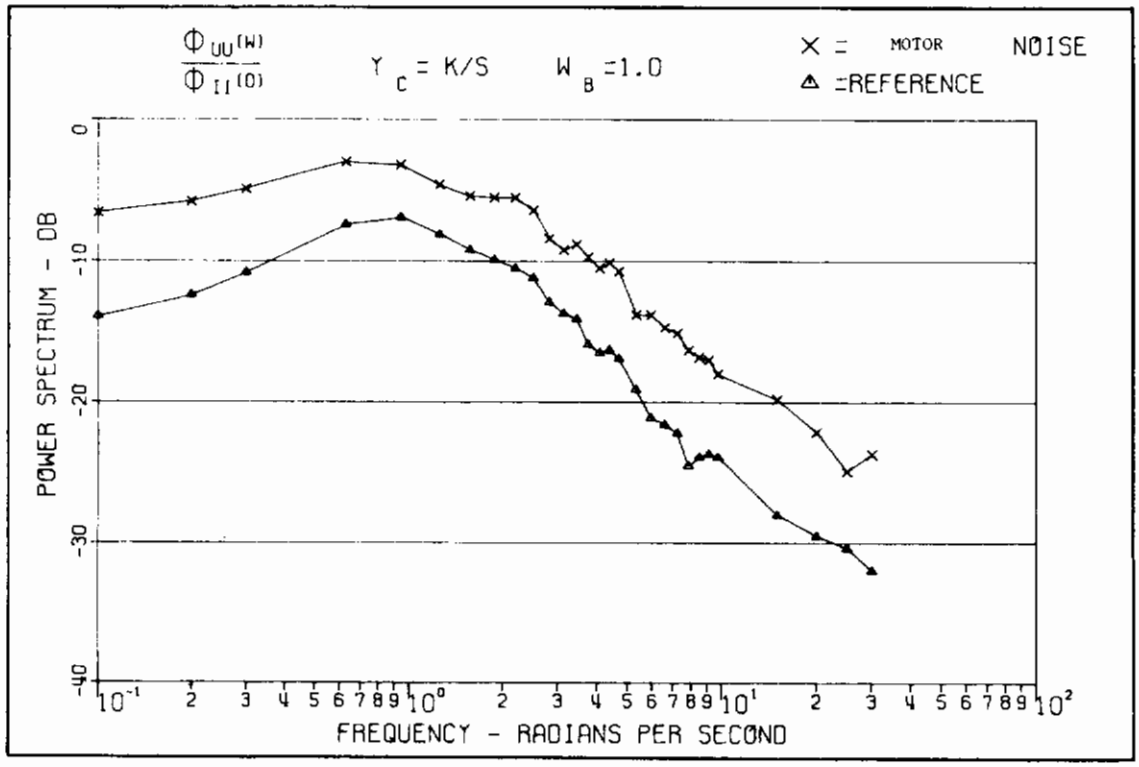

Figure 12. Motor Noise Effect Y_C = K/s

spectra for these plants in the low frequency range. Similarly, the steep drop off of gain (-40 db/decade) for the K/s^2 plant explains why there is a smaller high frequency (> 1.0 rad/sec) shift in the control spectra for this plant than for the remaining three. The shift for the remaining three should be essentially the same for ω greater than 0.1 rad/sec since the gains for these plants all fall off with the same slope of -20 db/decade.

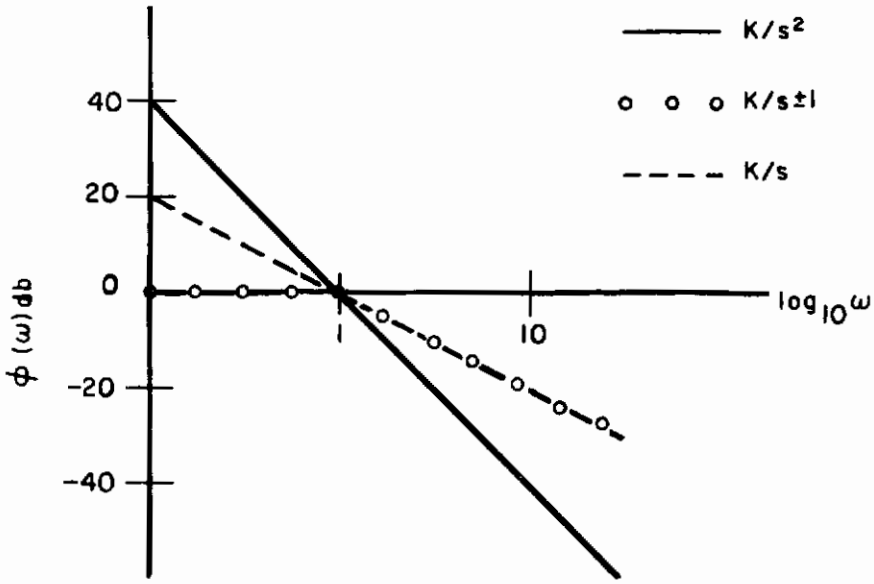

Figure 13. Power Spectral Density Asymptotes

Although there are significant changes in the shapes of the control spectra for the K/s and K/s^2 controlled elements, it was again decided not to develop a rationale for including the effects of motor noise in the model. This does not preclude the possibility of using motor noise as a parameter to obtain better correlation of model-operator power spectra if this becomes desirable. It will be concluded in the next section that the problems of developing a rational approach to including motor noise as an active model parameter are not warranted if one is only interested in the essential bandwidth and cutoff characteristics of the power spectral data. Thus the motor noise variance was fixed at the reference value of 1×10^{-6}.

At this point, all the model parameters have been discussed and fixed with the exception of the control weighting S. This parameter is the principal model parameter and its effect and the method of choosing it will now be discussed.

c. Control Weighting

The control weighting S is the primary parameter which is varied to match the model to the experimental data. To evaluate the effect of control weighting on model performance, the motor and observation noise variances were fixed at their reference values.

An initial trial of S = 0 indicated that the model output in no way matched human operator performance in any of the cases examined. With S = 0 the model performed the tracking task ideally in the sense that the NTEs were extremely low, the PSD of the plant output was an almost perfect reproduction of the PSD of the forcing function input, the PSD of the error signal was essentially zero, and the PSD of the control signal was the theoretical optimum. As an example of the controlled elements considered, the case for Y_c = K/s with S = 0 resulted in a NTE of 0.00084 (operator's NTE about 0.04) with PSD plots as shown in Figures 14 through 17. The error PSD is typical of the case when S = 0 for all of the controlled elements considered. By increasing the value of S from S = 0, the performance of the model is degraded and the error spectra and normalized tracking errors begin to match human operator performance.

The control weighting S is chosen to obtain a model-data match in the following manner. The value of S is varied in the digital simulation program to obtain a plot of NTE versus S for each controlled element. A value of S is chosen so the model value of NTE matches the mean value of NTE obtained experimentally at ω_B = 1.0 rad/sec. This value of S is fixed and the model simulation is repeated to predict NTE performance at the remaining bandwidth frequencies ω_B = 0.5, 1.5, and 2.0 rad/sec. PSD plots are obtained for each of these simulations for comparison with experimental PSD data.

Now that the procedures for fixing all of the system and model parameters have been described, the remainder of this section will be devoted to an analysis of the predicted and experimental NTE and PSD shapes.

2. EXPERIMENTAL RESULTS

The results of the experimental data runs will now be presented. The first data to be presented will be the NTE versus input forcing function bandwidth for both the compensatory and pursuit display situations.

a. Normalized Tracking Error

The results of the NTE data experiments for one subject are presented in Table III and IV and are representative of the data collected. The experimental mean and 1-sigma

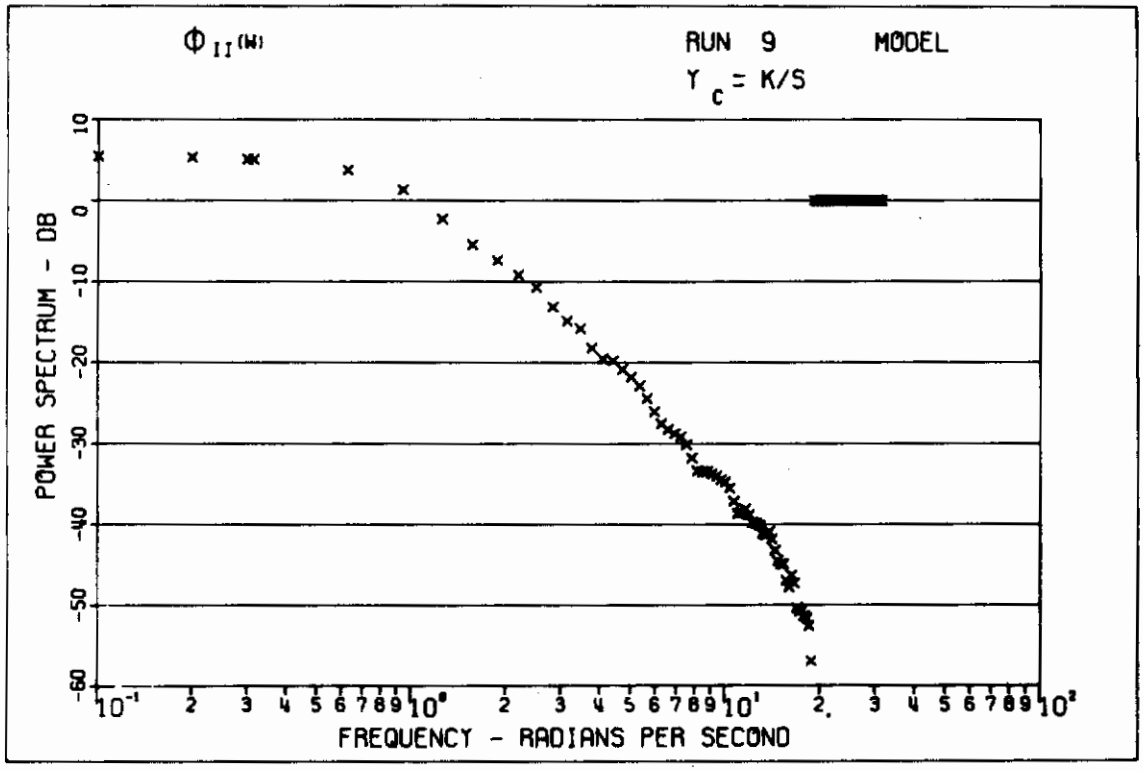

Figure 14. Input Power Spectral Density

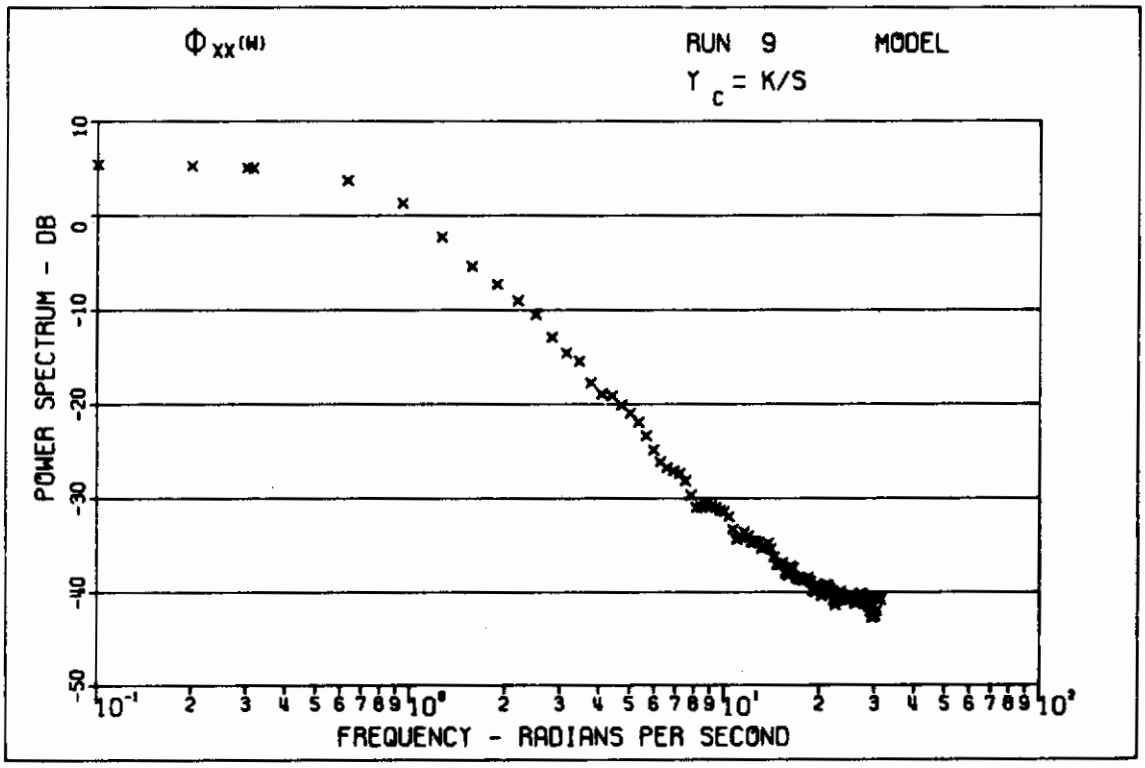

Figure 15. Output Power Spectral Density

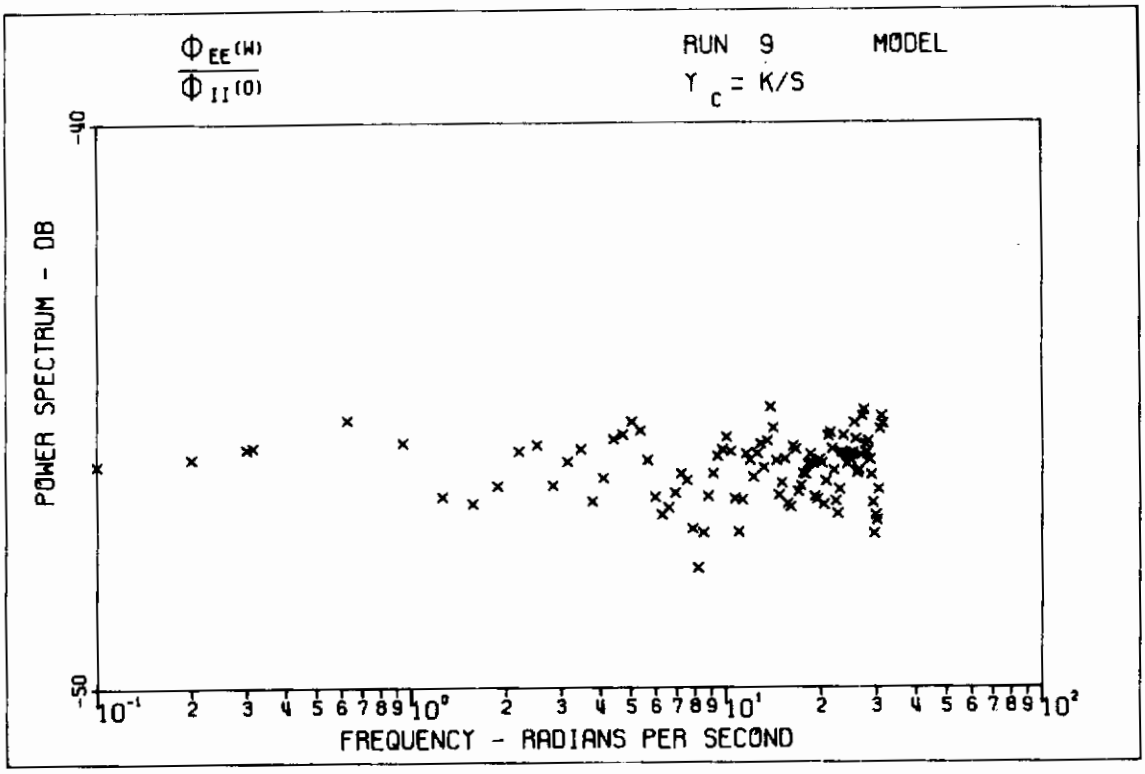

Figure 16. Error Power Spectral Density

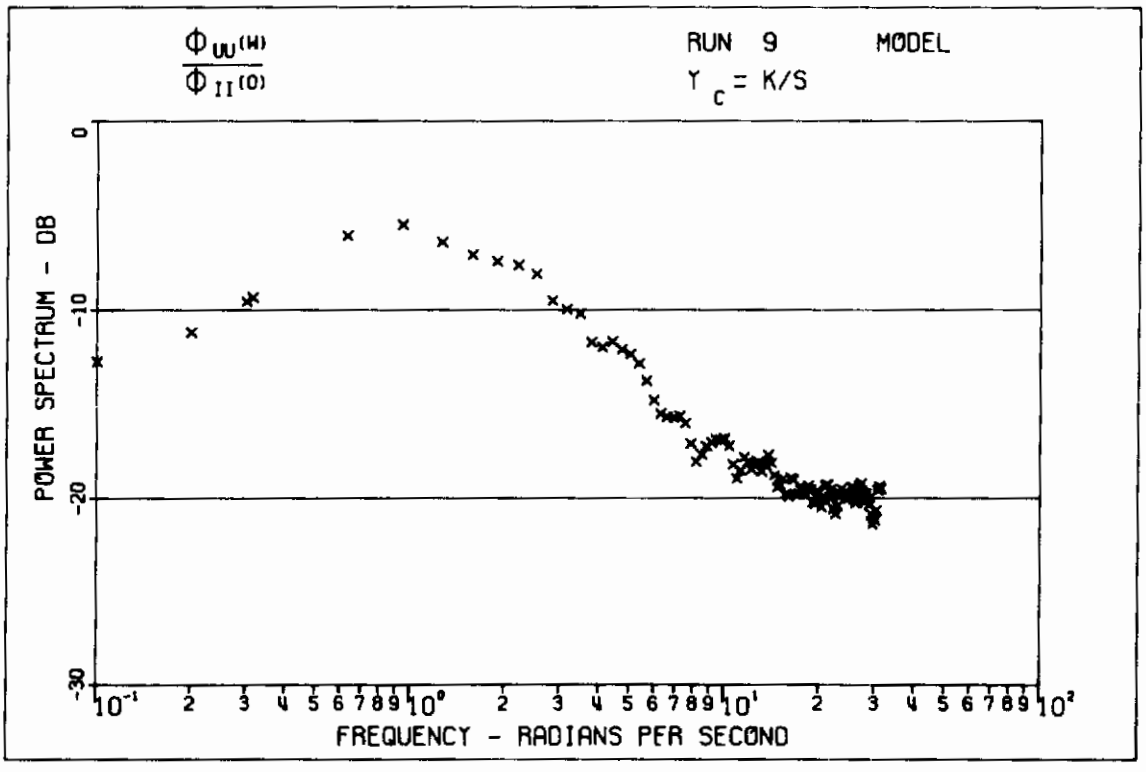

Figure 17. Control Power Spectral Density

TABLE III

EXPERIMENTAL NTE DATA

		Controlled Element							
		K/s		K/s+1		K/s−1		K/s^2	
	ω_B rad/sec	Mean	1 σ	Mean	1 σ	Mean	1 σ	Mean	1 σ
Pursuit	0.5	0.016	0	0.013	0	0.015	0	0.031	0.01
	1.0	0.042	0	0.038	0	0.047	0	0.11	0.022
	1.5	0.082	0.020	0.095	0.010	0.093	0.010	0.25	0.032
	2.0	0.15	0.024	0.16	0.014	0.17	0.010	0.33	0.030
Compensatory	0.5	0.014	0	0.019	0	0.025	0	0.030	0
	1.0	0.038	0	0.037	0	0.067	0.010	0.030	0.017
	1.5	0.096	0.010	0.11	0.020	0.13	0.010	0.38	0.014
	2.0	0.17	0.014	0.16	0.020	0.21	0.028	0.59	0.030

TABLE IV

EXPERIMENTAL VS MODEL NTE DATA

		Controlled Element							
		K/s		K/s+1		K/s-1		K/s^2	
	ω_B rad/sec	P	C	P	C	P	C	P	C
Experimental Data	0.5	0.016	0.014	0.013	0.019	0.015	0.025	0.031	0.030
	1.0	0.042	0.038	0.038	0.037	0.047	0.069	0.11	0.14
	1.5	0.082	0.096	0.095	0.11	0.093	0.13	0.25	0.38
	2.0	0.15	0.17	0.16	0.16	0.17	0.21	0.33	0.59
Model Prediction	0.5	0.006		0.016		0.020	0.033	0.019	0.027
	1.0	0.040		0.040		0.047	0.070	0.11	0.14
	1.5	0.102		0.081		0.091	0.13	0.25	0.31
	2.0	0.178		0.134		0.15	0.20	0.40	0.47
	S	0.200		0.112		0.125	0.170	0.030	0.050

P = Pursuit Tracking C = Compensatory Tracking

values of the NTE data as a function of forcing function bandwidth, controlled element, and type display are listed in Table III. The mean values of NTE are repeated in Table IV along with the corresponding values of NTE obtained from the model simulation. The value of the control weighting parameter S is also included in Table IV. The results in Table IV are presented graphically in Figures 18 through 21. These figures illustrate two items of interest. First, they show the comparison between pursuit and compensatory tracking performance (as measured by NTE data) for each of the controlled elements considered. Figures 18 and 21 show that, for K/s-1 and K/s^2 controlled elements, the pursuit tracking performance is increasingly better than compensatory as ω_B increases. These results agree with those obtained by Wasicko, et al (Reference 33:44). Figure 19 indicates essentially no difference in pursuit and compensatory performance for the K/s+1 controlled element and for the K/s plant. Figure 20 indicates slightly better compensatory performance at low bandwidth inputs and slightly better pursuit performance at higher bandwidth inputs. Wasicko (Reference 33:44) found compensatory performance for the K/s plant to be slightly better than the pursuit at both low and high bandwidth inputs with essentially no difference for moderate bandwidth inputs. Reid (Reference 29:24), however, found no significant difference between compensatory and pursuit NTE scores for the K/s controlled element. With respect to the data for K/s^2 and K/s-1 controlled elements, the differences for K/s plant dynamics between pursuit and compensatory are small enough to consider, as Reid does, that there is no significant difference between pursuit and compensatory tracking performance. There is no comparative data in the literature for the K/s+1 controlled element. The data presented here supports the conclusion of Wasicko (Reference 33:46) that, in general, the NTE performance improvement with a pursuit display is largest for the more difficult controlled elements and inputs.

The second item of interest in Figures 18 through 21, is the comparison between measured and predicted values of NTE. As mentioned earlier, the predicted values of NTE are obtained by first choosing the control weighting S so the model NTE matches the experimental NTE at a forcing function bandwidth of $\omega_B = 1.0$ rad/sec. Then with all the model parameters fixed, the system parameter ω_B is varied to obtain model NTE predictions at values of $\omega_B = 0.5$, 1.5, and 2.0 rad/sec. These data points are plotted and joined by a smooth curve in the figures. In the K/s-1 and K/s^2 cases, where the compensatory performance differed significantly from the pursuit, a model match was accomplished separately for each display condition. Note that the model does not distinguish between pursuit and compensatory tracking. All that is varied in the model, regardless of the display situation, is the value of the control weighting S.

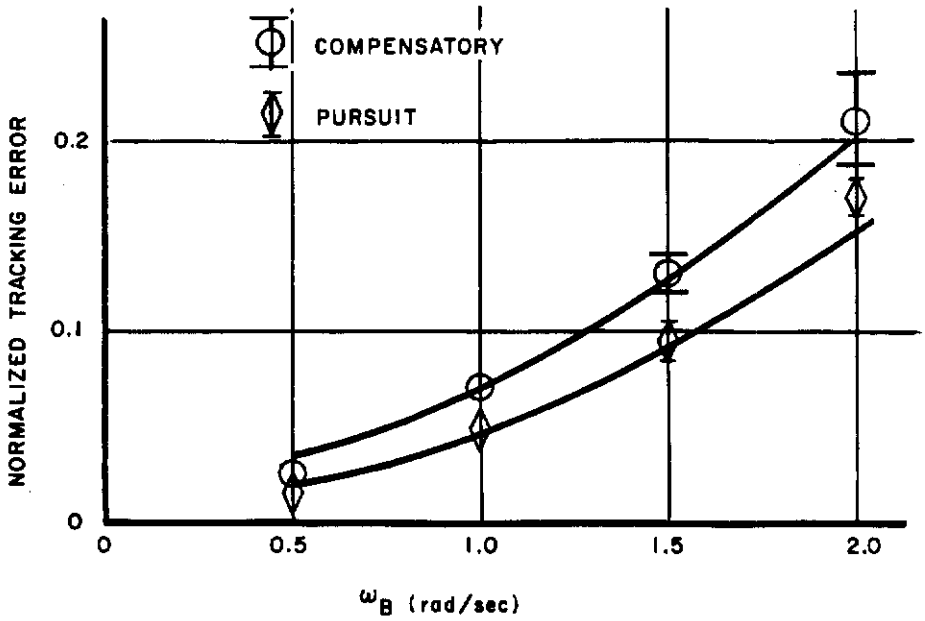

Figure 18. NTE vs ω_B Y_C = K/s-1

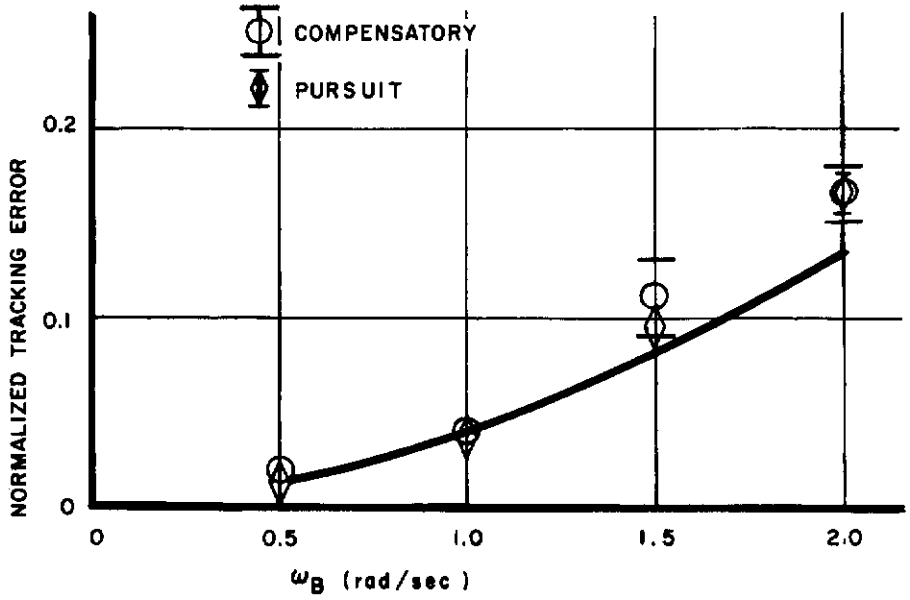

Figure 19. NTE vs ω_B Y_C = K/s+1

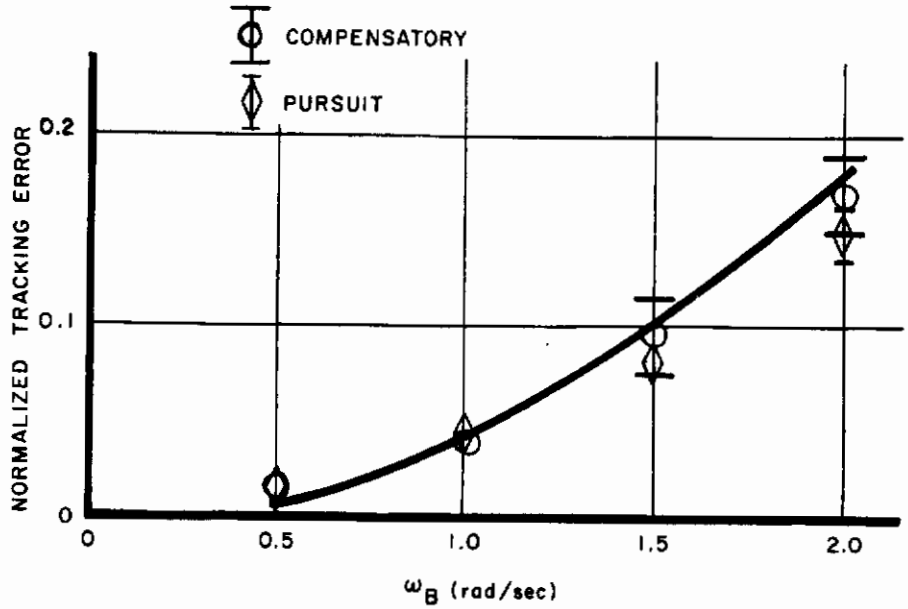

Figure 20. NTE vs ω_B Y_C = K/s

Figures 18 through 20 show the results for the first-order controlled elements. The experimental mean values of NTE for these cases generally conform to the predicted values with deviations above and below as shown. At most of the data points, the ±1-sigma range of experimental NTE include the predicted value. For the second-order controlled element (Figure 21), the experimental NTE is greater than predicted for the compensatory situation at ω_B = 1.5 and 2.0 rad/sec. The trend towards higher than predicted NTE in the compenastory case is predictable on the basis of compensatory tracking data collected by McRuer (Reference 19). McRuer found that, in general, the operator remnant increases with task difficulty, and for a given controlled element, task difficulty increases as ω_B increases. Since remnant is associated with the control output not correlated with the desired input, it is expected that NTE will increase as remnant increases. Thus as remnant increases, the human operator characteristics depart from the linear model and hence the actual NTE is higher than that predicted. For the pursuit situation at ω_B = 2.0 rad/sec, the operator NTE is lower than predicted. As mentioned earlier, this behavior might be attributed to a decrease in effective time delay as noted by McRuer (Reference 19). It should be noted that no attempt was made to compute describing functions for the experiments conducted, and hence there were no quantitative measures of remnant or effective time delay to support the above discussion. Some qualitative measure of remnant can be made from the PSD plots and this will be done in the next subsection.

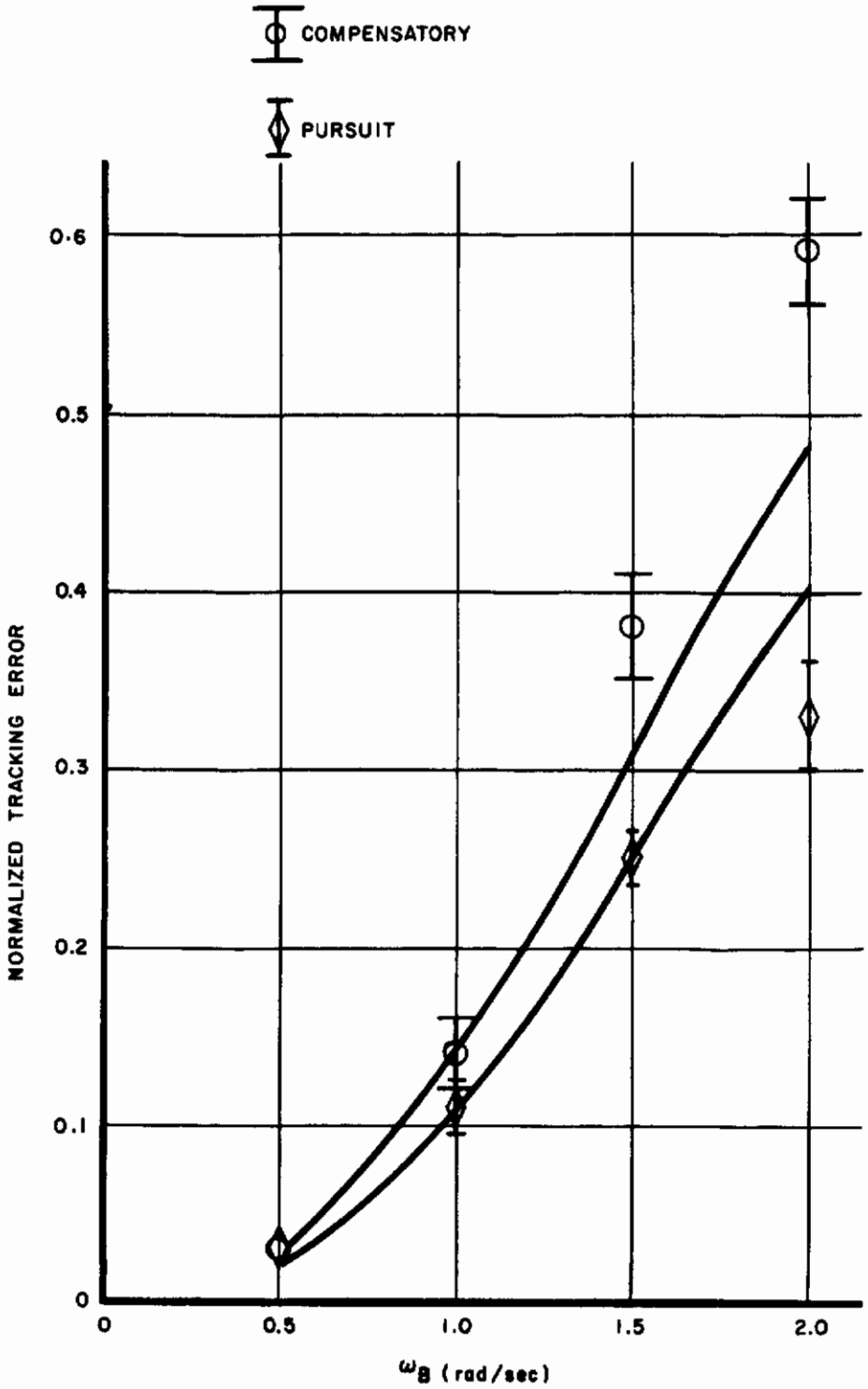

Figure 21. NTE vs $\omega_B Y_C = K/s^2$

Thus although there are some departures of the actual from the predicted values of NTE in Figures 18 through 21, they all have plausible explanations, and, consequently, the predictions are close enough to warrant their use in evaluating the effects of input bandwidth changes on a given controlled element-display situation.

b. Power Spectral Densities

Experimental and model power spectral densities were computed and plotted for the following tracking loop signals

1. System forcing function $i(t)$
2. System output $x(t)$
3. System error $e(t) = i(t) - x(t)$
4. Control signal $u(t)$

Power spectra were computed using a modification to the computation routine described by Bendat (Reference 4). This modification is discussed in Appendix III. The data reduction was done on an IBM 7094 digital computer. The analog data tape recorded during the experimental data runs was digitized at a rate of 417 samples/second/channel for use on the IBM 7094. This sampling rate is well within the minimum required to recover the highest frequency of interest in the data. With the highest frequency of interest taken to be 30 rad/sec, a minimum sampling rate of 9.06 samples/sec is required in accordance with Shannon's sampling theorem (Reference 28:17). The sampling rate in the model is 10 samples/second and the digitized experimental data was sampled at 13.9 samples/second for PSD calculations.

Since the error spectrum characterizes the desired input-output data match and can be interpreted more readily than individual input and output spectra, the input and output spectra will not be presented. Instead, the normalized error and control PSD data will be used to compare model and experimental results and characterized system and operator performance. As mentioned earlier, the normalization $\phi_{ii}(0)$ in the PSD plots is really $\phi_{ii}(0.1 \text{ rad/sec})$ and is an approximation to $\phi_{ii}(0)$. The model and experimental results are plotted simultaneously for comparison purposes. The results will be grouped first by the type of display, second by the type of controlled element, and finally by forcing function bandwidth.

c. Pursuit Display

The first PSD data to be presented are the results for the K/s controlled element, a pursuit display, and ω_B = 1.0 rad/sec. The PSD data for each of the four subjects are presented (Figures 22 through 25) to show the range of operator-to-operator variability. The model PSD data for each operator was generated using the value of S which resulted in the NTE match for that operator. This was done in lieu of matching the average value of NTE across operators because individual variances from the optimum are of interest. In every instance, the operator error PSD is consistently above the model PSD at the higher frequencies (> 1.0 rad/sec). This is to be expected, as an analysis of the control PSD shows that the operator consistently has more control power than the model across the frequency spectrum, particularly in the 2-10 rad/sec frequency range. This excess of control power (over the model) can be explained by realizing that the operator does not operate in a perfectly optimum manner. Extensive quasi-linear modeling data (References 19 and 33) have shown that there is definitely a portion of the operator's control output which is not linearly correlated with the input and can be considered as an additive white noise to the operator's output. This would explain an excess of control power across the frequency range. The emphasized excess of control power in the 2-10 rad/sec range has been observed by Smith (Reference 32) and McRuer (Reference 19). They have concluded that this peaking at the high frequency end of the spectrum is not due to nonlinear or periodic behavior by the operator but is most likely caused by the neuromuscular system. The intraoperator control spectra do show some variability in the extent of this high frequency excess which could be attributed to the variability of the individual characteristics of each operator's neuromuscular system. Finally, note that, although there is some variability between operators, all operator output spectra have essentially the same bandwidth and cutoff characteristics and they match the model output with the exception of the excess in control power mentioned above. Since this is the case, the remaining PSD data will not be shown on an individual basis, but rather will be the results of the most experienced of the four operators.

The remaining pursuit display data are shown in Figures 26 through 40. For each controlled element there are PSD plots of normalized error and control at values of ω_B = 0.5, 1.0, 1.5, and 2.0 rad/sec. The value of S for each controlled element is determined by the model-data NTE match at ω_B = 1.0 rad/sec and is then held constant for prediction of NTE and PSD data at the remaining values of ω_B. As would be expected, the characteristics of the error PSD do not vary with controlled element bandwidth, but the control PSD characteristics do.

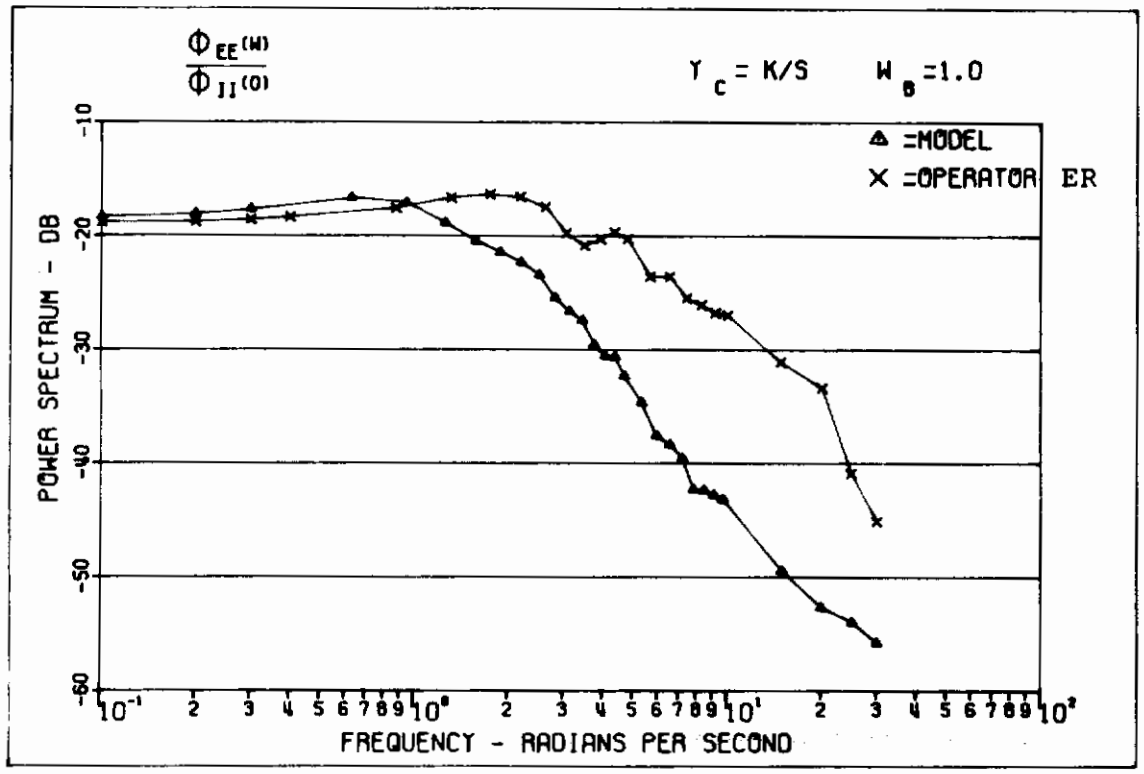

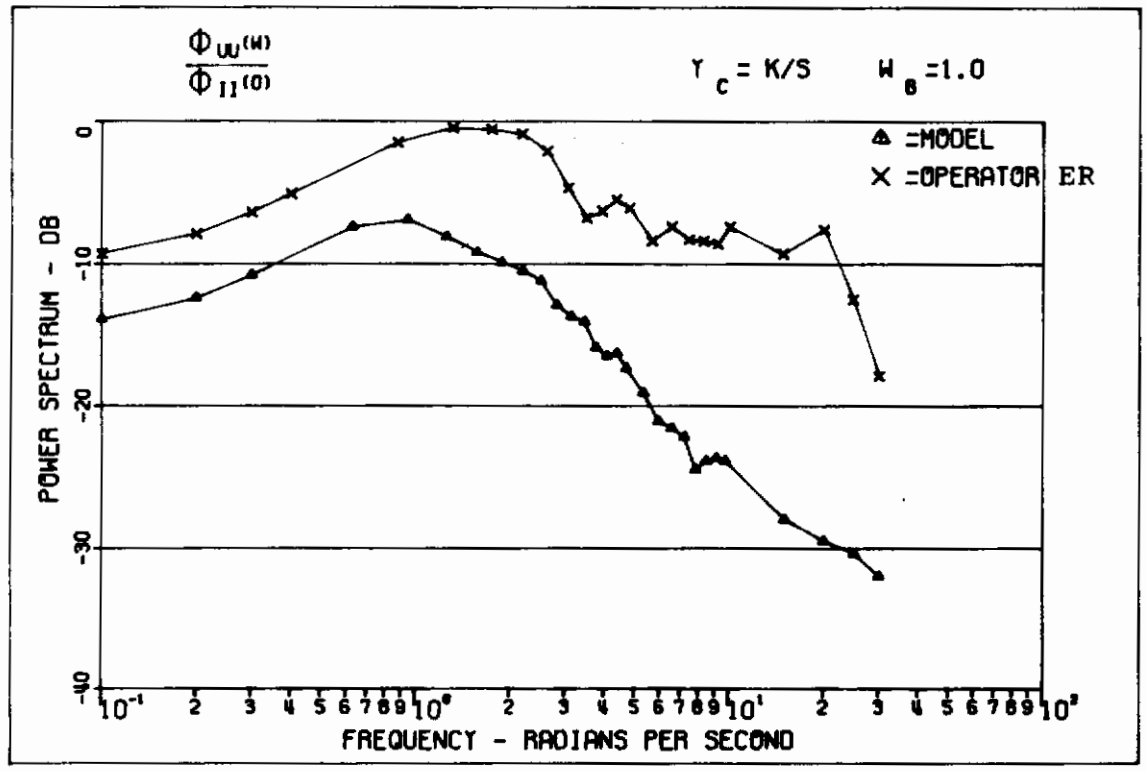

Figure 22. Power Spectral Densities Y_C = K/s Pursuit

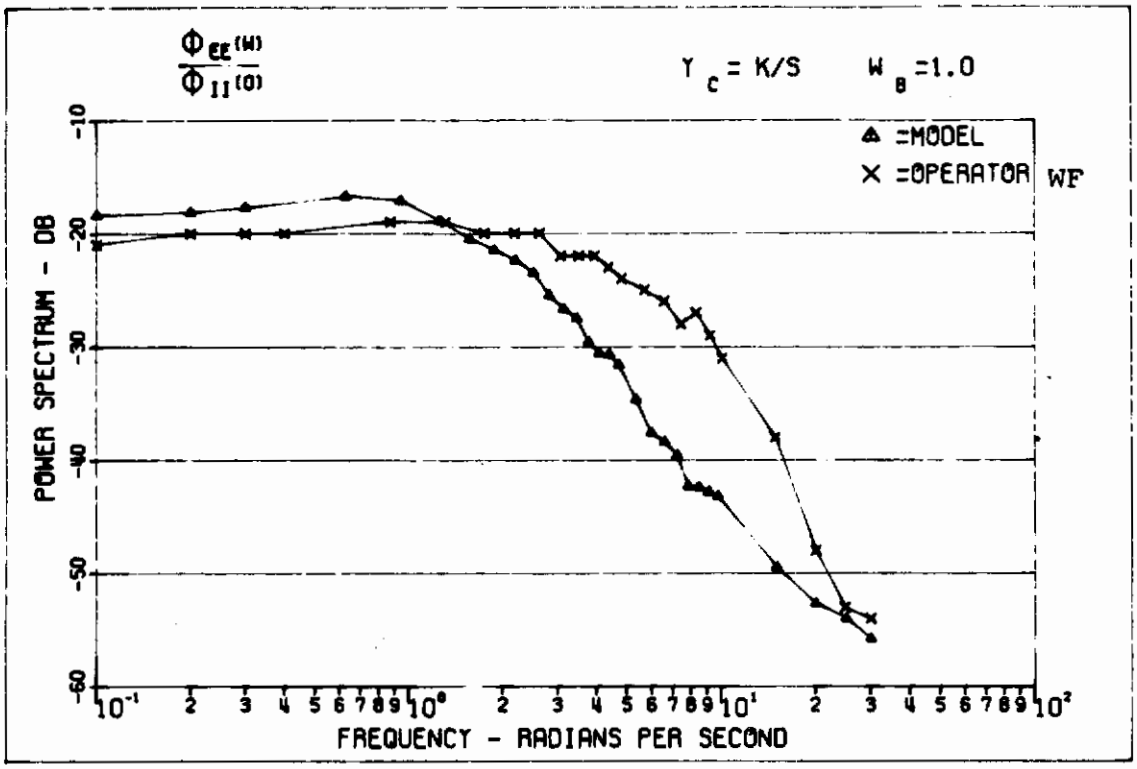

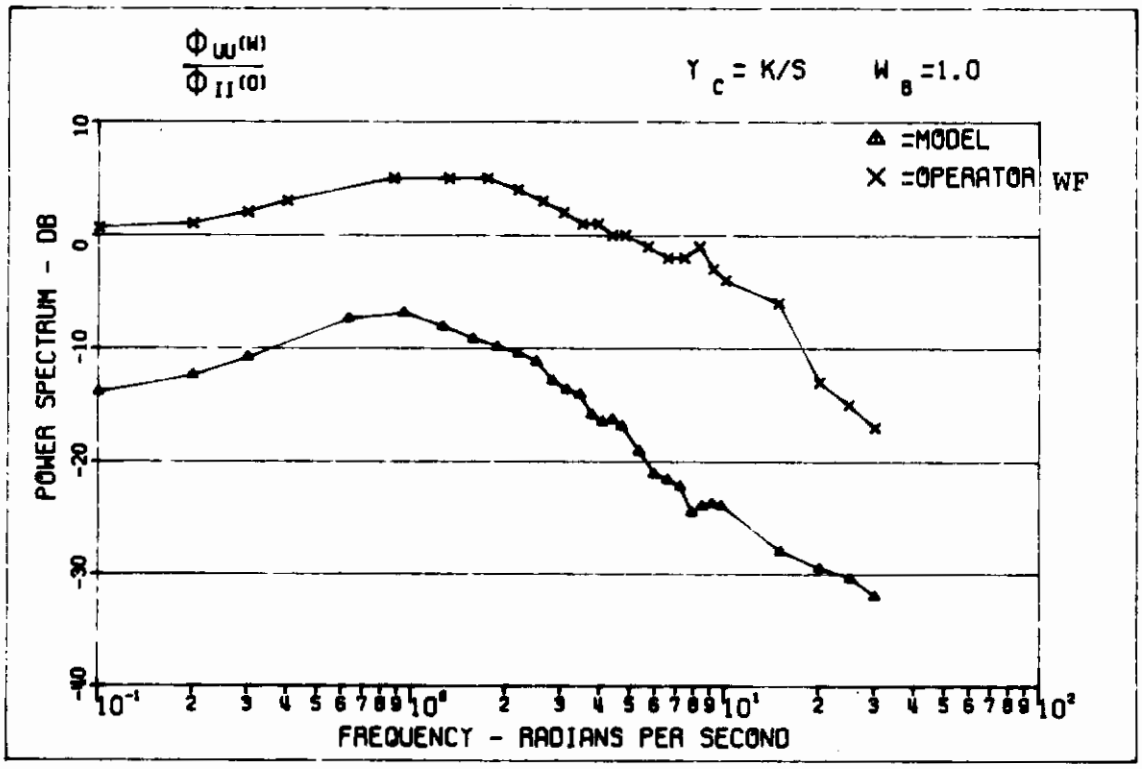

Figure 23. Power Spectral Densities Y_C = K/s Pursuit

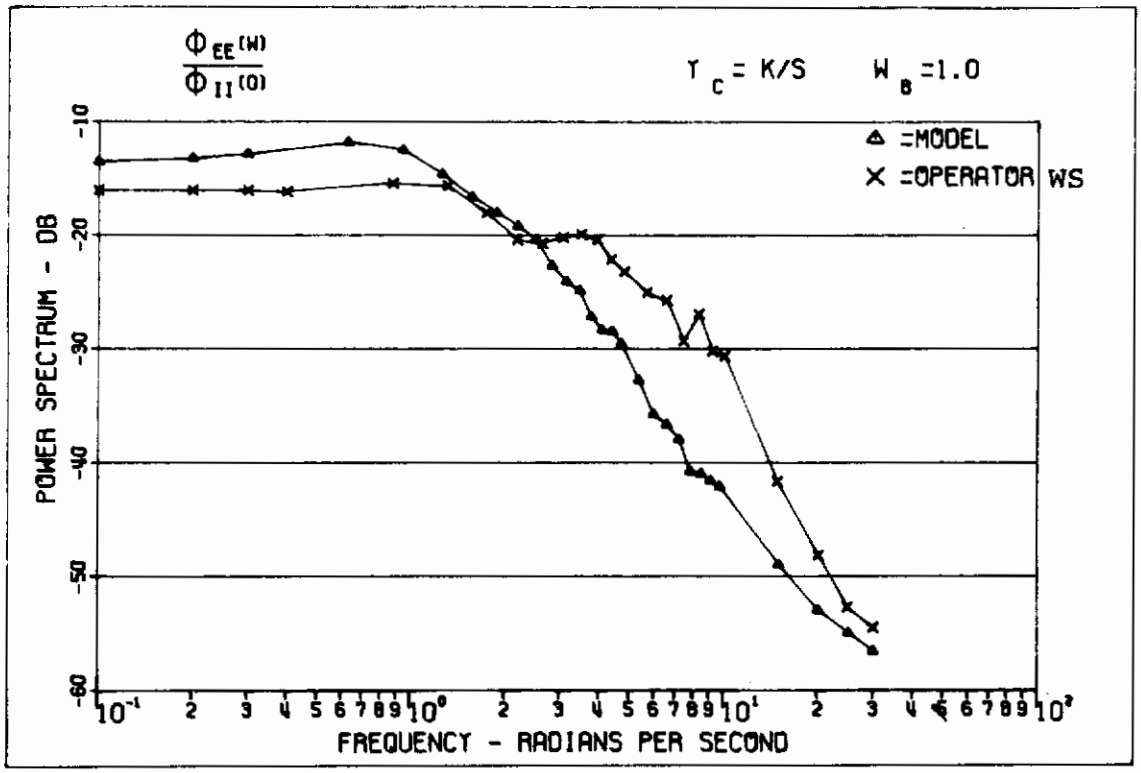

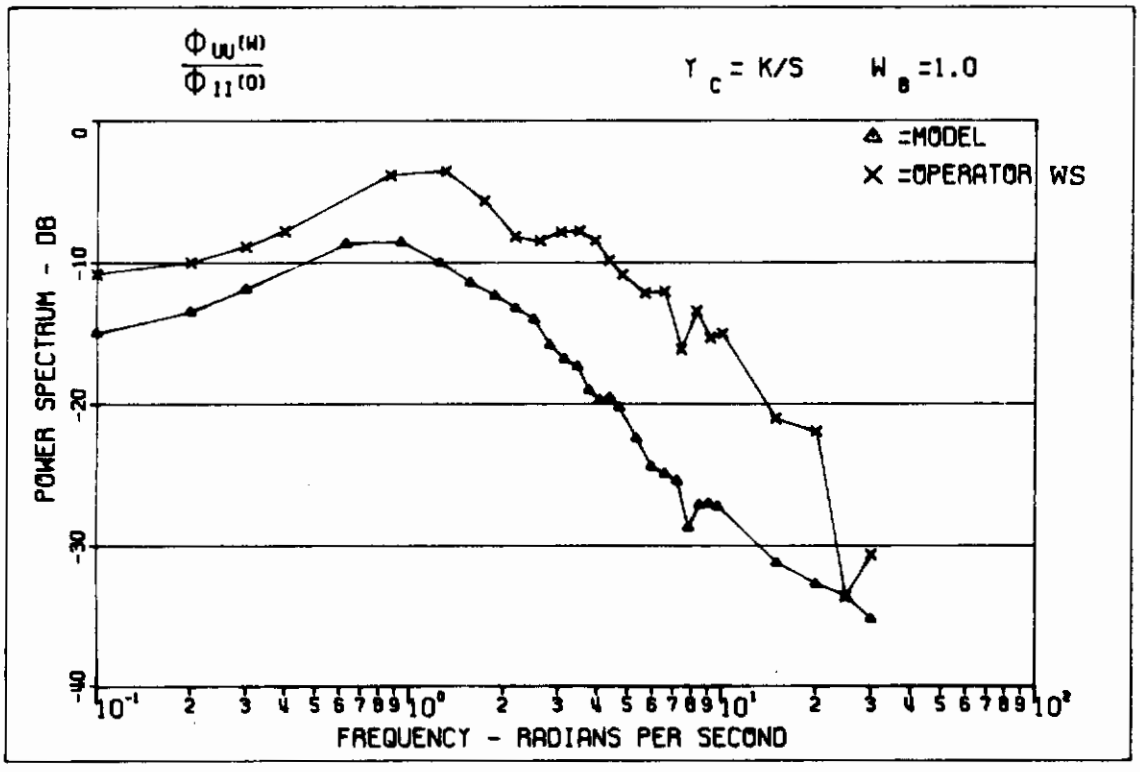

Figure 24. Power Spectral Densities Y_C = K/s Pursuit

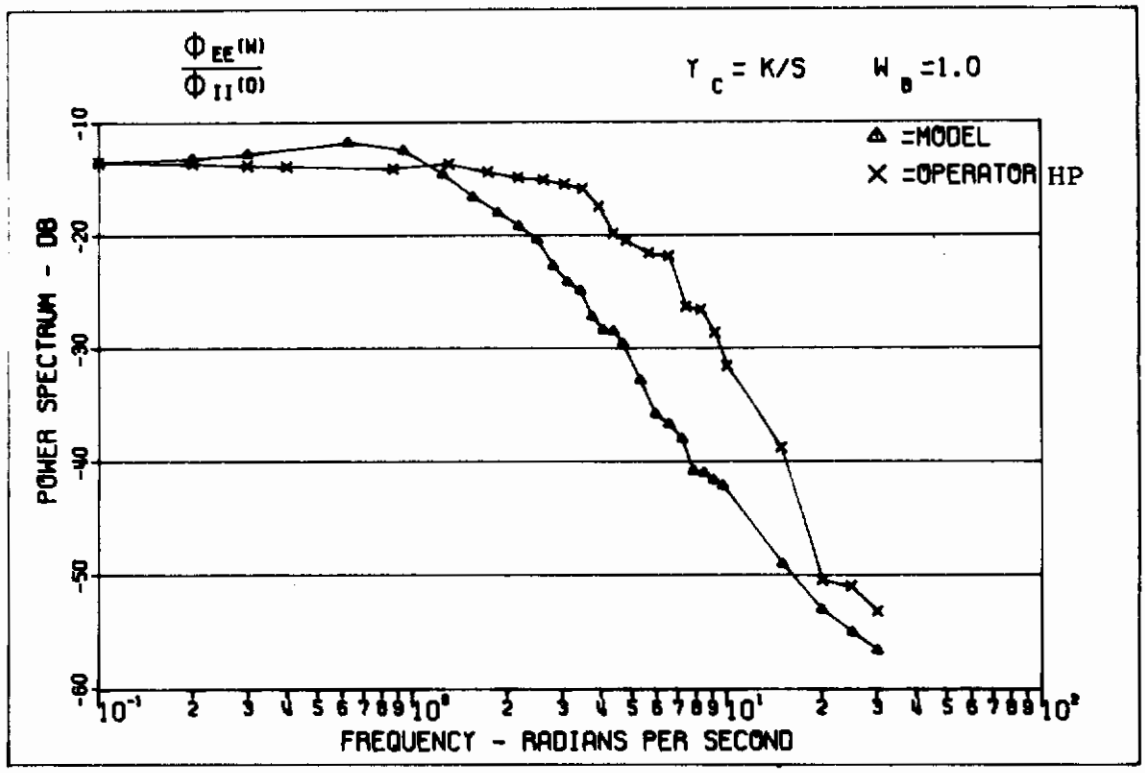

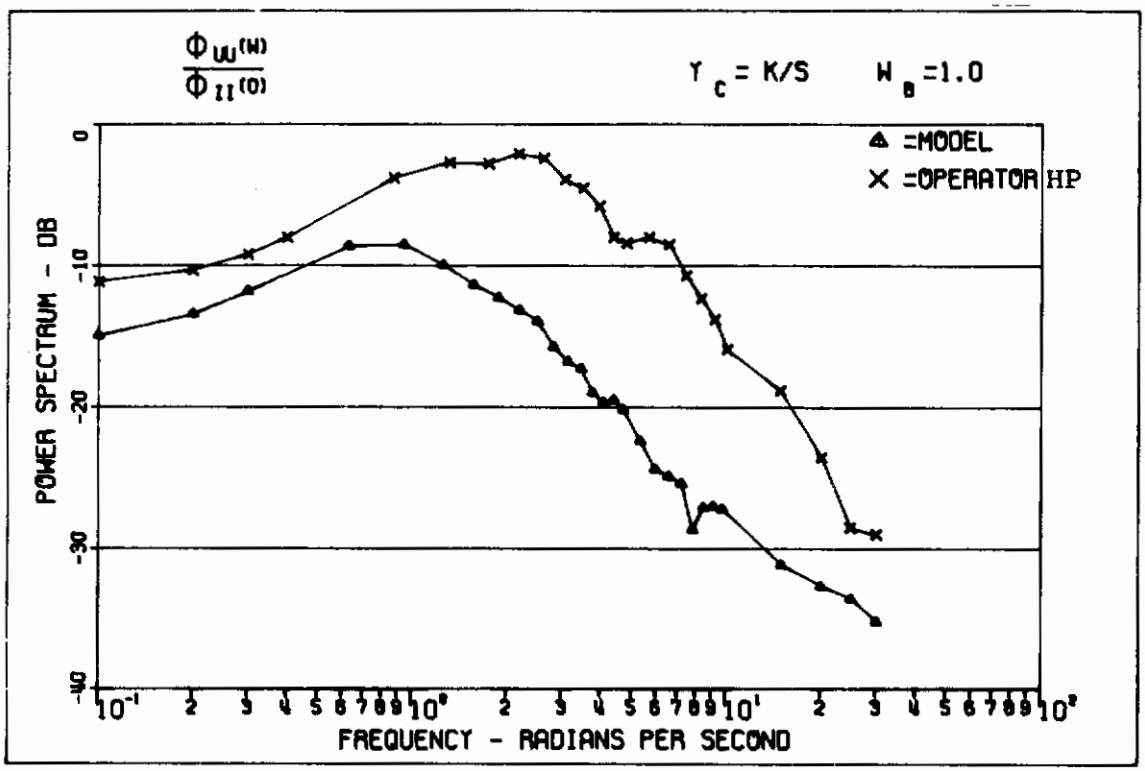

Figure 25. Power Spectral Densities Y_C = K/s Pursuit

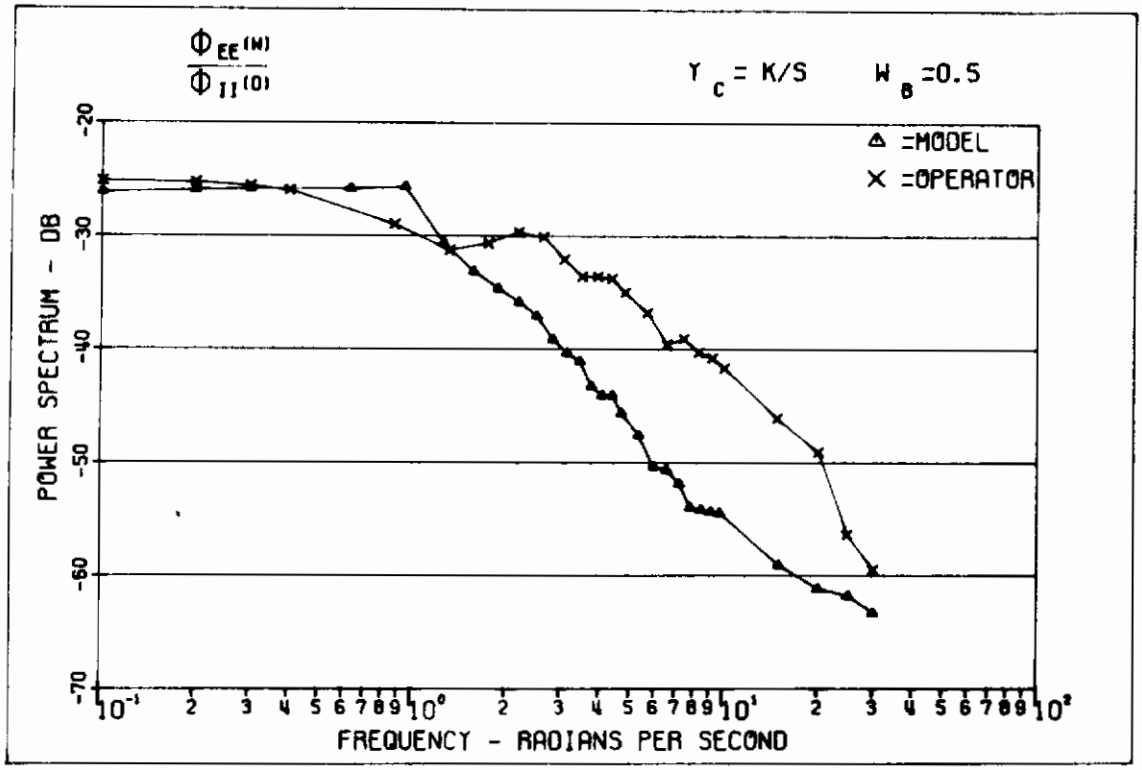

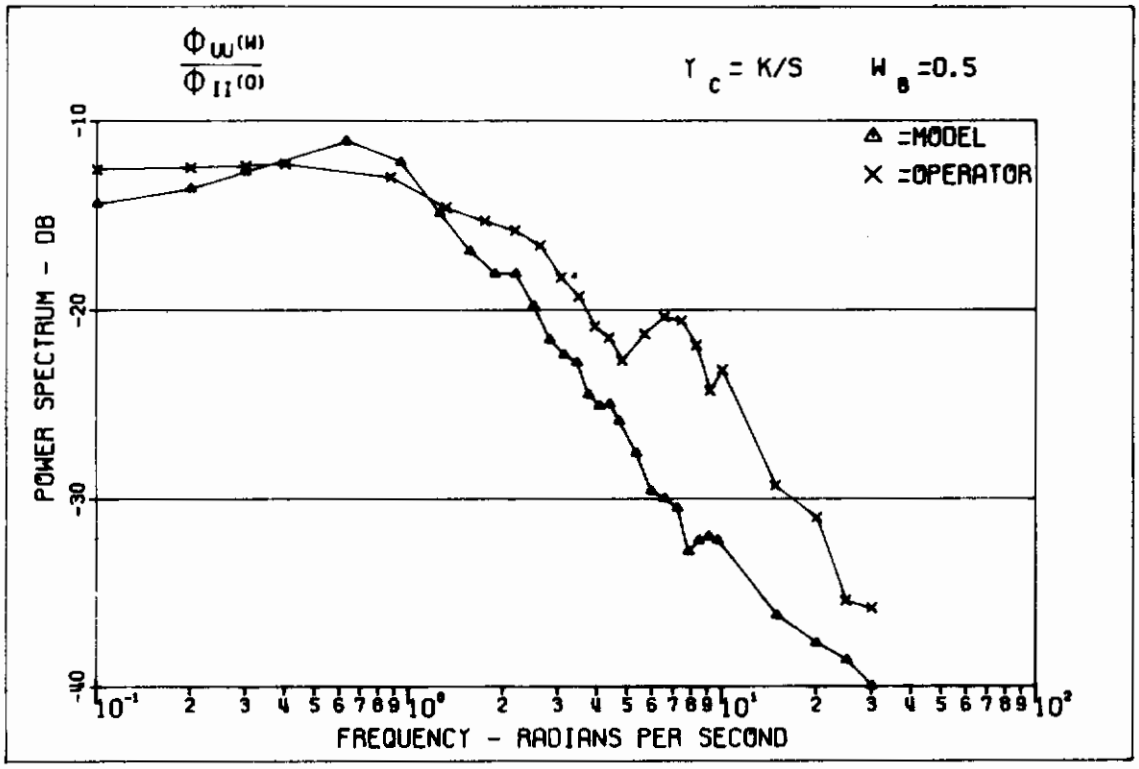

Figure 26. Power Spectral Densities Y_C = K/s Pursuit

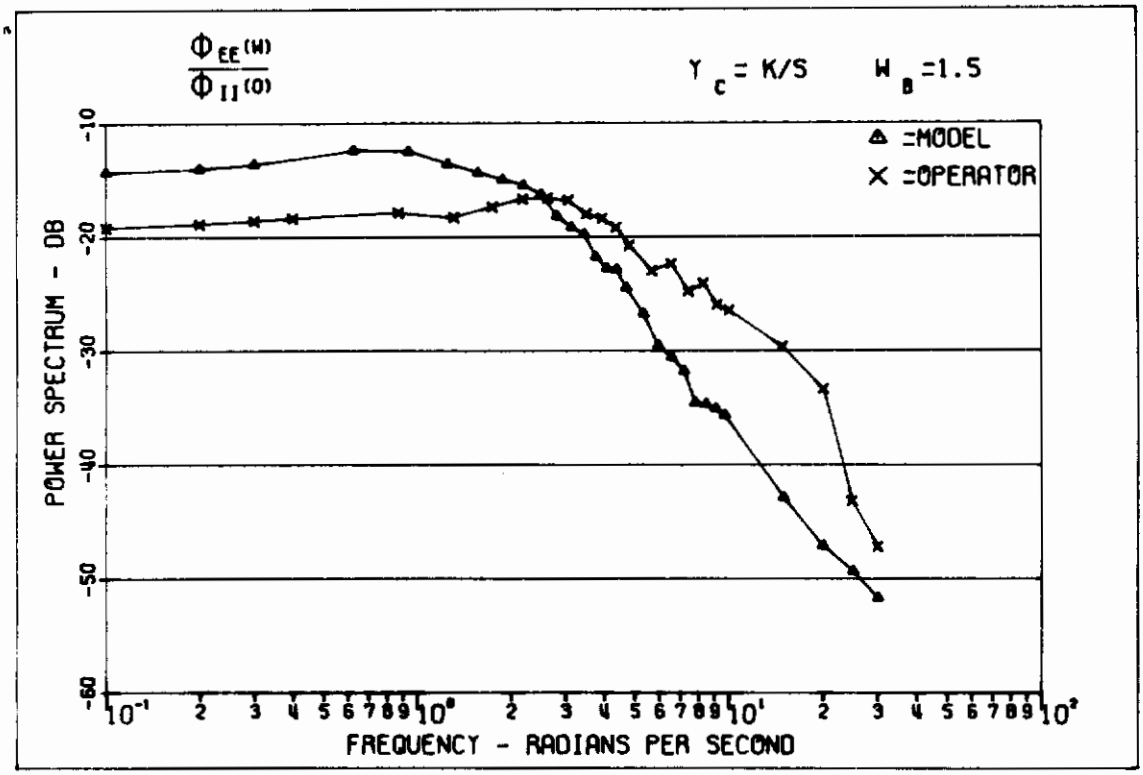

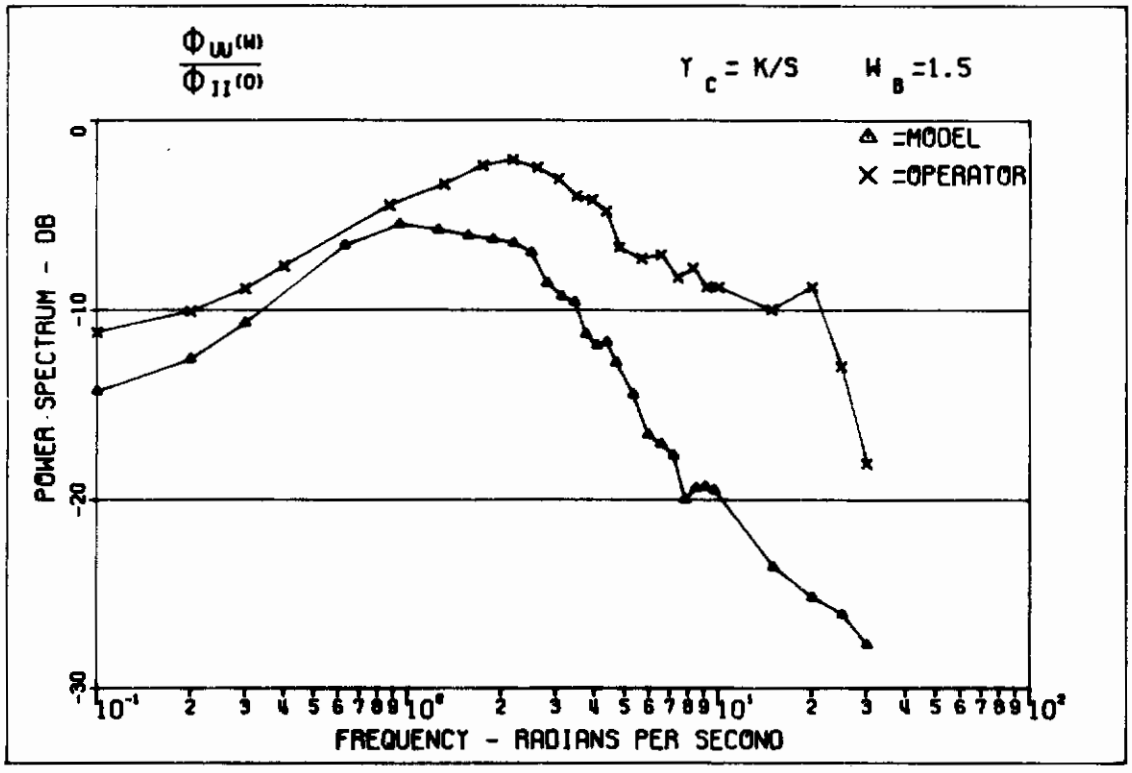

Figure 27. Power Spectral Densities Y_C = K/s Pursuit

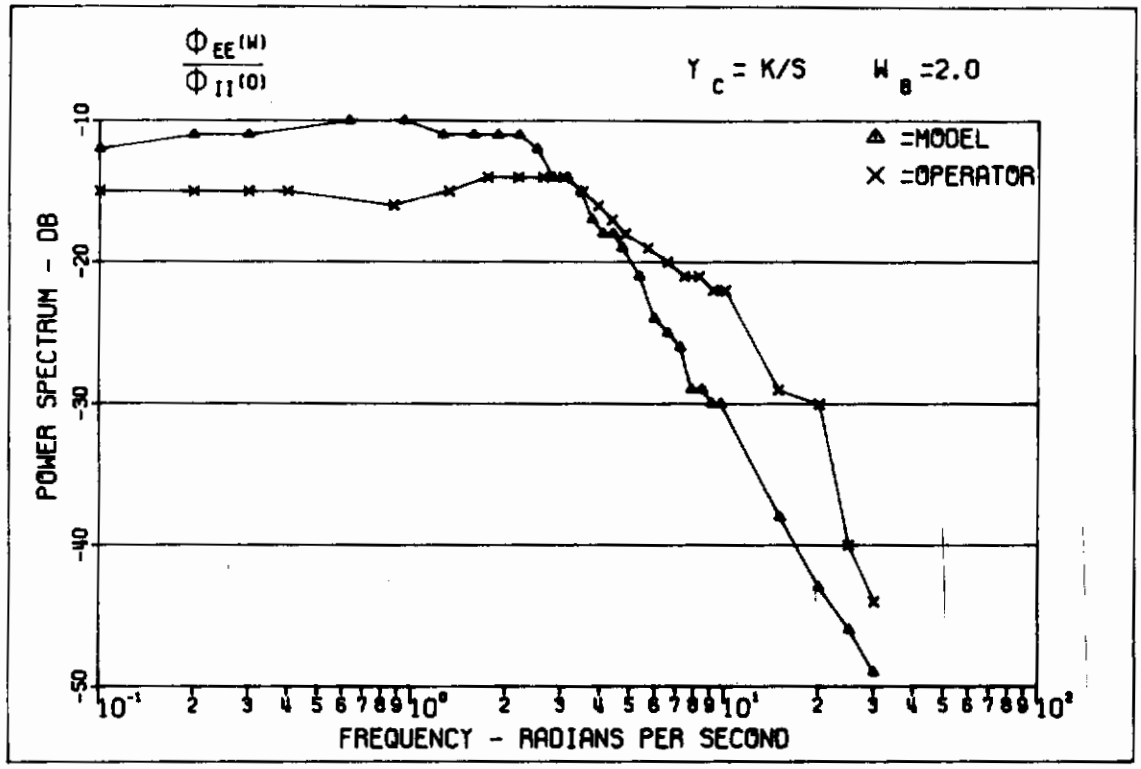

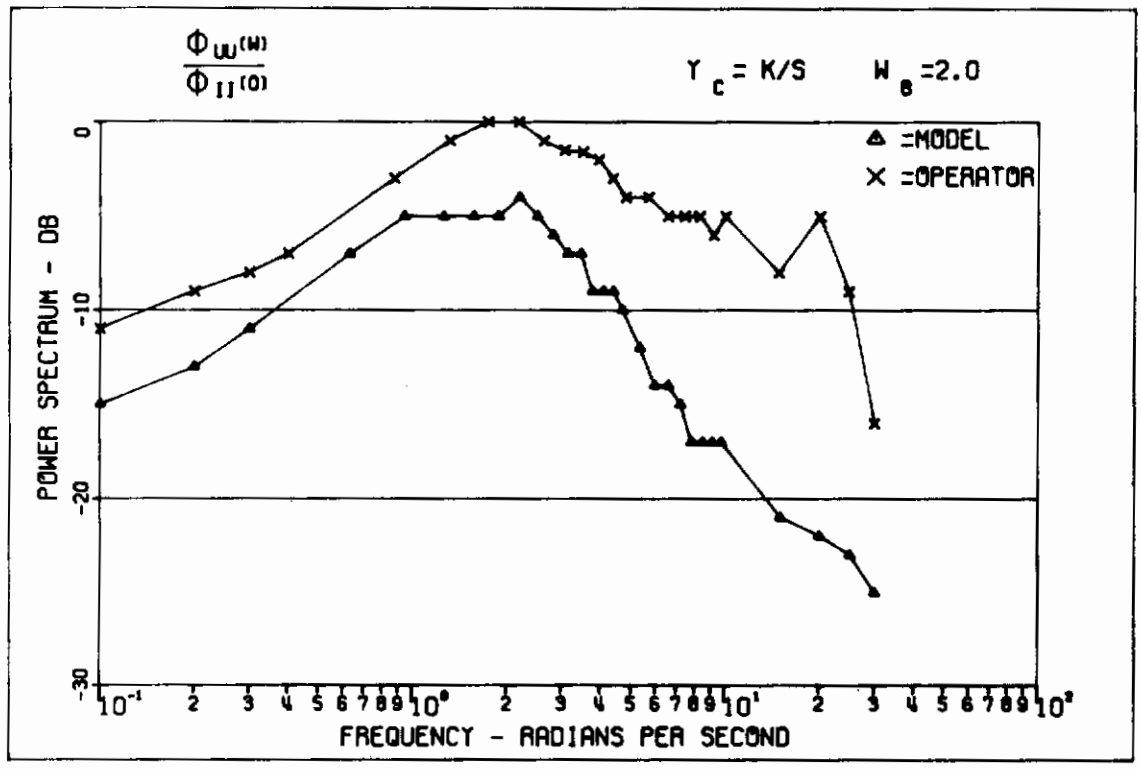

Figure 28. Power Spectral Densities Y_C = K/s Pursuit

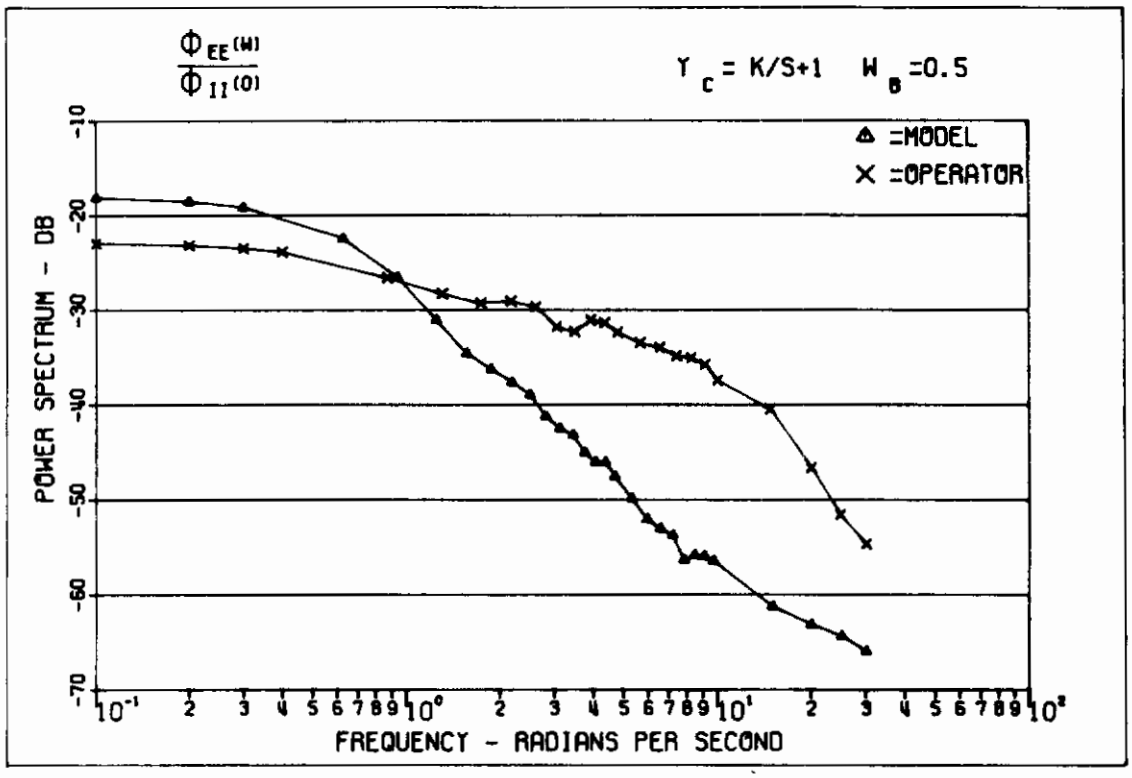

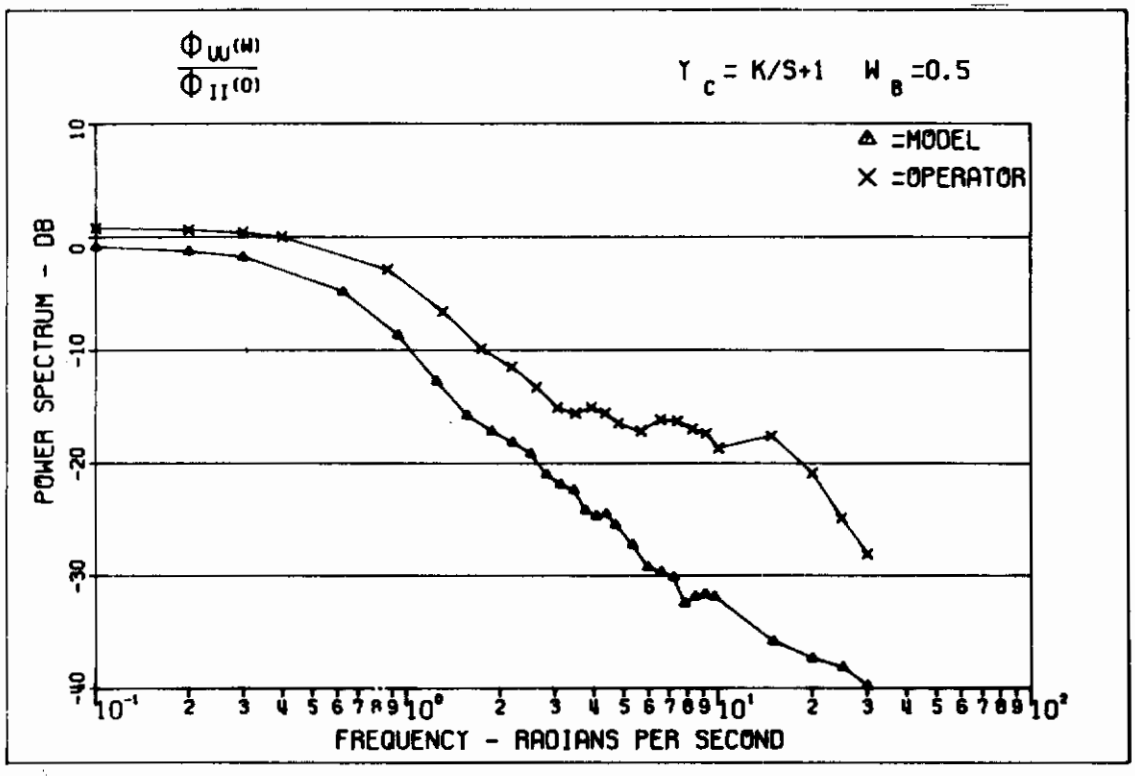

Figure 29. Power Spectral Densities Y_C = K/s+1 Pursuit

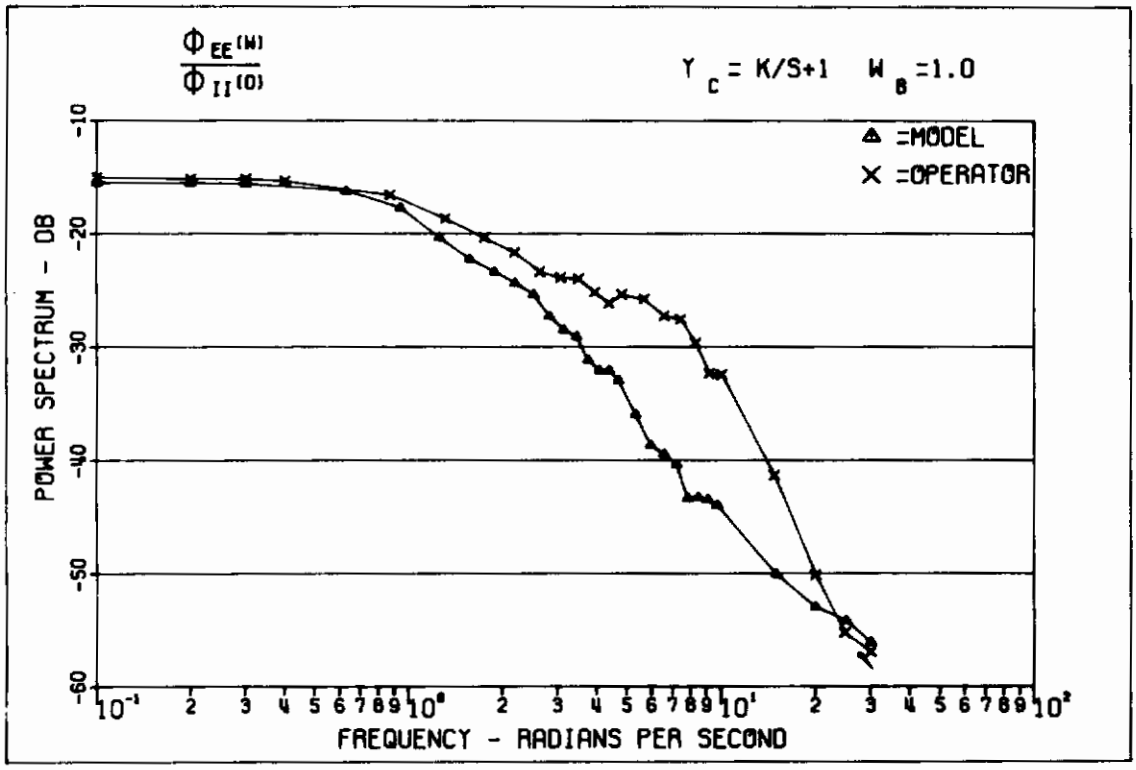

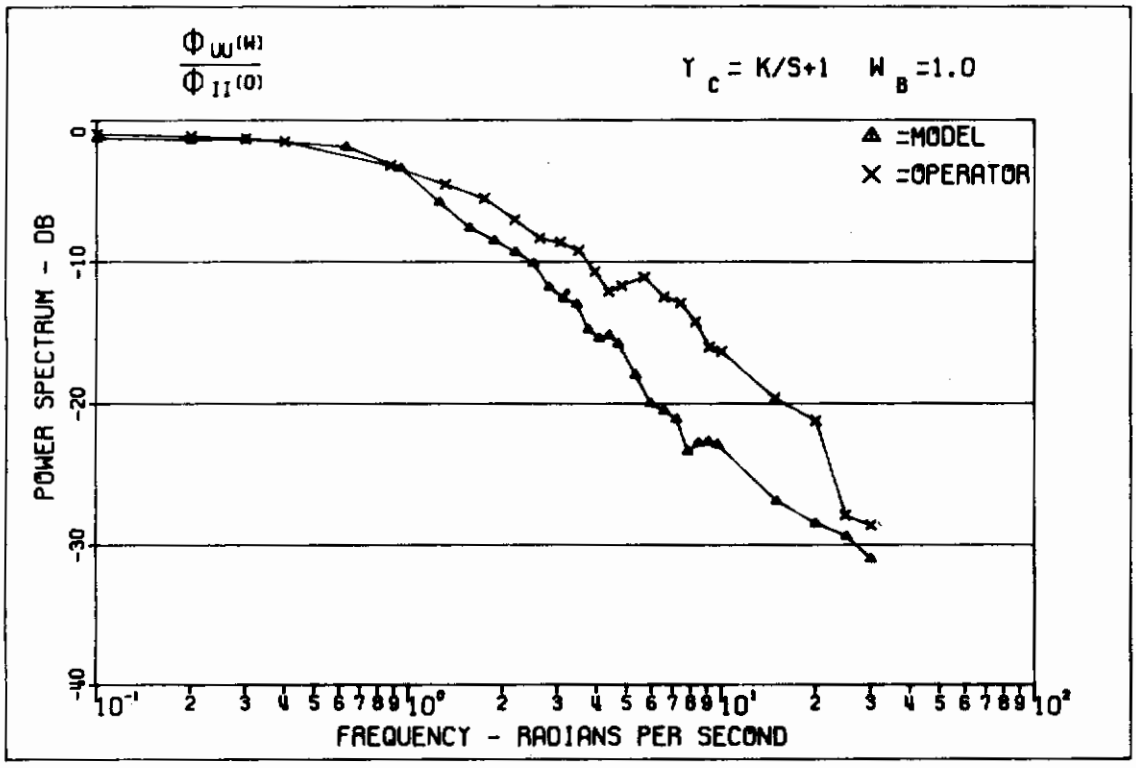

Figure 30. Power Spectral Densities Y_C = K/s+1 Pursuit

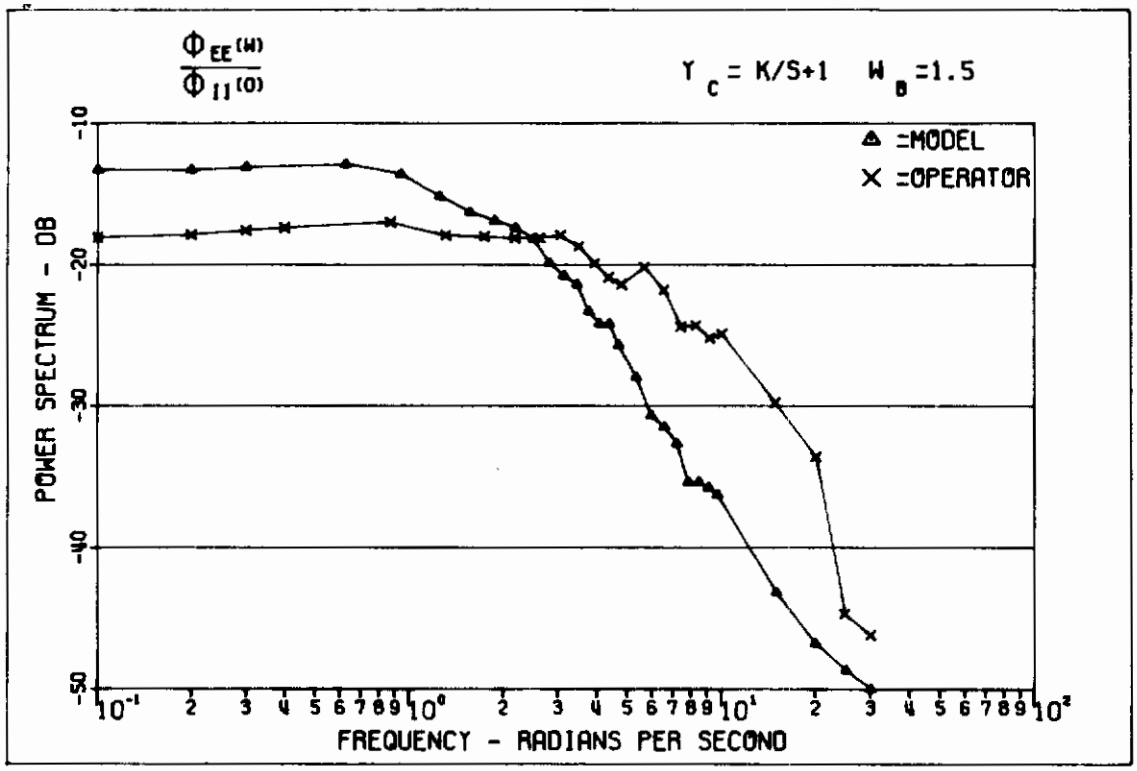

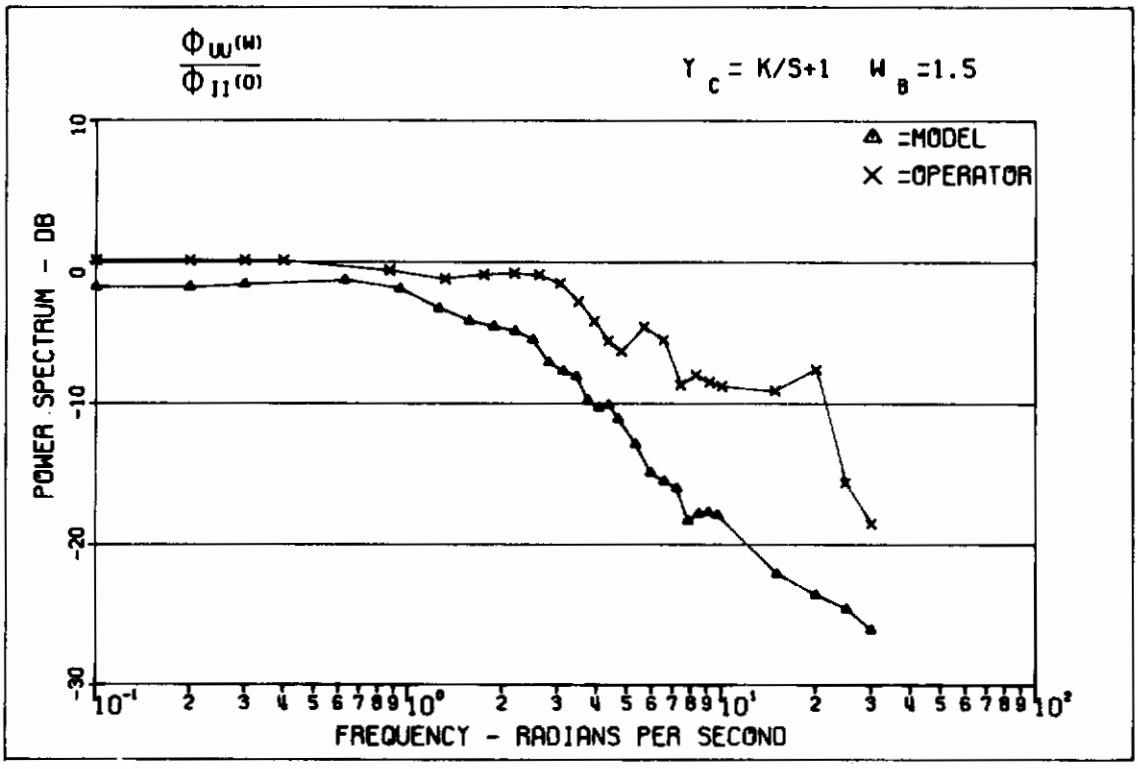

Figure 31. Power Spectral Densities Y_C = K/s+1 Pursuit

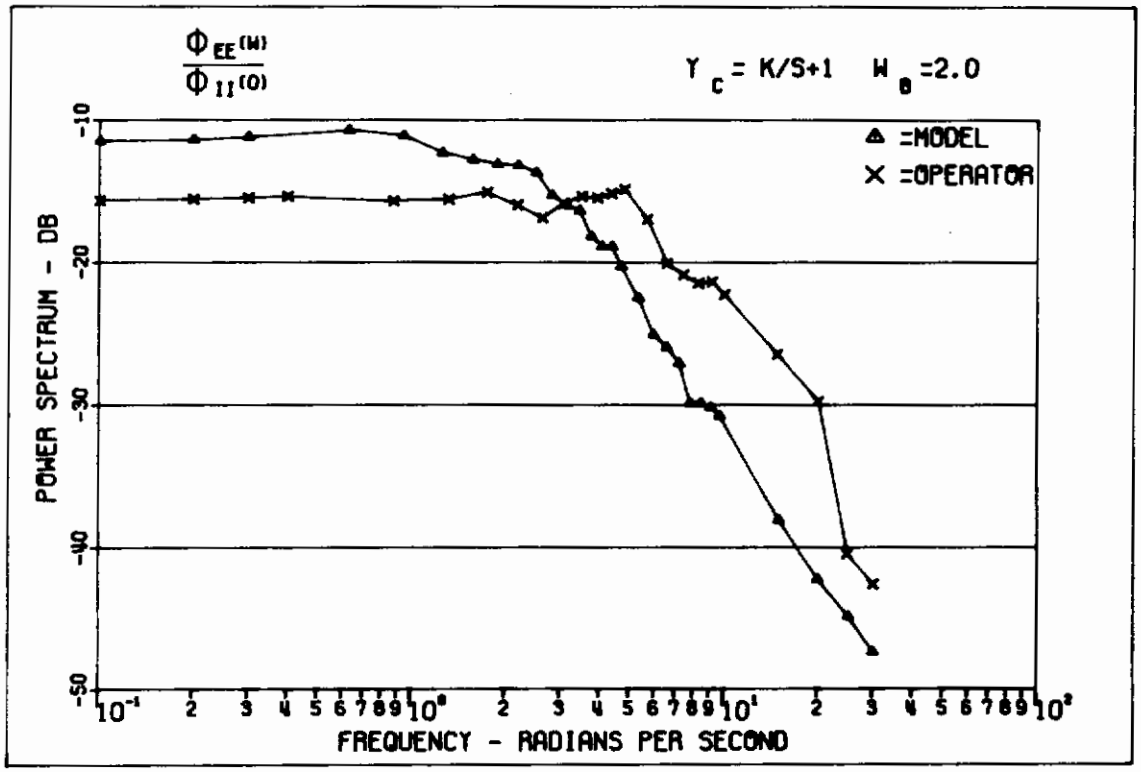

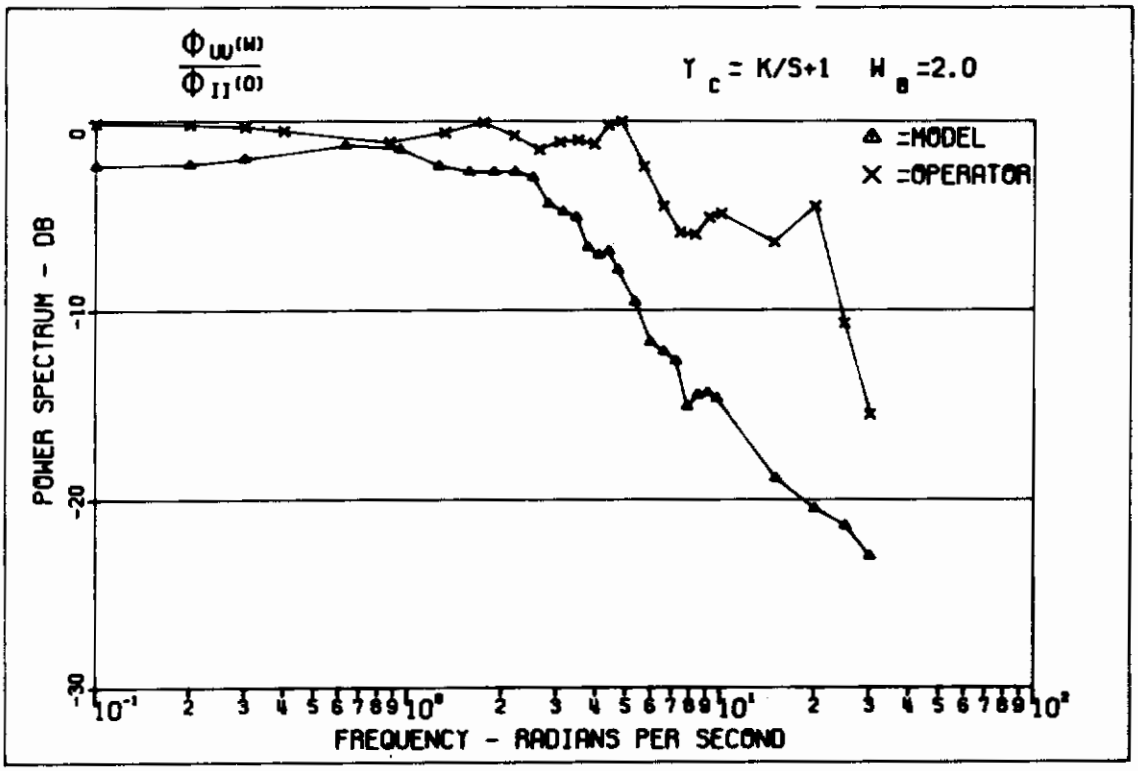

Figure 32. Power Spectral Densities Y_C = K/s+1 Pursuit

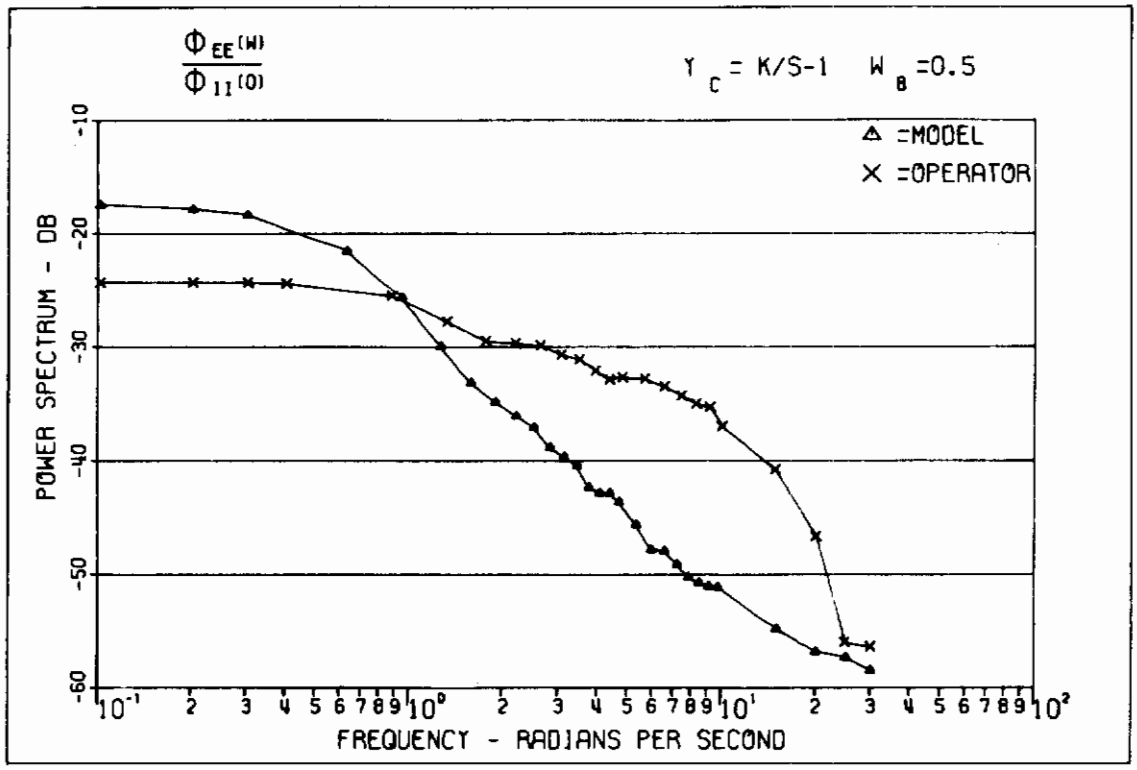

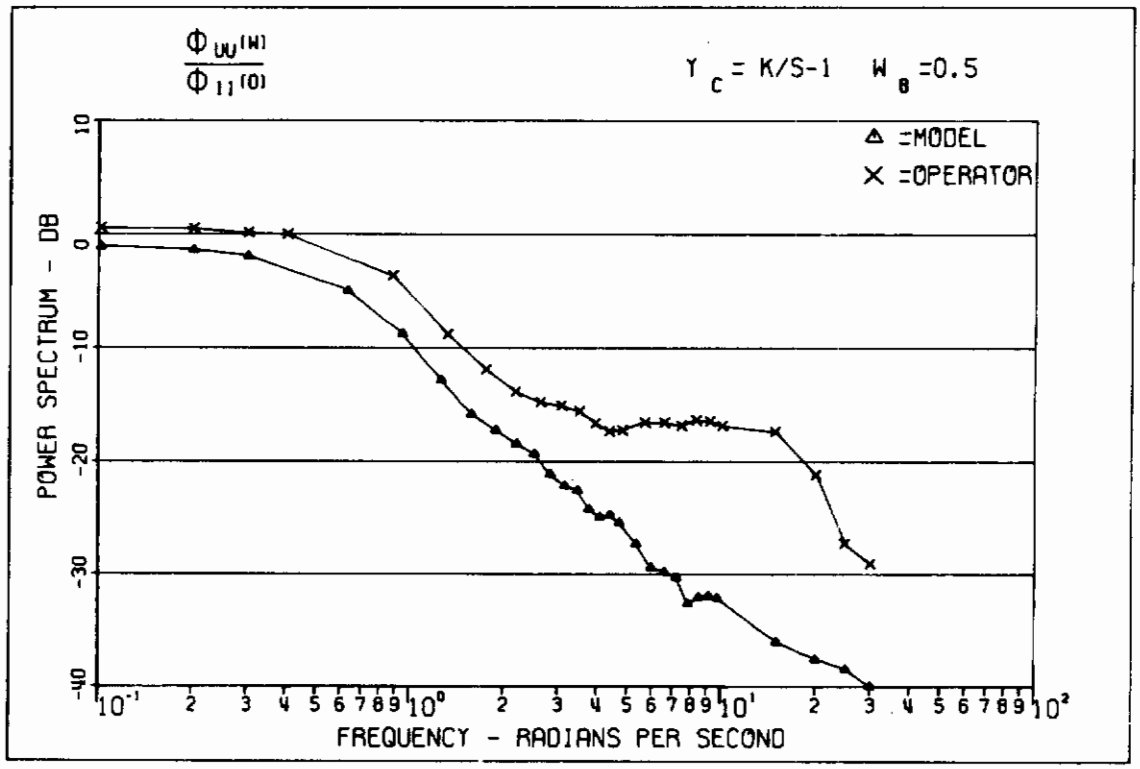

Figure 33. Power Spectral Densities Y_C = K/s-1 Pursuit

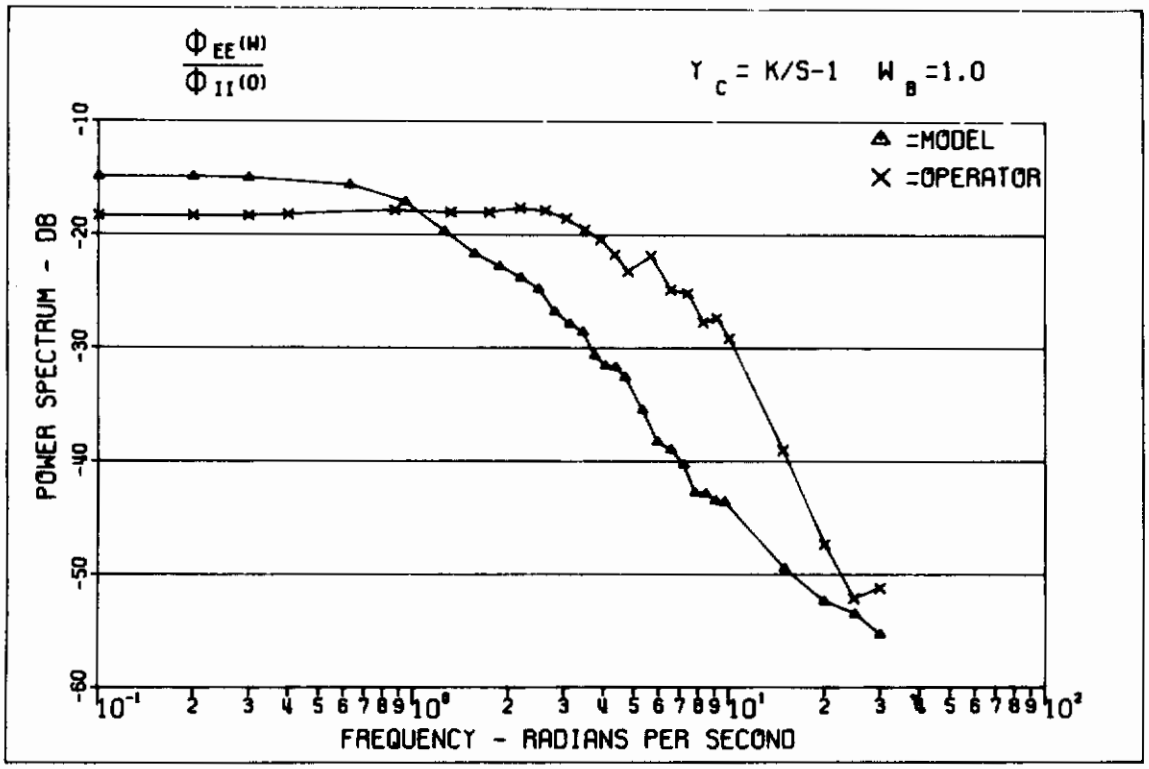

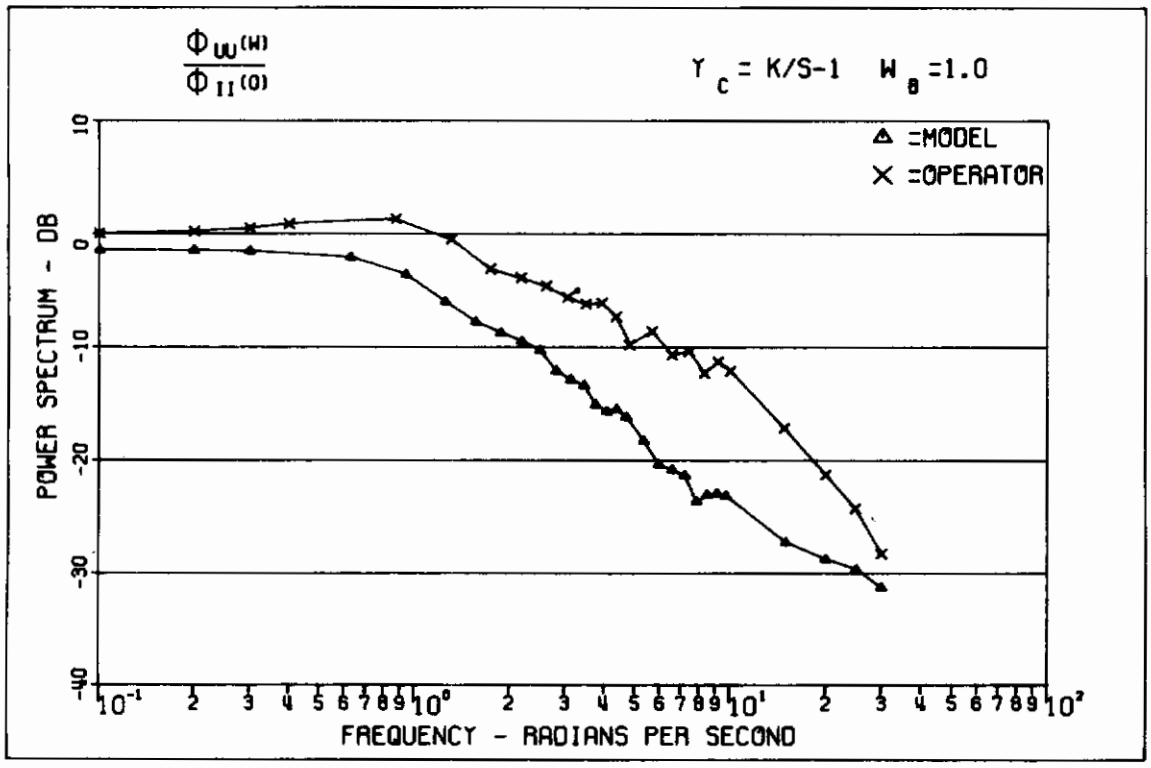

Figure 34. Power Spectral Densities Y_C = K/s-1 Pursuit

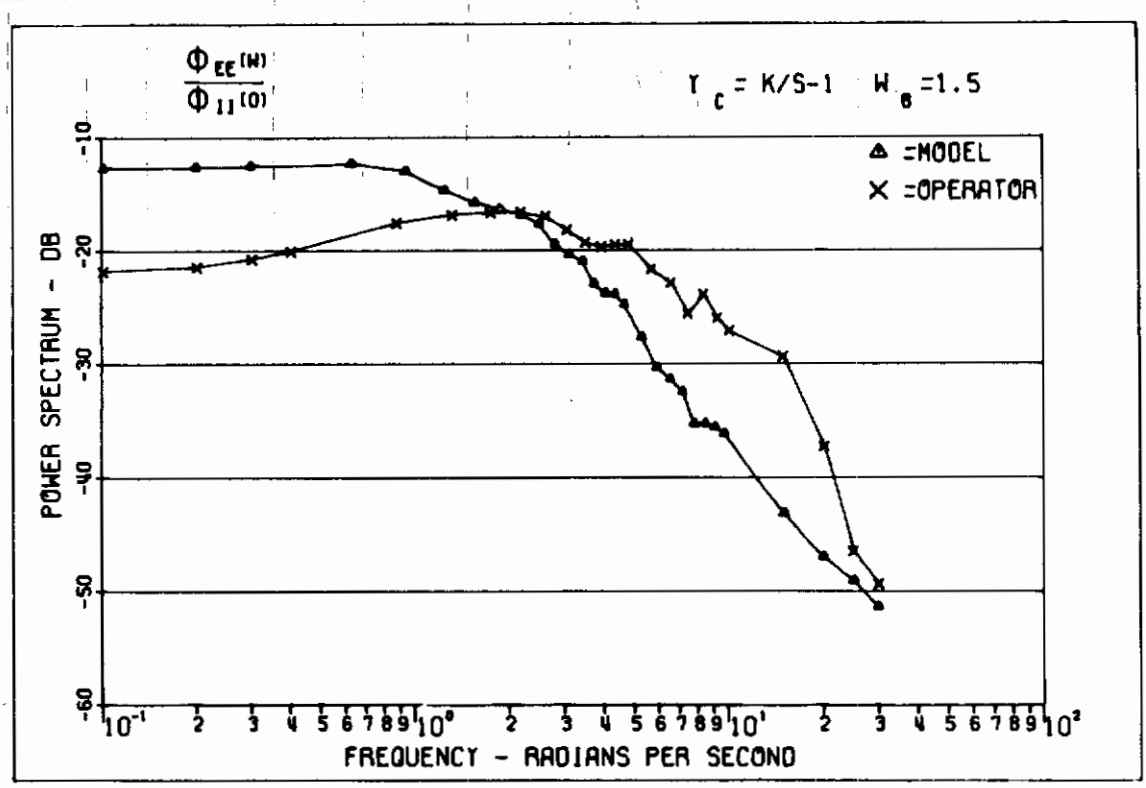

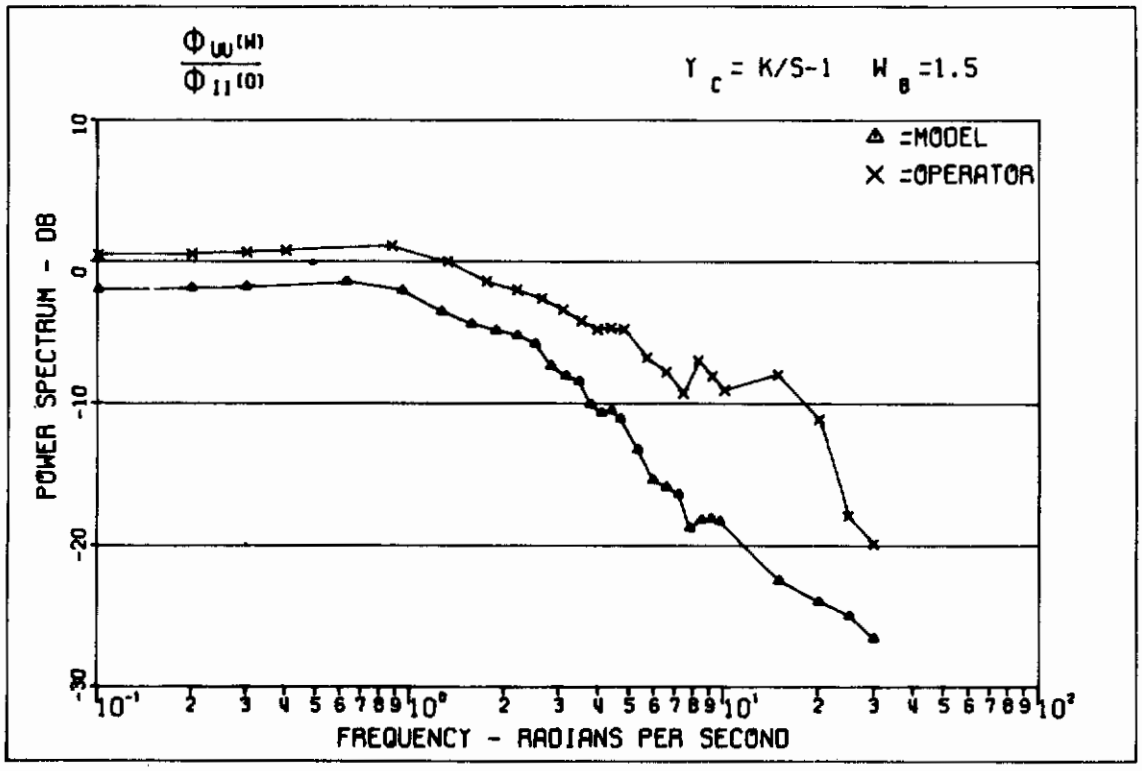

Figure 35. Power Spectral Densities Y_C = K/s-1 Pursuit

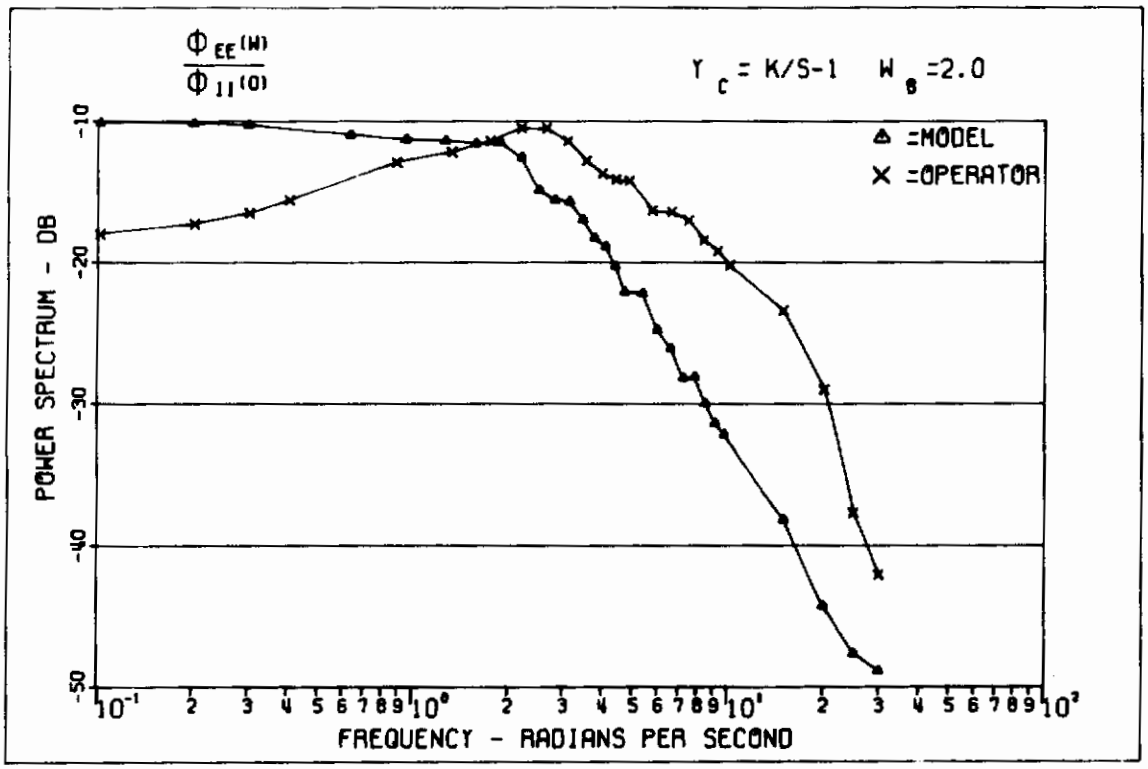

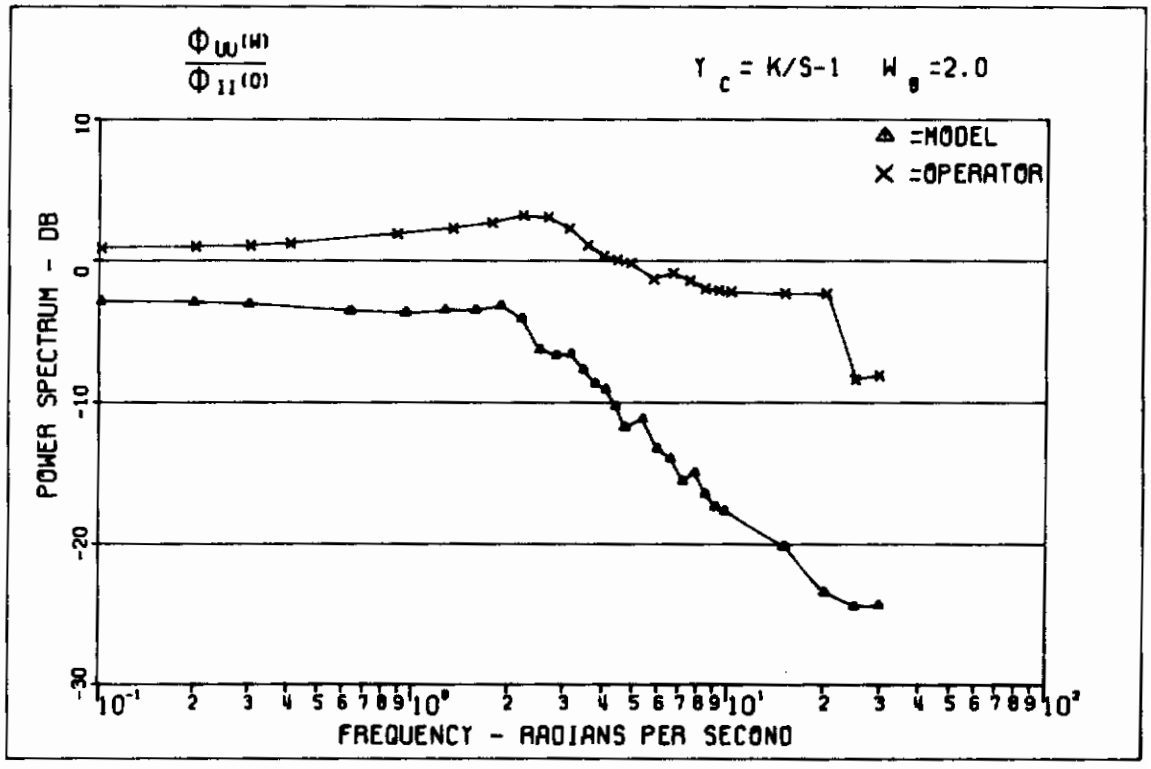

Figure 36. Power Spectral Densities Y_C = K/s-1 Pursuit

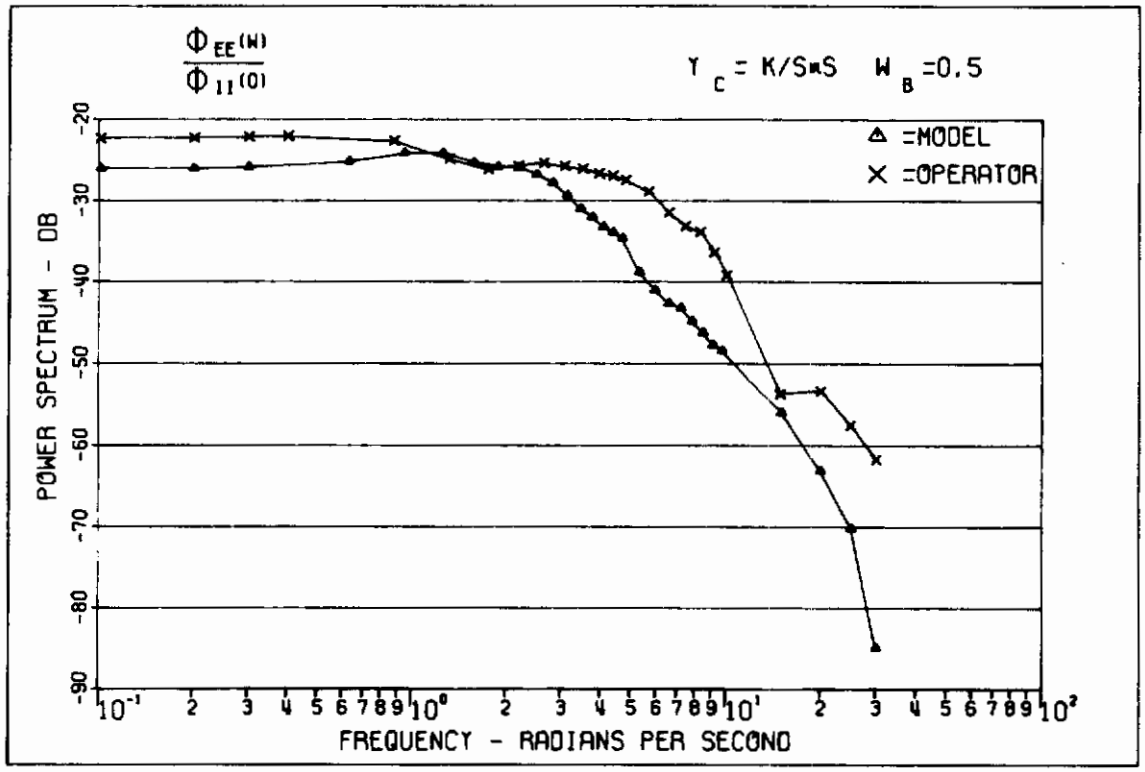

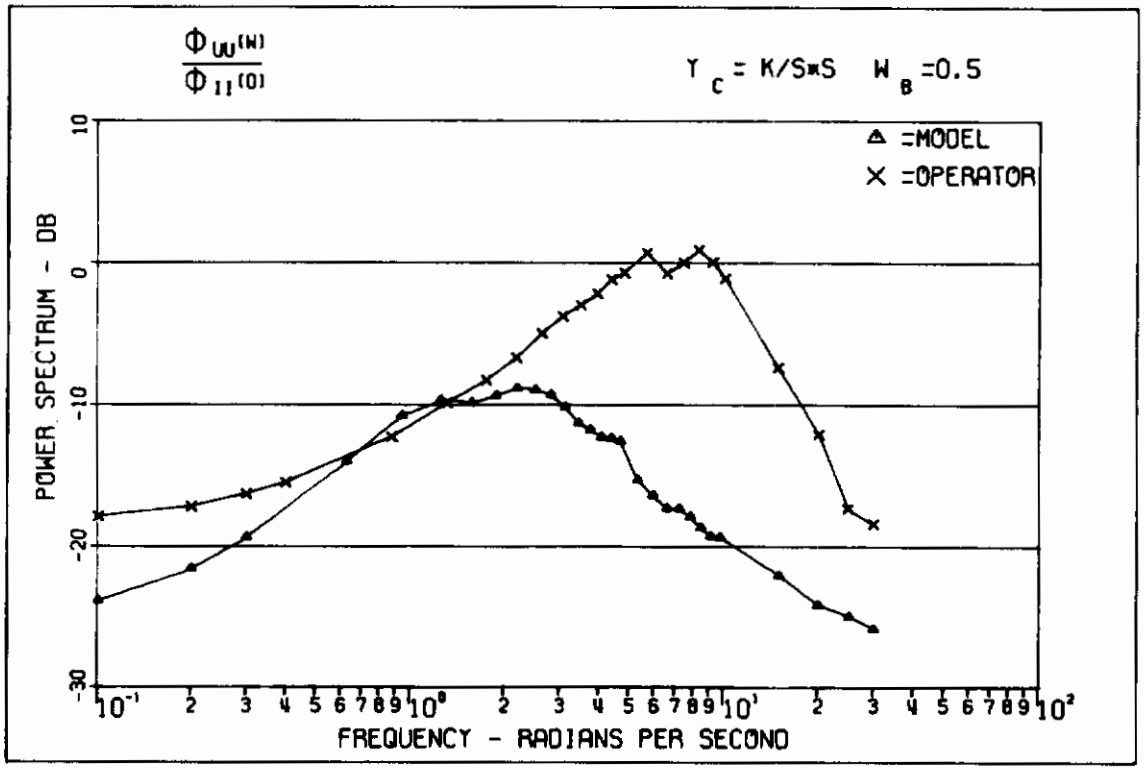

Figure 37. Power Spectral Densities $Y_C = K/s^2$ Pursuit

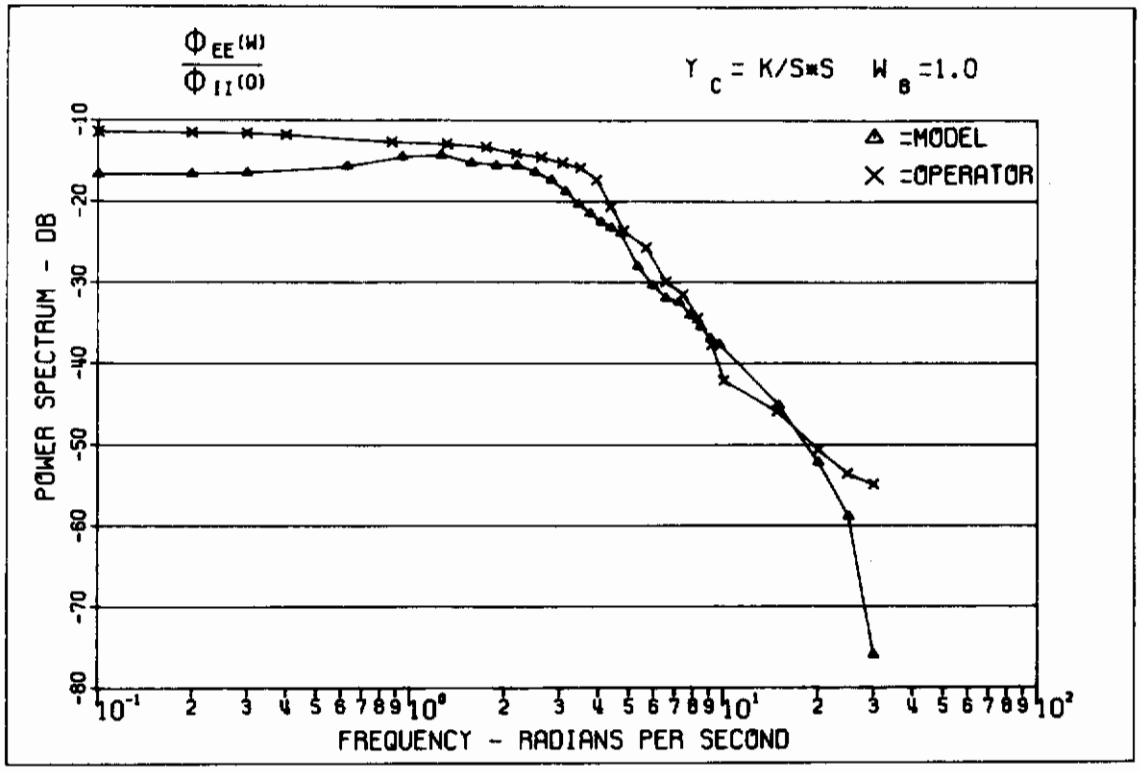

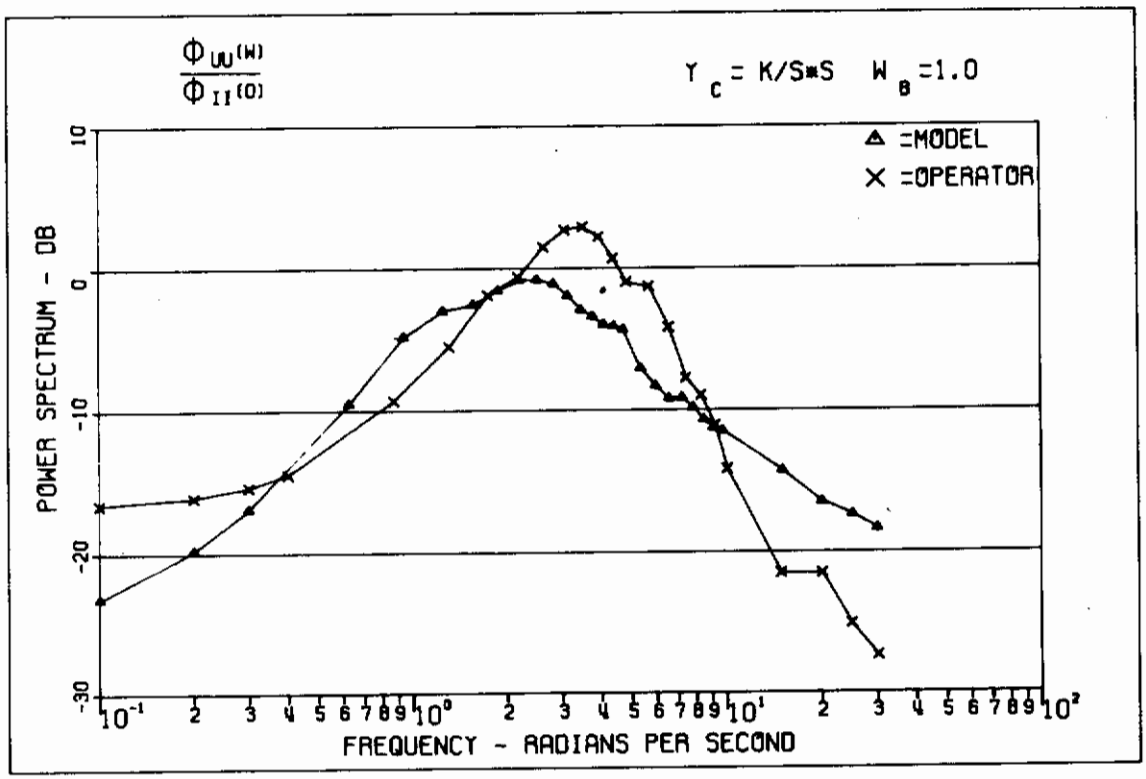

Figure 38. Power Spectral Densities $Y_C = K/s^2$ Pursuit

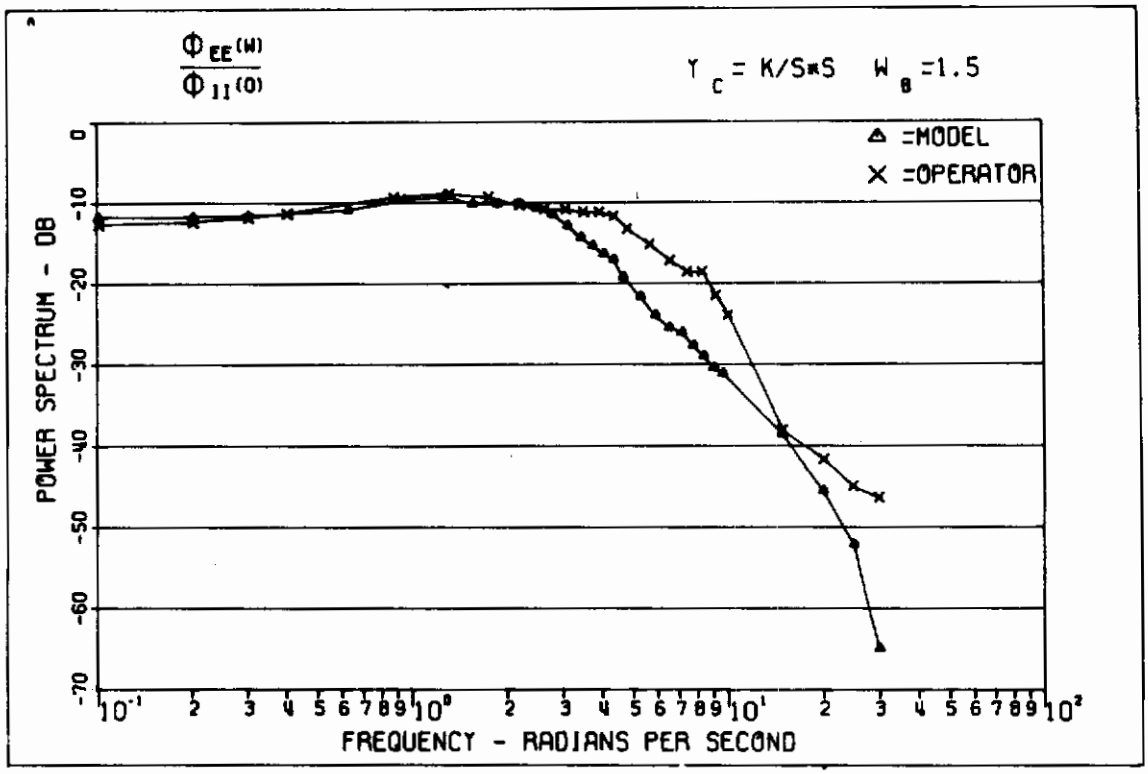

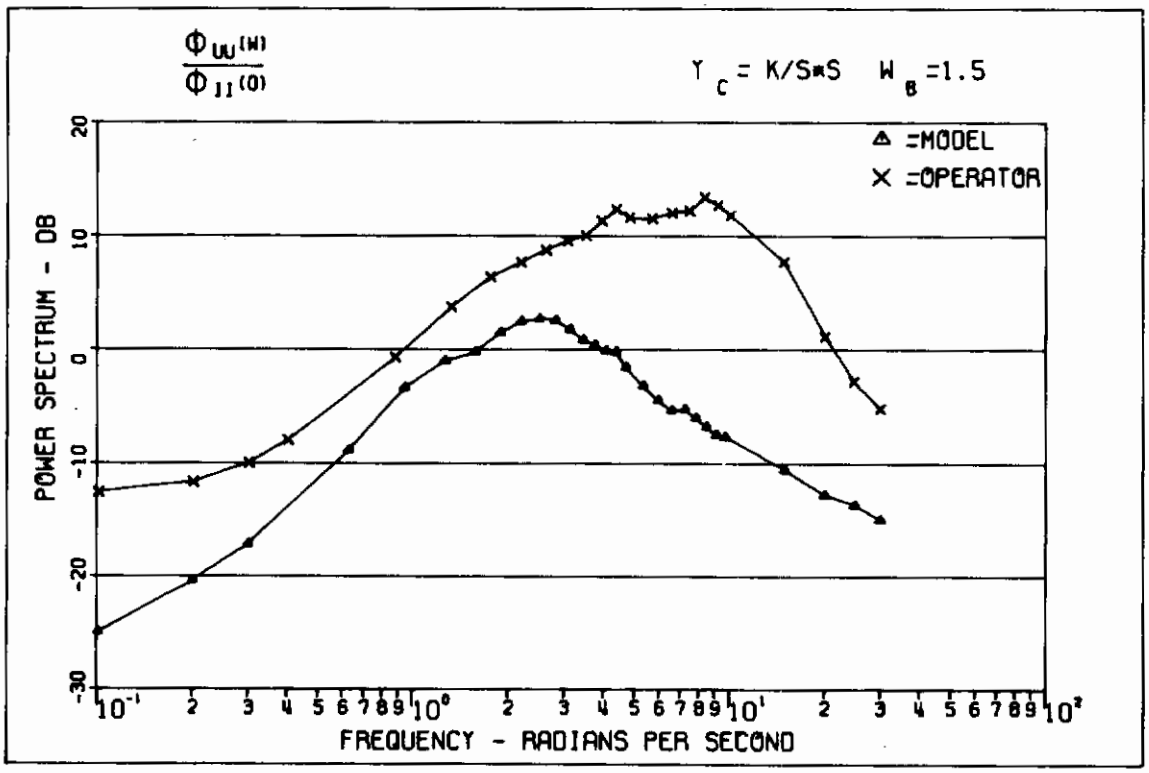

Figure 39. Power Spectral Densities $Y_C = K/s^2$ Pursuit

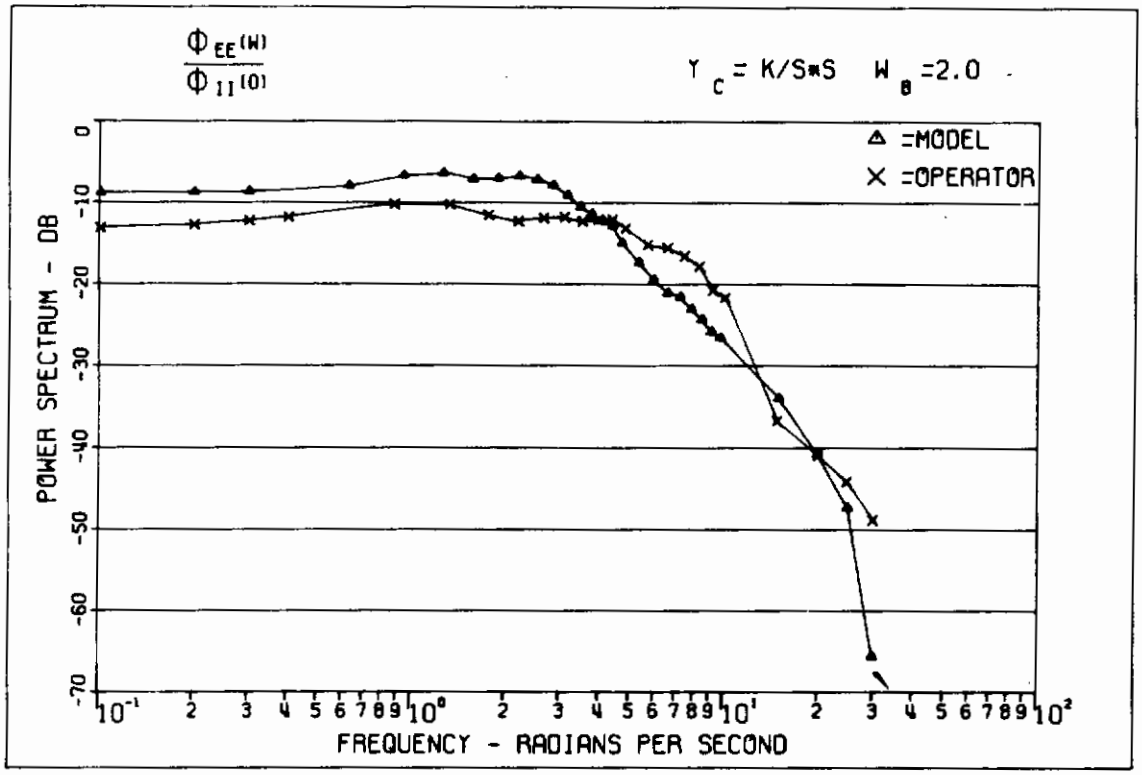

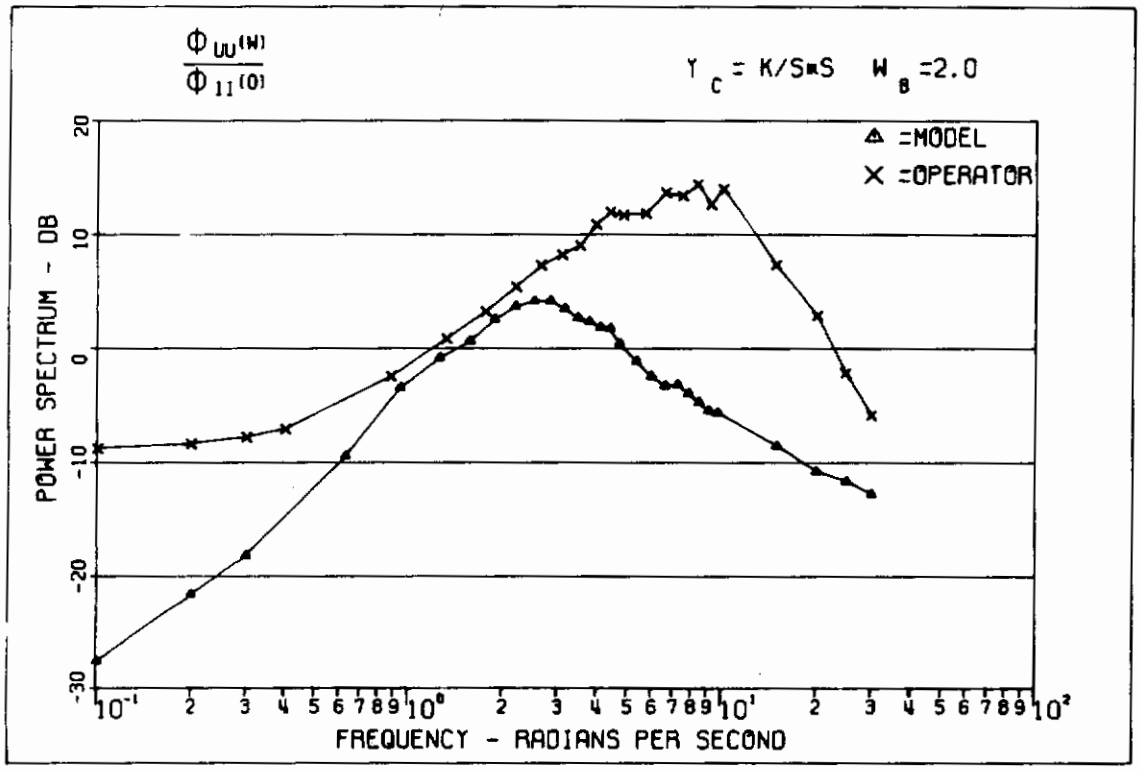

Figure 40. Power Spectral Densities $Y_C = K/s^2$ Pursuit

The basic characteristics of the control PSD for each of the controlled elements considered can be predicted by the following analysis. As the cost function indicates, the optimal control will be such as to make the system output follow the system input at each sampling instant. If this is accomplished successfully, the PSD of the output will match that of the input. Thus, if the Fourier transform of the impulse response of the controlled element is denoted by $Y_c(j\omega)$, then the power spectrum of its output in response to an input u is given by $\phi_{uu}(\omega)\left|Y_c(j\omega)\right|^2$ (Reference 27:347). If this PSD is to match the PSD of the input, the required control PSD is

$$\phi_{uu}(\omega) = \frac{\phi_{ii}(\omega)}{\left|Y_c(j\omega)\right|^2} \tag{76}$$

For the input PSD (Equation 3) and the first- and second-order controlled elements used, the corresponding required control power spectra are

$$\phi_{uu}(\omega) = \frac{K^4(\omega^2+a^2)}{\omega^4+2\omega_B^2\omega^2+\omega_B^4} \tag{77}$$

$$\phi_{uu}(\omega) = \frac{K^4\omega^4}{\omega^4+2\omega_B^2\omega^2+\omega_B^4} \tag{78}$$

These control spectra are plotted in Figure 41 as a function of ω. A comparison between Figure 41 and the control spectra in Figures 22 through 40 shows that the model and operator control PSD characteristics are as predicted except for the effects of control weighting in the model and the physiological limitations of the operator.

d. Compensatory Display

The PSD data for the compensatory display are shown in Figures 42 through 47. Note that the characteristics of both the control and error power spectra are the same as for the pursuit case and conform to the predicted results. This result is to be expected, since, regardless of the display situation, the task of the controller is to generate an input to the controlled element such that its output follows the system input.

Thus, for both the pursuit and compensatory display situations, the predicted power spectra reproduce the essential bandwidth and cutoff characteristics of the experimental data and thus can be useful in the design of control system augmentation devices.

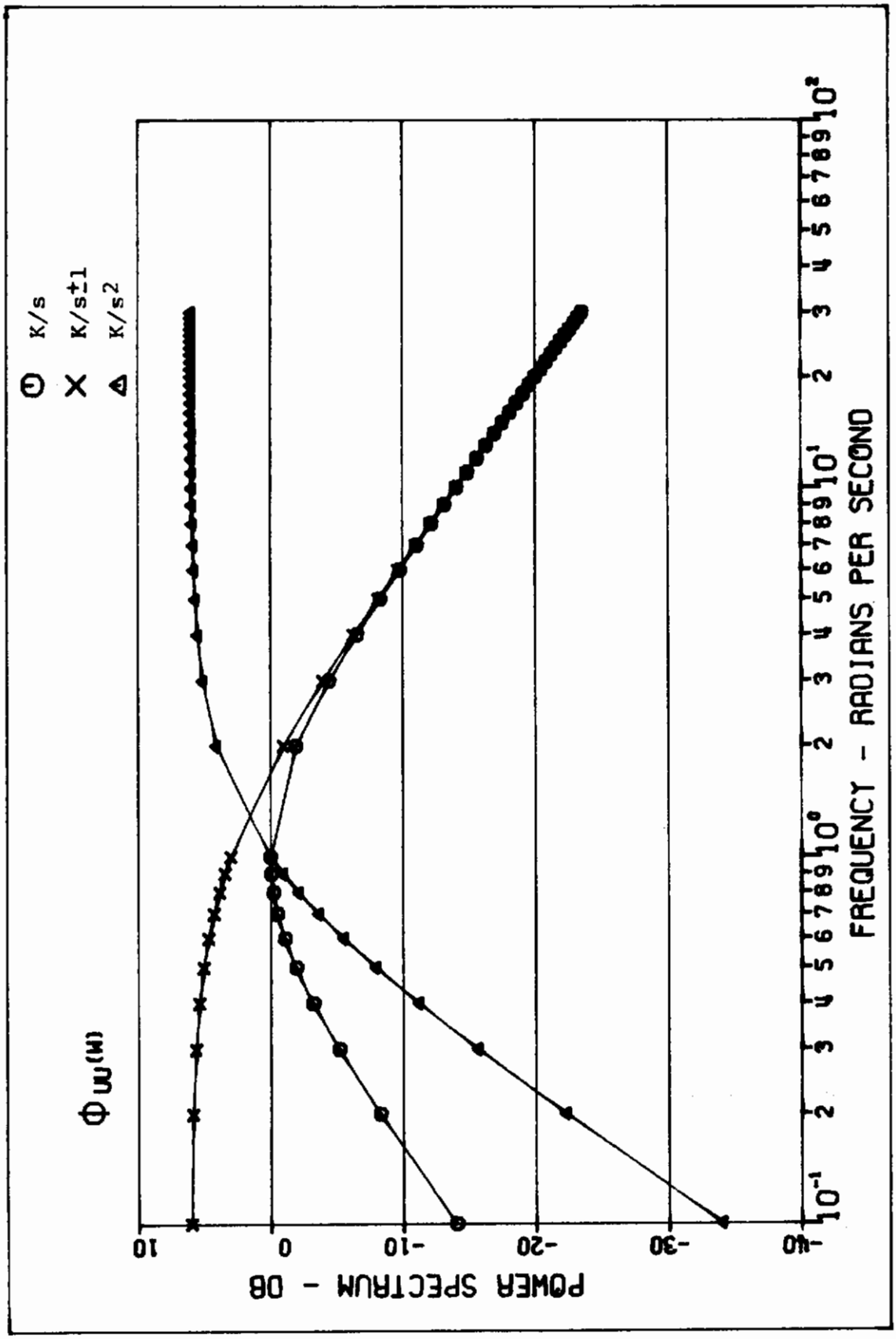

Figure 41. Theoretical Control Power Spectra

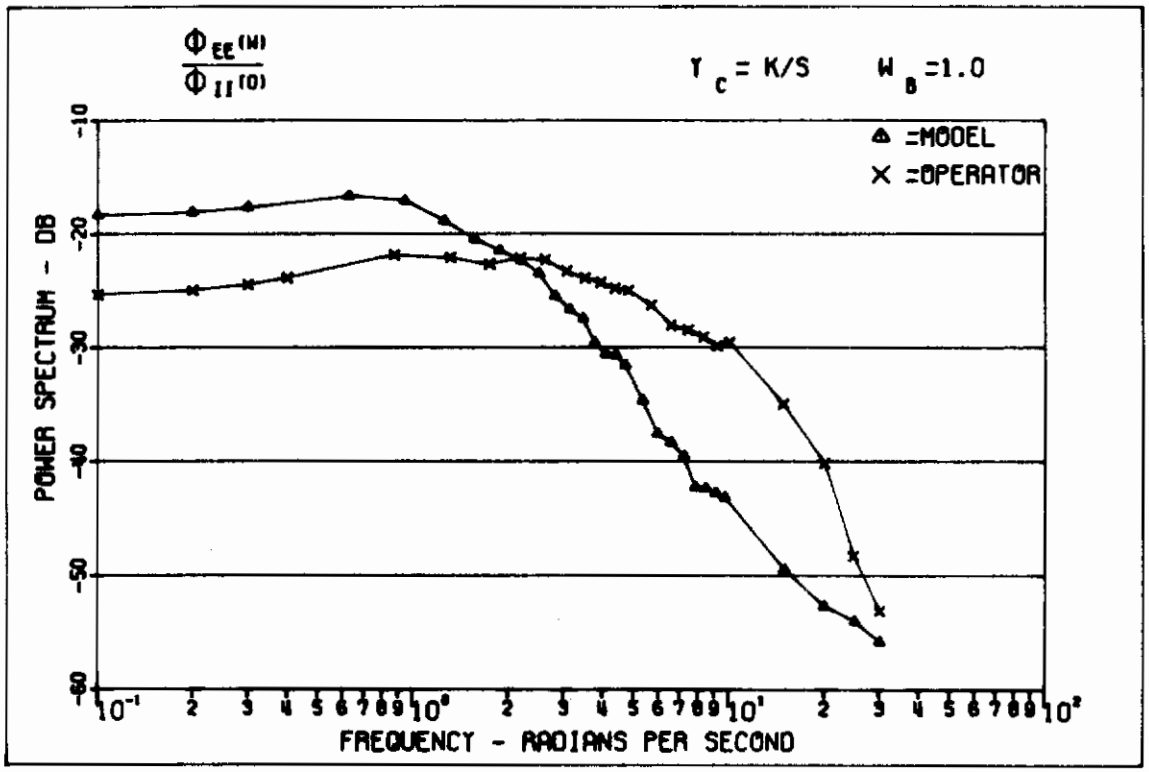

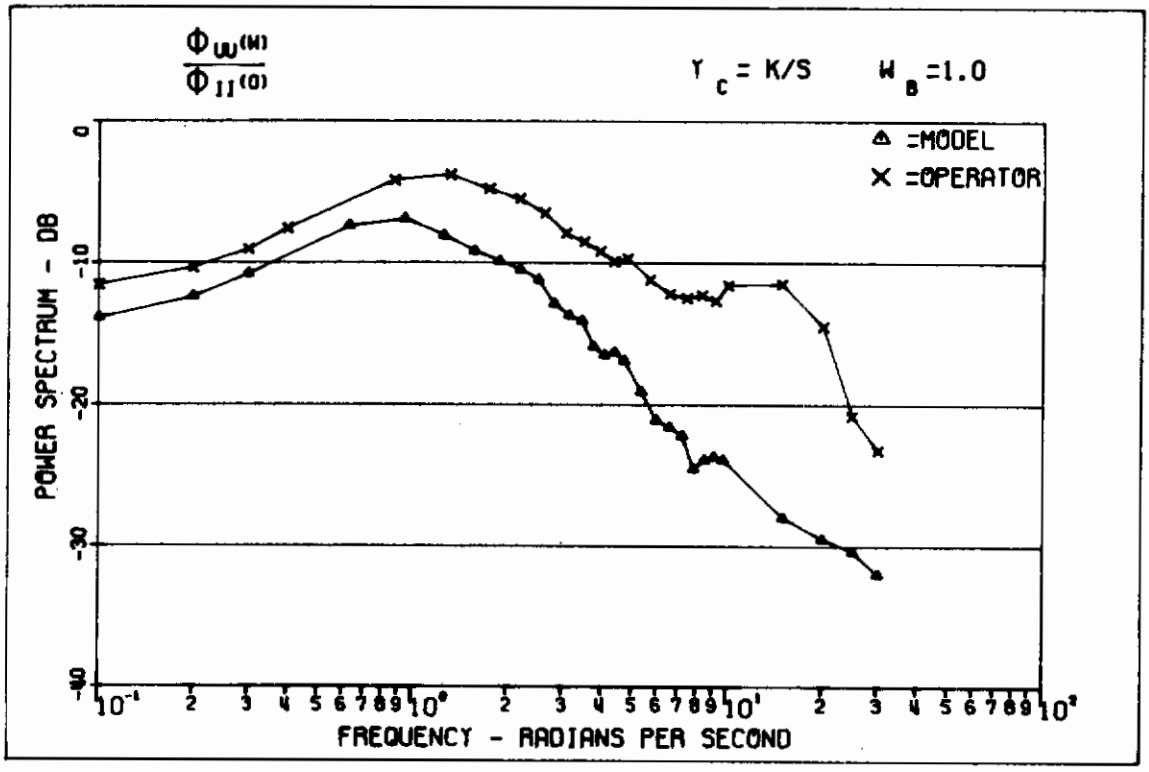

Figure 42. Power Spectral Densities Y_C = K/s Compensatory

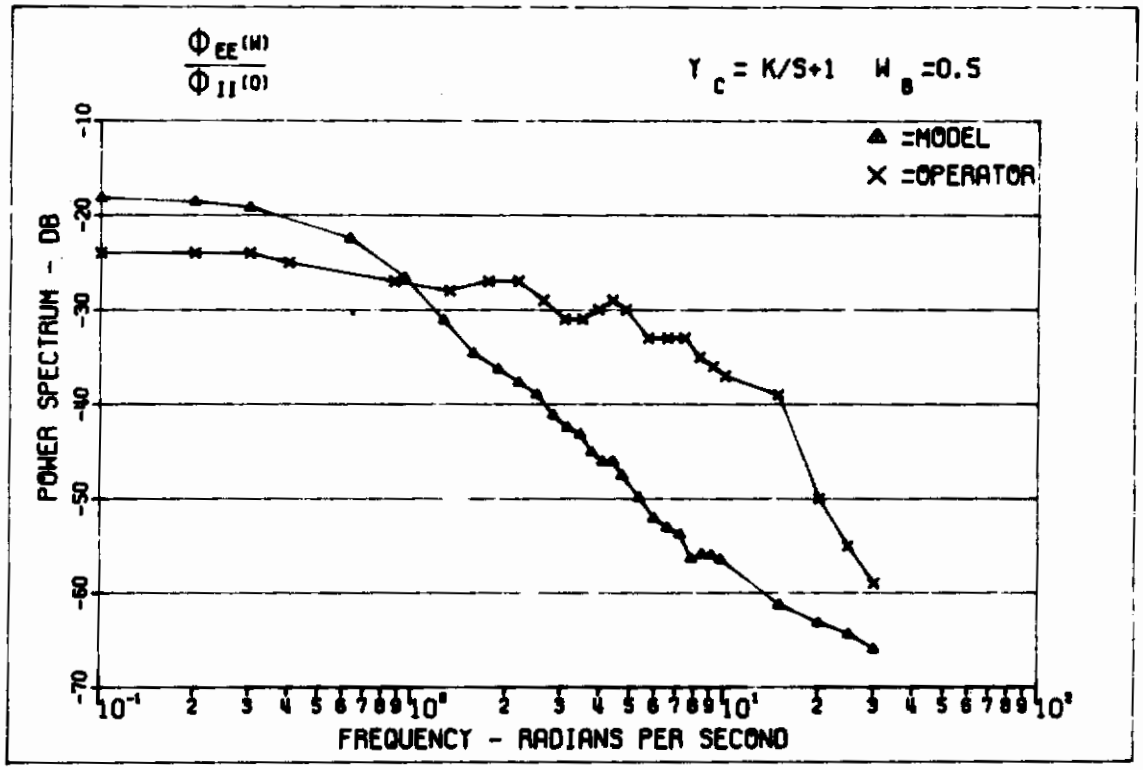

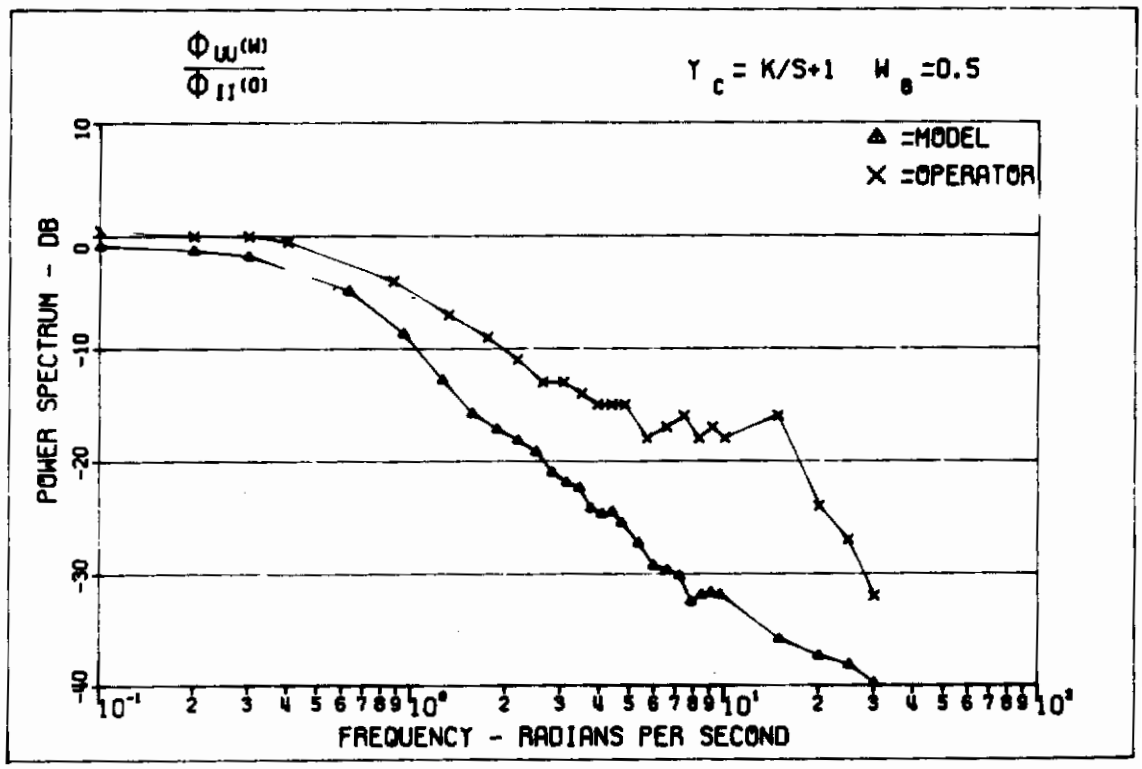

Figure 43. Power Spectral Densities Y_C = K/s+1 Compensatory

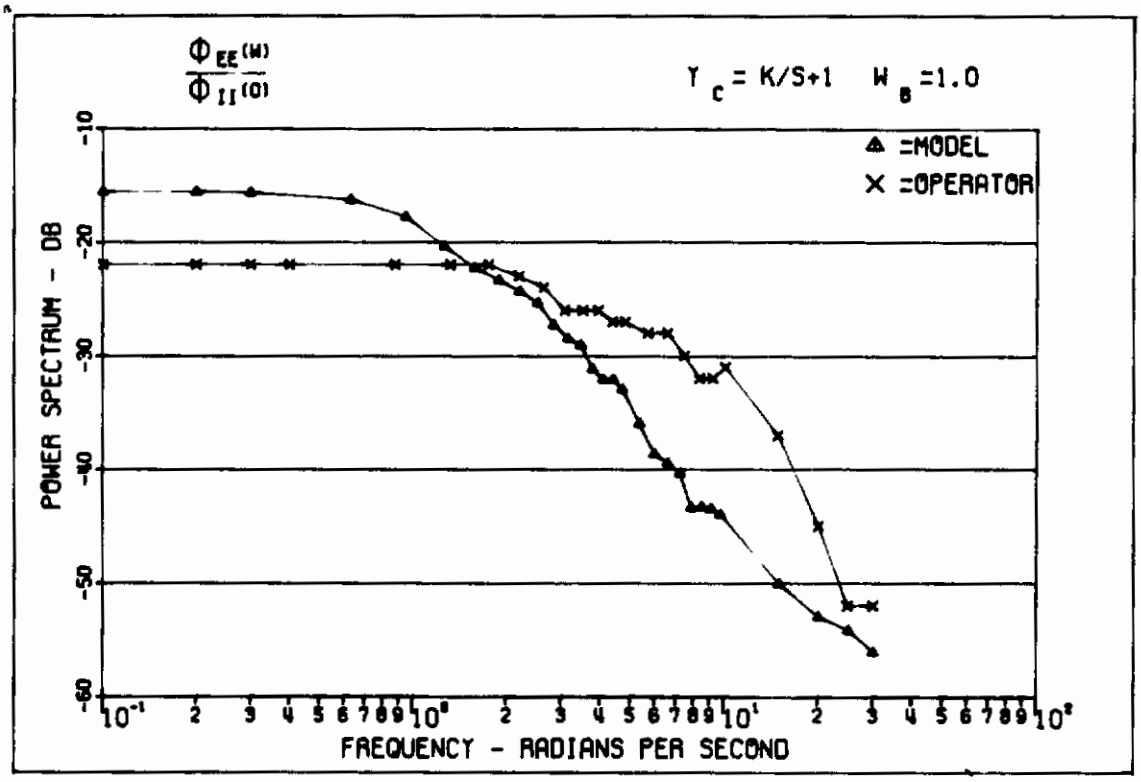

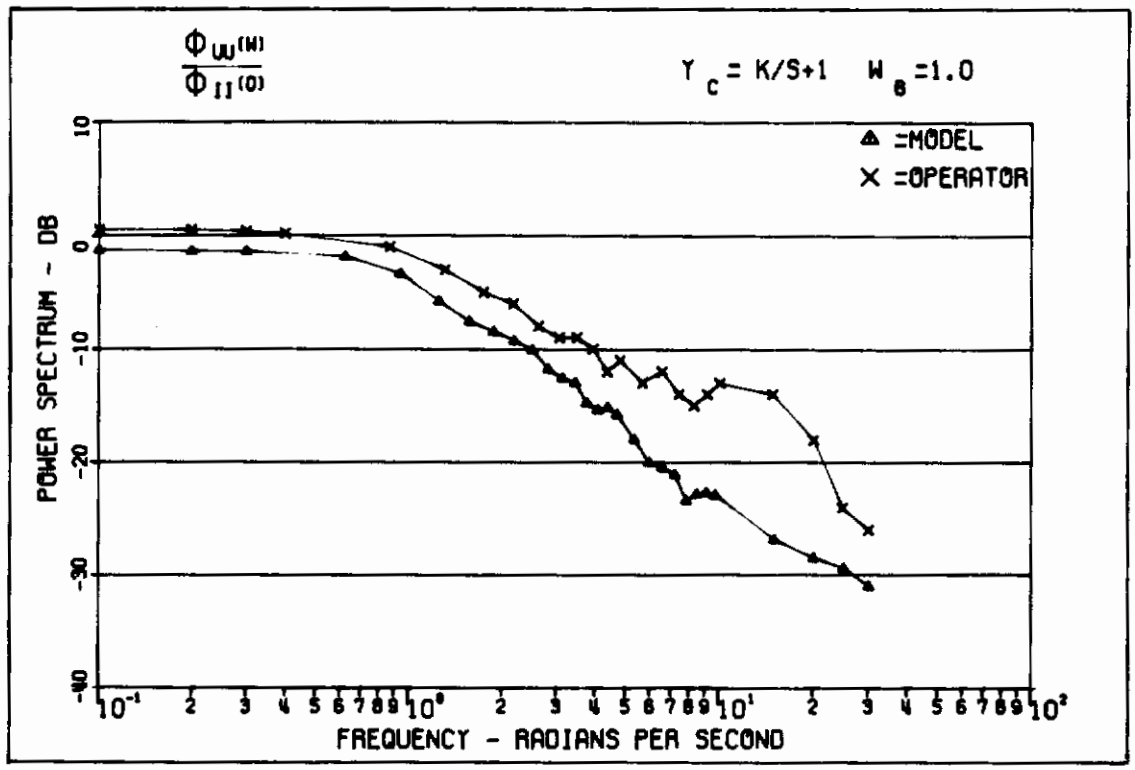

Figure 44. Power Spectral Densities Y_C = K/s+1 Compensatory

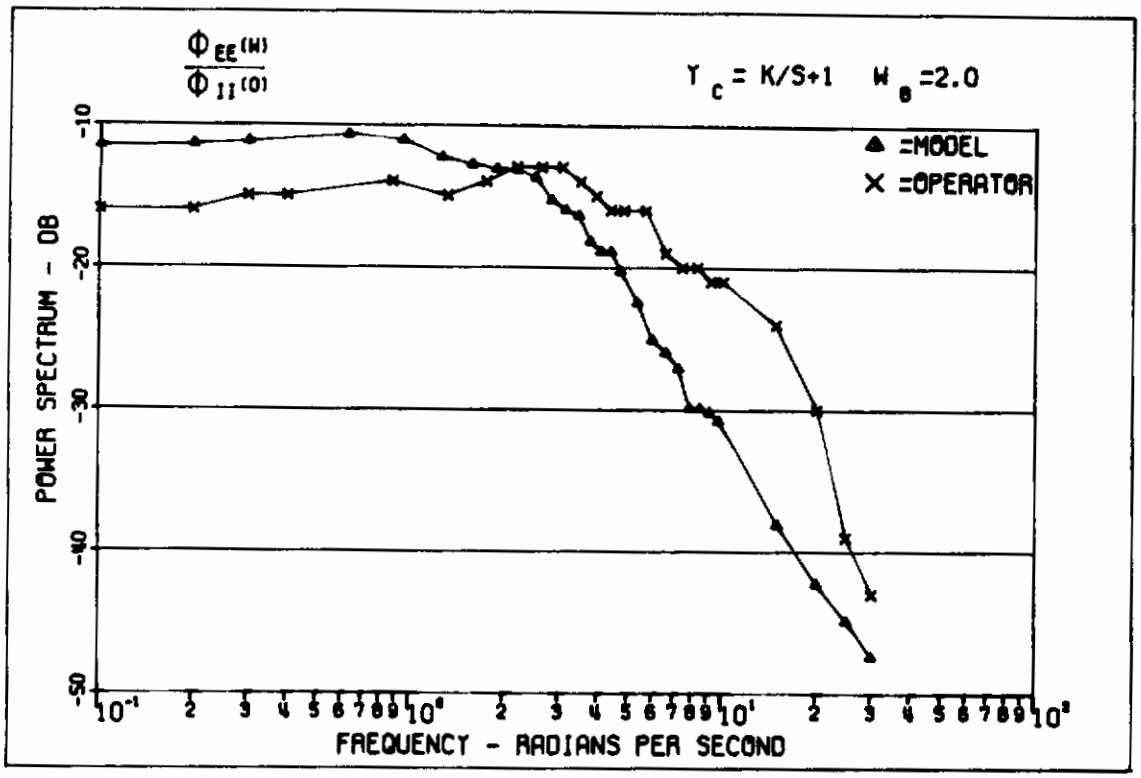

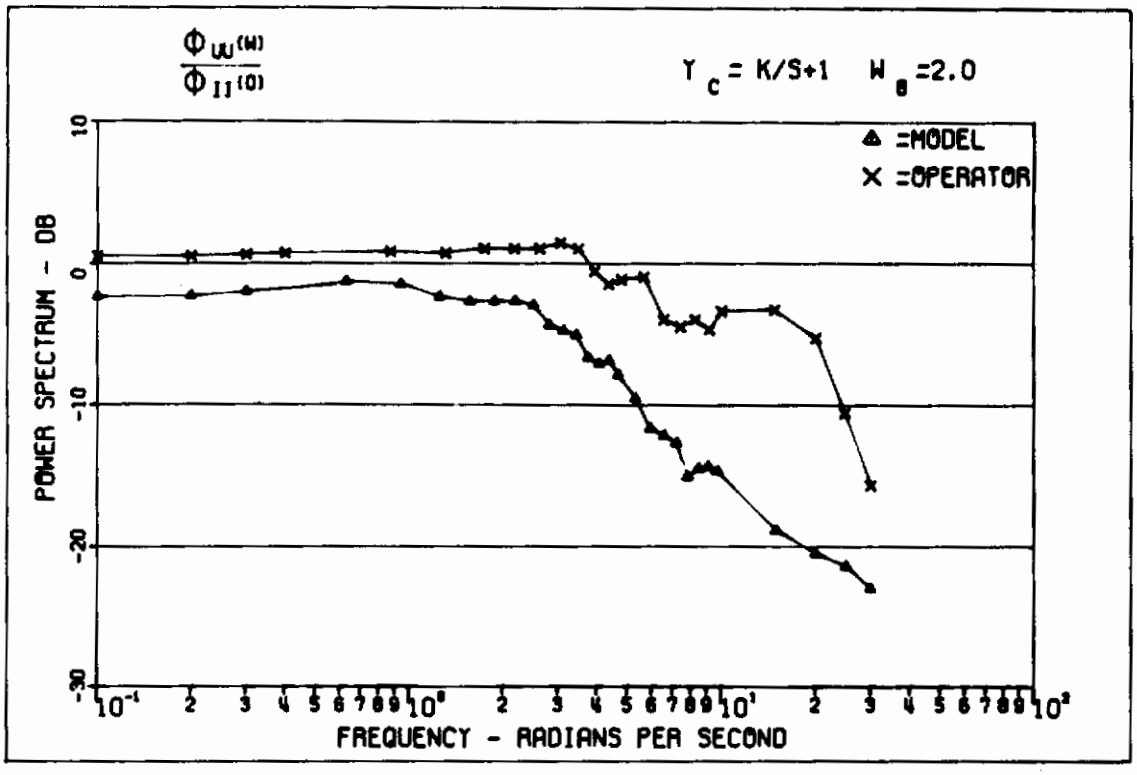

Figure 45. Power Spectral Densities Y_C = K/s+1 Compensatory

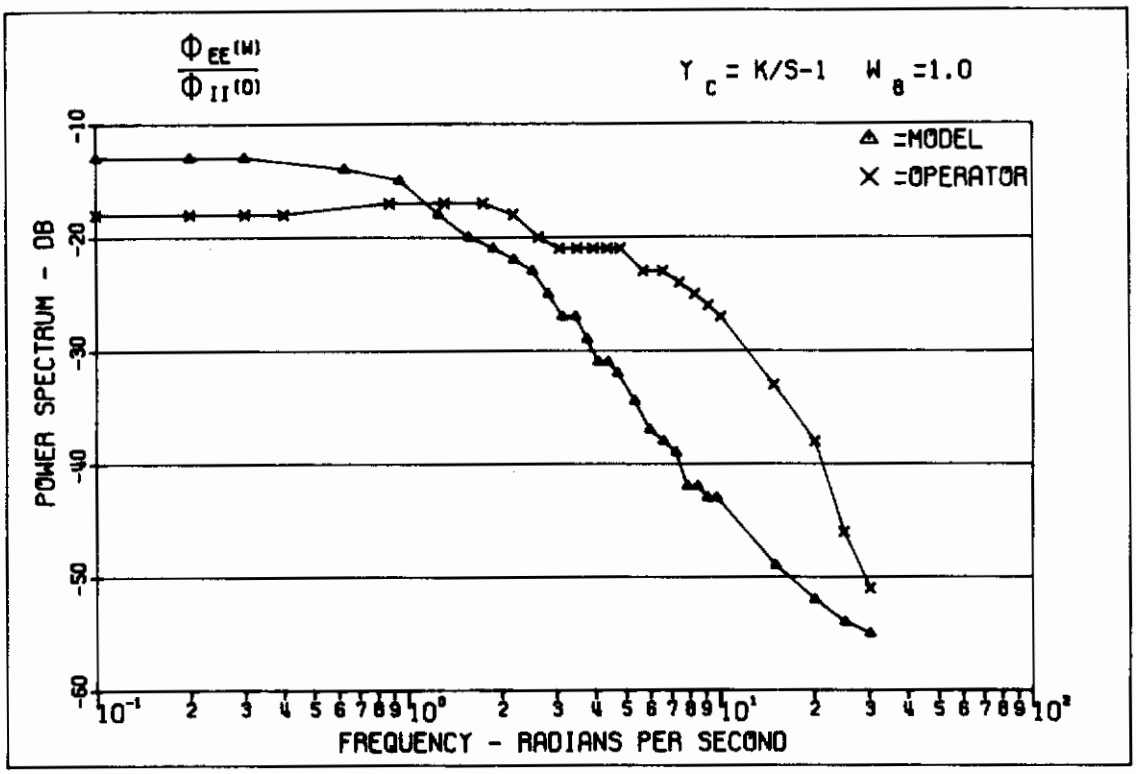

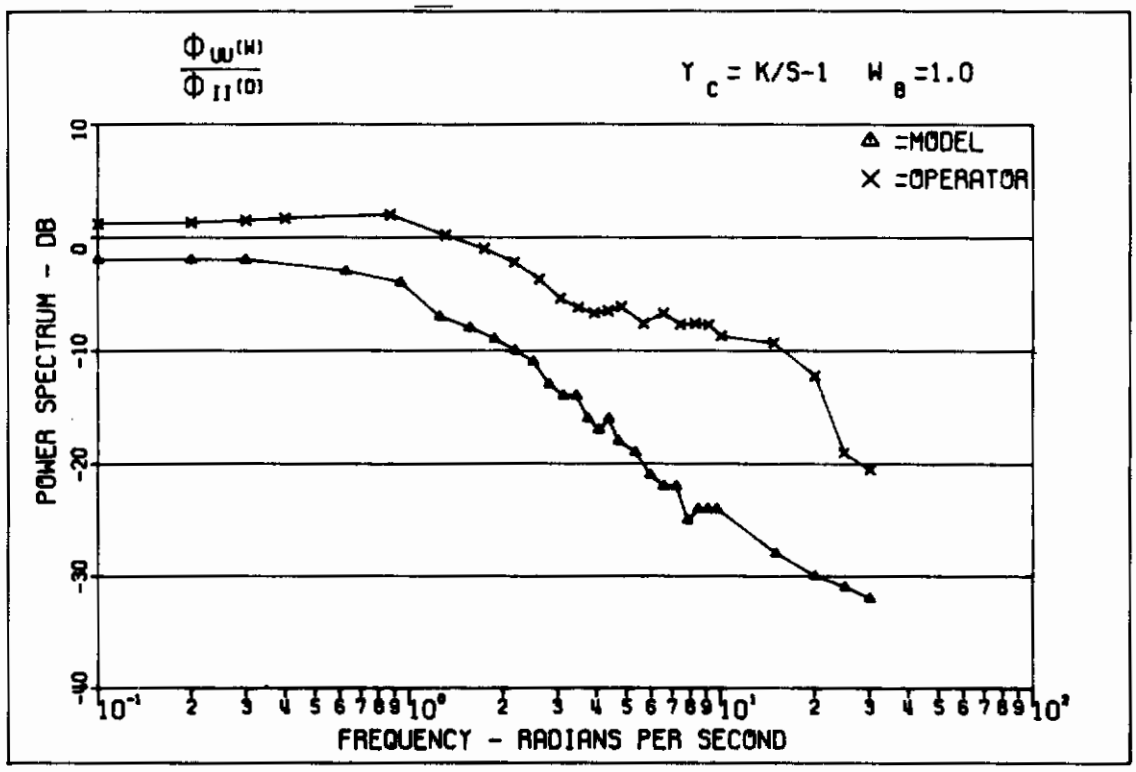

Figure 46. Power Spectral Densities Y_C = K/s-1 Compensatory

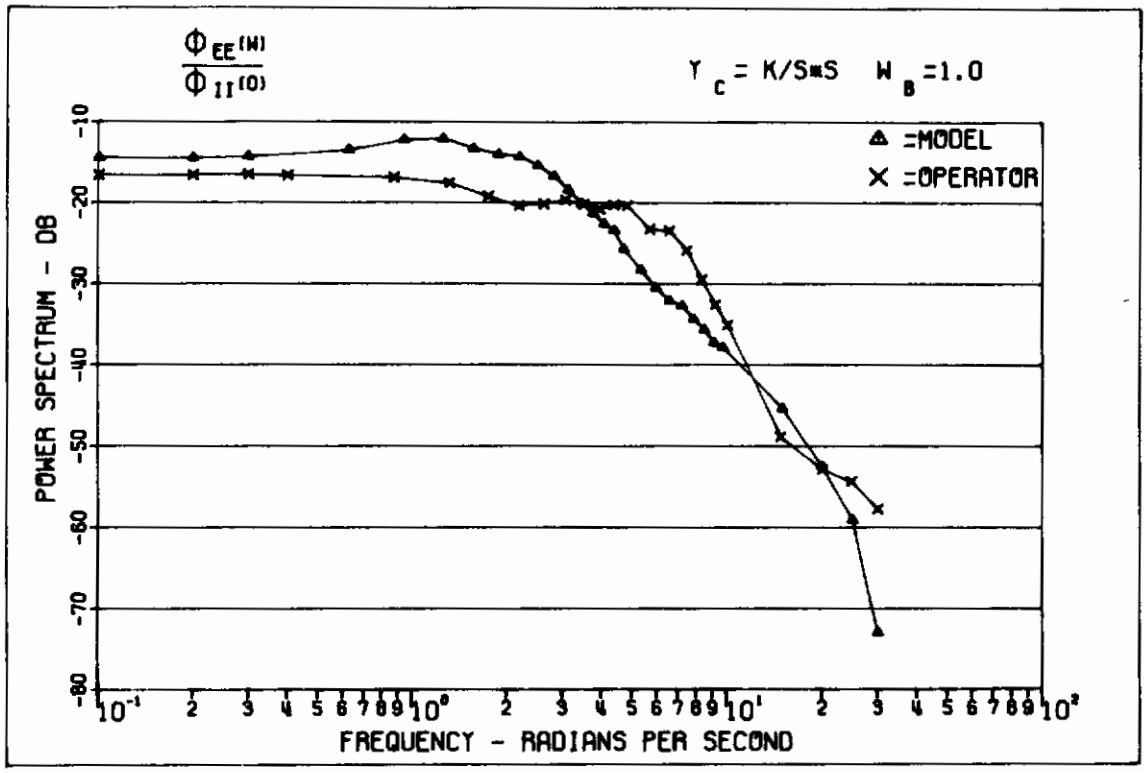

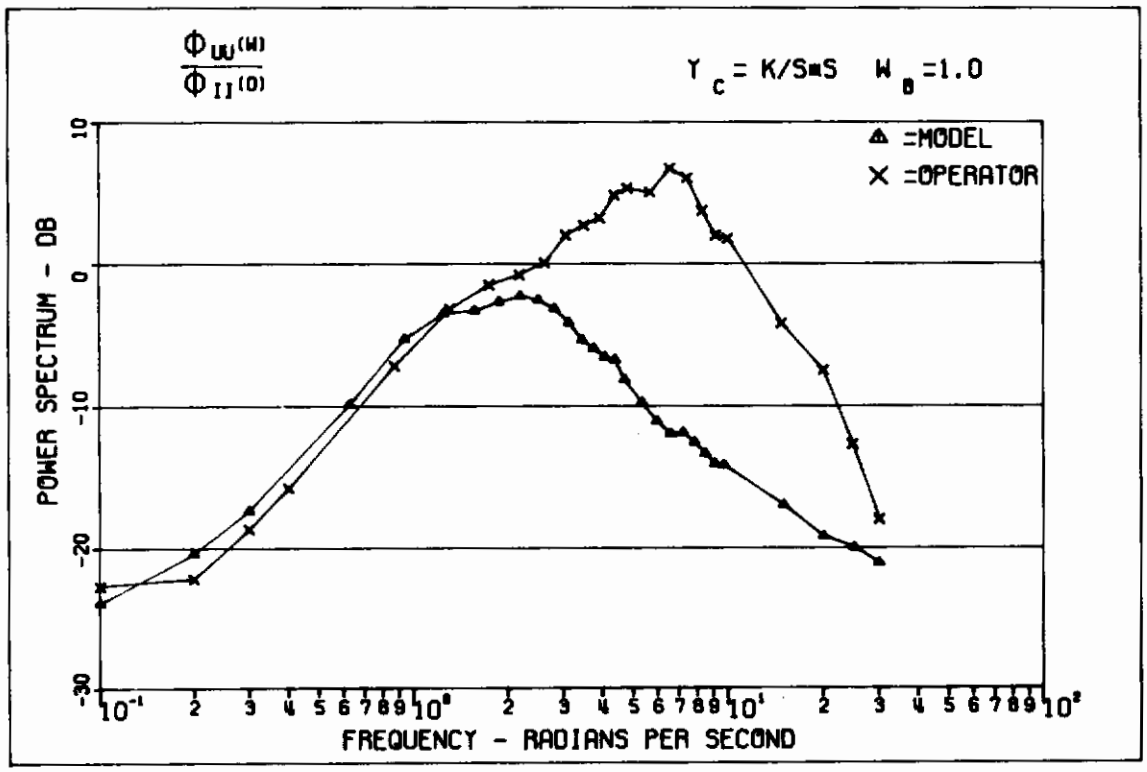

Figure 47. Power Spectral Densities $Y_C = K/s^2$ Compensatory

3. PURSUIT-COMPENSATORY COMPARISONS

As mentioned in Section I, most human operator modeling to date has been applied to the compensatory display situation. The two most successful results (quasi-linear describing function and optimal control models) have relied heavily on a close association of the model parameters with known and assumed physiological properties of the operator. In the pursuit display, the operator is presented with more information than in the compensatory case (Figure 2), and, as a result, the association of operator behavior with specific input stimuli becomes very difficult (References 1, 7, and 33).

Because of the system approach to modeling developed in this investigation, there is no need to distinguish between compensatory and pursuit tracking situations, and hence the model results can be compared with both pursuit and compensatory experimental data. More specifically, the PSD of the control signal of both the operator and the model are the most significant results to examine. The control signal spectrum is examined not with the idea of relating it to a specific input stimulus but rather by noting that it is the result of a controller trying to minimize a given cost function. In the case of the model, the cost function is given by Equation 47. By varying the value of the control weighting S in this equation, it has been demonstrated (Figures 22 through 47) that the characteristics of the model control spectra match those of the human operator. This does not infer, however, that the operator is trying to minimize the same cost function. As mentioned in Section I, McRuer et al (Reference 21:123) assumed this to be the case and tried to determine the value of S in the cost function by analyzing experimental data. They found a trend towards small negative values of S, although the S values for the K/s and K/s^2 controlled elements were provisional because of discrepancies in the experimental data. The direct optimal control approach used in this dissertation is based on a positive value of S in the cost function and has been adequate to reproduce the basic human operator control characteristics manifested in the power spectral density data and normalized tracking errors. It may be inferred then that the human operator is acting in an optimal manner when tracking and by analogy must be trying to minimize some equivalent form of cost function. It is significant to note that the form of the cost function in the model does not vary over the range of controlled elements considered. Only the value of the control weighting S changed.

SECTION VI

CONCLUSIONS AND RECOMMENDATIONS

1. CONCLUSIONS

As mentioned in Section IV, the experimental objectives of this investigation were to "validate" the proposed model. As a result of the normalized tracking error and power spectral density data collected and analyzed in the last section, it is concluded that the model is valid over the range of controlled elements and forcing function bandwidths investigated.

Because of the system approach taken, i.e., modeling the complete operator-display-controlled element tracking loop, it is possible to consider both the compensatory and pursuit display situations with a single model. Although the model formulation does not distinguish between the two display situations, the model outputs correlate with the pursuit and compensatory tracking data obtained experimentally. Thus the model overcomes the difficulties encountered when trying to apply describing function techniques (Section I3) to pursuit tracking situations and provides insight into operator behavior in this tracking mode.

Furthermore, this approach has substantially confirmed the hypothesis that the human operator behaves in some optimum manner when performing a closed-loop tracking task and tends to minimize a cost function equivalent to that minimized in the model formulation. It is significant to note that the form of this cost function (at least in the model) is invariant with respect to the controlled elements, forcing function bandwidths, and displays investigated.

An important aspect of the model is its ease of application. The system equations can be derived once the type of input, type of controlled element, and type of manipulator are specified. These equations can then be digitized to obtain the equations necessary for digital simulation of the optimum controller. The model-operator match is accomplished by varying the control weighting parameter S to match the model NTE to measured or estimated operator performance for the compensatory or pursuit tracking situation. System parameters can then be varied to investigate their effects on performance in terms of NTE and PSD plots. Thus, the model has sufficient simplicity and predictive capability to make it useful in manual vehicular control system design.

2. RECOMMENDATIONS

In the interest of developing a model which can be applied with a minimum of engineering "artistry," no attempt was made to use the motor noise variance as an additional model parameter. Although NTE and PSD comparisons between model and operator are close enough to warrant the use of the model as a preliminary design tool, one might be interested in obtaining closer correlation between model and experimental data. A more detailed investigation into the effects of motor noise variance might provide a means of affecting this data match; however, the addition of this parameter must be accompanied by some rationale for choosing the noise variance over the range of conditions investigated and predicted.

The general framework of modern optimal control theory is ideally suited for formulating and solving multiaxis and multiloop control problems. There has even been developed (Reference 26:527) a means of determining an optimal observation or measurement strategy based on the minimization of an observation cost function. Thus the modeling procedure developed in this dissertation could be extended to the multiaxis and multiloop tracking situations. Actual tracking experiments would then have to be conducted to determine the validity of this model extension. If this technique is successful, the model might then be expanded to predict the optimum sampling strategy required for the multidisplay situation. If this prediction is successful, the model would then have application in display design and sensor selection.

APPENDIX I

COMPUTATION OF $\Phi(t)$, A, AND B

Φ (t) is computed using Sylvester's Theorem (Reference 10:279) and $\underline{A}$ and $\underline{B}$ are computed using Equations 28 and 29. The method is illustrated for Case I.

$$A = \begin{bmatrix} -\omega_B & 0 & 0 \\ k & -\omega_B & 0 \\ 0 & 0 & a \end{bmatrix}$$

Compute the eigenvalues of A.

$$|A - I\alpha| = \begin{vmatrix} -\omega_B - \alpha & 0 & 0 \\ k & -\omega_B - \alpha & 0 \\ 0 & 0 & a - \alpha \end{vmatrix}$$

Set $|A - I\alpha| = 0$ to obtain the characteristic equation

$$(\alpha + \omega_B)(\alpha + \omega_B)(\alpha - a) = 0$$

$$\alpha_1 = \alpha_2 = -\omega_B$$

$$\alpha_3 = a$$

Sylvester's Theorem (confluent form) is stated as follows (Reference 34:609):

Let A be a constant nxn matrix with characteristic equation

$$p(\alpha) = |A - I\alpha| = (\alpha - \alpha_1)^{m_1} (\alpha - \alpha_2)^{m_2} \cdots (\alpha - \alpha_\sigma)^{m_\sigma}$$

where $\alpha_1 \neq \alpha_2 \neq \alpha_3 \neq \cdots \neq \alpha_\sigma$

α_i has multiplicity m_i

Let f be an analytic function such that f maps the space of real numbers onto the space of real numbers. Then there exist constant matrices $Z_0(\alpha_1)$, $Z_1(\alpha_1)$, ..., $Z_{m_1-1}(\alpha_1)$, $Z_0(\alpha_2)$, ..., $Z_{m_2-1}(\alpha_2)$, ... dependent only on A such that

$$f(A) = \sum_{i=1}^{\sigma} \sum_{j=0}^{m_i - 1} f^{(j)}(\alpha_i) Z_j(\alpha_i)$$

where $f^{(j)}(\alpha_i)$ is the j^{th} derivative of f evaluated at α_i.

Thus for Case I,

$$f(A) = f(\alpha_1) Z_0(\alpha_1) + f'(\alpha_1) Z_1(\alpha_1) + f(\alpha_3) Z_0(\alpha_3)$$

Note that the $Z_j(\alpha_i)$ are independent of the function f and hence can be evaluated by a judicious choice of trial functions.

Pick $f(x) = (x-\alpha_1)^2$

Then $f'(x) = 2(x-\alpha_1)$

$$f(\alpha_1) = 0 \qquad f'(\alpha_1) = 0$$

$$f(\alpha_3) = (\alpha_3 - \alpha_1)^2 = (a+\omega_B)^2$$

and

$$f(A) = (A-I\alpha)^2 = f(\alpha_3) Z_0(\alpha_3)$$

Solve for $Z_0(\alpha_3)$

$$Z_0(\alpha_3) = \frac{(A-I\alpha_1)^2}{f(\alpha_3)} = \frac{(A+I\omega_B)^2}{f(a)}$$

$$Z_0(\alpha_3) = \frac{\begin{bmatrix} 0 & 0 & 0 \\ k & 0 & 0 \\ 0 & 0 & a+\omega_B \end{bmatrix}^2}{(a+\omega_B)^2}$$

$$Z_0(\alpha_3) = \frac{\begin{bmatrix} 0 & 0 & 0 \\ 0 & 0 & 0 \\ 0 & 0 & (a+\omega_B)^2 \end{bmatrix}}{(a+\omega_B)^2}$$

$$Z_0(\alpha_3) = \begin{bmatrix} 0 & 0 & 0 \\ 0 & 0 & 0 \\ 0 & 0 & 1 \end{bmatrix}$$

Now pick $f(x) = x - \alpha_1$

Then $f'(x) = 0$

$$f(\alpha_1) = 0 \qquad f'(\alpha_1) = 1$$

$$f(\alpha_3) = \alpha_3 - \alpha_1 = a + \omega_B$$

and

$$f(A) = A - I\alpha_1 = Z_1(\alpha_1) + (a+\omega_B) Z_0(\alpha_3)$$

Solve for $Z_1(\alpha_1)$

$$Z_1(\alpha_1) = A - I\alpha_1 - (a+\omega_B) Z_0(\alpha_3)$$

$$Z_1(\alpha_1) = \begin{bmatrix} 0 & 0 & 0 \\ 0 & 0 & 0 \\ 0 & 0 & -(a+\omega_B) \end{bmatrix} + \begin{bmatrix} 0 & 0 & 0 \\ k & 0 & 0 \\ 0 & 0 & a+\omega_B \end{bmatrix}$$

$$Z_1(\alpha_1) = \begin{bmatrix} 0 & 0 & 0 \\ k & 0 & 0 \\ 0 & 0 & 0 \end{bmatrix}$$

Finally pick $f(x) = 1$

Then $f'(x) = 0$

$$f(\alpha_1) = 1$$

$$f(\alpha_3) = 1$$

and

$$f(A) = I = Z_0(\alpha_1) + Z_0(\alpha_3)$$

Solve for $Z_0(\alpha_1)$

$$Z_0(\alpha_1) = I - Z_0(\alpha_3)$$

$$Z_0(\alpha_1) = \begin{bmatrix} 1 & 0 & 0 \\ 0 & 1 & 0 \\ 0 & 0 & 0 \end{bmatrix}$$

Thus

$$f(A) = f(\alpha_1)\begin{bmatrix} 1 & 0 & 0 \\ 0 & 1 & 0 \\ 0 & 0 & 0 \end{bmatrix} + f'(\alpha_1)\begin{bmatrix} 0 & 0 & 0 \\ k & 0 & 0 \\ 0 & 0 & 0 \end{bmatrix} + f(\alpha_3)\begin{bmatrix} 0 & 0 & 0 \\ 0 & 0 & 0 \\ 0 & 0 & 1 \end{bmatrix}$$

Now the particular f(A) of interest is $f(A) = \exp(At) = \Phi(t)$

Thus

$$f(x) = \exp(xt)$$

$$f'(x) = t\exp(xt)$$

So

$$\Phi(t) = \exp(\alpha_1 t)\begin{bmatrix} 1 & 0 & 0 \\ 0 & 1 & 0 \\ 0 & 0 & 0 \end{bmatrix} + t\cdot\exp(\alpha_1 t)\begin{bmatrix} 0 & 0 & 0 \\ k & 0 & 0 \\ 0 & 0 & 0 \end{bmatrix} + \exp(\alpha_3 t)\begin{bmatrix} 0 & 0 & 0 \\ 0 & 0 & 0 \\ 0 & 0 & 1 \end{bmatrix}$$

$$\Phi(t) = \begin{bmatrix} \exp(\alpha_1 t) & 0 & 0 \\ k\cdot t\cdot\exp(\alpha_1 t) & \exp(\alpha_1 t) & 0 \\ 0 & 0 & \exp(\alpha t) \end{bmatrix}$$

$$\Phi(t) = \begin{bmatrix} \exp(-\omega_B t) & 0 & 0 \\ k\cdot t\cdot\exp(-\omega_B t) & \exp(-\omega_B t) & \\ 0 & 0 & \exp(\alpha t) \end{bmatrix}$$

$$A = \Phi(T) = \begin{bmatrix} \exp(-\omega_B T) & 0 & 0 \\ kT\exp(-\omega_B T) & \exp(-\omega_B T) & 0 \\ 0 & 0 & \exp(aT) \end{bmatrix}$$

$$\int_0^T \Phi(\xi)\, d\xi = H$$

$$h_{11} = \frac{1}{\omega_B}\left[1-\exp(-\omega_B T)\right]$$

$$h_{12} = h_{13} = 0$$

$$h_{21} = \frac{k}{\omega_B^2}\left[1-\exp(-\omega_B T)\,(1+\omega_B T)\right]$$

$$h_{22} = h_{11}$$

$$h_{23} = 0$$

$$h_{31} = h_{32} = 0$$

$$h_{33} = \frac{1}{a}\left[\exp(aT)-1\right]$$

$$\int_0^T \Phi(\xi)\, d\xi\, B = \underline{B}$$

$$\underline{B} = \begin{bmatrix} 0 \\ 0 \\ \frac{b}{a}\left[\exp(aT)-1\right] \end{bmatrix}$$

$$\int_0^T \Phi(\xi)\, d\xi W = \underline{W}$$

$$\underline{W} = \begin{bmatrix} \frac{k}{\omega_B}\left[1-\exp(-\omega_B T)\right] w_1(n) \\ \\ \frac{k^2}{\omega_B^2}\left[1-\exp(-\omega_B T)\,(1+\omega_B T)\right] w_1(n) \\ \\ 0 \end{bmatrix}$$

APPENDIX II

DIGITAL SIMULATION PROGRAM FOR OPTIMAL CONTROL MODEL

This appendix contains the Fortran IV digital computer program which implements the discrete stochastic model of the human operator in a closed-loop tracking task. A complete set of comment cards is included in the program to explain its operation.

```
$IBFTC MAIN    DECK
C****DISCRETE STOCHASTIC OPTIMAL CONTROL MODEL
C
C          CASE I  LINEAR PLANT YC=B/S-A
C
C          PURPOSE
C             TO GENERATE A SERIES OF DATA POINTS FOR EACH OF THE
C             FOLLOWING PURSUIT TRACKING LOOP SIGNALS
C                   I(K)  FORCING FUNCTION INPUT
C                   X(K)  PLANT OUTPUT
C                   E(K)=I(K)-X(K)  SYSTEM ERROR
C                   U(K)  CONTROL
C
C          DESCRIPTION OF PARAMETERS
C             T----SAMPLING PERIOD (SEC)
C             WB---TIME CONSTANT OF INPUT NOISE FILTER (RAD/SEC)
C             SIG--STANDARD DEVIATION OF FORCING FUNCTION INPUT
C             BB---PLANT GAIN
C             AA---PLANT TIME CONSTANT
C             S----CONTROL WEIGHTING
C             N----NUMBER OF SAMPLES TO BE GENERATED
C             QSQ--MOTOR NOISE VARIANCE
C             VAR1-INTERMEDIATE NOISE OBSERVATION NOISE VARIANCE
C             VAR2-FORCING FUNCTION INPUT OBSERVATION NOISE VARIANCE
C             VAR3-PLANT OUTPUT OBSERVATION NOISE VARIANCE
C
C          REMARKS
C             1) N IS LIMITED TO 5000 OR LESS BY THE DIMENSION STATEMENT
C             2) THE CHARACTERISTICS OF THE PSEUDO WHITE NOISE GENERATOR,
C             RANDNM, ARE AS FOLLOWS..GIVEN A LARGE SAMPLE OF POINTS
C             X(K) GENERATED BY X(K)=RANDNM(W) THEN
C                   MEAN(X)=0.0
C                   VAR(X)=1.0
C                   PSDXX(W)=0.1 WHERE PSDXX(W) IS THE POWER SPECTRAL
C             DENSITY OF X AS A FUNCTION OF FREQUENCY
C                   10LOG(PSDXX(W))=-10  (DB)
C             3) IF A NEW SET OF SAMPLE POINTS IS GENERATED BY
C                   Y(K)=VAR*X(K)=VAR*RANDNM(W)
C             THEN THE STATISTICS OF Y ARE
C                   MEAN(Y)=0.0
C                   VAR(Y)=VAR
C                   PSDYY(W)=VAR*PSDXX(W)=0.1*VAR
C                   10LOG(PSDYY(W))=-10 + 10LOG(VAR)  (DB)
C             4) THE POWER SPECTRAL DENSITY OF THE FORCING FUNCTION INPUT
C             AT W=0 RAD/SEC IS
C                   PSDII(0)=10LOG(4.*SIG*SIG/WB)
C             5) THE POWER SPECTRAL DENSITY LEVELS OF THE WHITE MOTOR AND
C             OBSERVATION NOISE PROCESSES ARE SET AS DESIRED BY CHOOSING
C             THE VARIANCES AS FOLLOWS..
C                   PSDN(W)=NVAR*0.1   WHERE PSDN(W) IS THE DESIRED
C             POWER SPECTRAL DENSITY LEVEL OF THE NOISE PROCESS AND NVAR
C             IS THE REQUIRED VARIANCE OF THE NOISE BEING CONSIDERED
C             6) AA IS POSITIVE FOR UNSTABLE PLANT AND NEGATIVE FOR
C             STABLE PLANT
C
      DIMENSION A(3,3),V(3,3),R(3,3),Q(3,3),D(3,3),ATP(3,3),P(3,3),B(3),
     1AHAT(3,3),BDEL(3,3),BTP(3,3),X1(3),ONE(3,3),CAY(3,3)
      DIMENSION DEL(5001,3)
      DIMENSION AX(3),ZETA(3),GNU(3),X2(3),X2A(3),X1A(3),BU(3),Y(3)
101   FORMAT(6F10.4)
102   FORMAT(1HB,5X,2HT=,F5.2,5X,3HWB=,F5.2,5X,4HSIG=,F10.4,5X,2HB=,F5.2
```

```
     1,5X,2HS=,F10.6,5X,2HA=,F6.2)
103   FORMAT(1HB,5X,4HQSQ=,F10.6,5X,5HVAR1=,F10.6,5X,5HVAR2=,F10.6,5X,5H
     1VAR3=,F10.6,5X,2HN=,I6)
109   FORMAT(4F10.6,I10)
110   FORMAT(1HB,5X,26HNORMALIZED TRACKING ERROR=,E10.3)
150   READ(5,101)T,WB,SIG,BB,AA,S
      READ(5,109)QSQ,VAR1,VAR2,VAR3,N
      WRITE(6,102)T,WB,SIG,BB,S,AA
      WRITE(6,103)QSQ,VAR1,VAR2,VAR3,N
      JJ=3
      DO 41 I=1,JJ
      DO 41 J=1,JJ
      V(I,J)=0.0
      R(I,J)=0.0
      Q(I,J)=0.0
      ONE(I,J)=0.0
41    A(I,J)=0.0
C**COMPUTE A MATRIX AND B VECTOR
      IF(AA)201,200,201
201   A(3,3)=EXP(AA*T)
      GAM=(A(3,3)-1.0)/AA
      GO TO 202
200   A(3,3)=1.0
      GAM=T
202   A(1,1)=EXP(-WB*T)
      C2=SQRT(2.0*WB*SIG)
      C2=C2*SQRT(SQRT(10.0*WB))
      C3=(1.0-A(1,1))/WB
      C3=C2*C3
      C4=C2*T*A(1,1)
      A(2,1)=C4
      A(2,2)=A(1,1)
      B(1)=0.0
      B(2)=0.0
      B(3)=GAM*BB
C**COMPUTE V MATRIX
      V(2,2)=1.0
      V(2,3)=-1.0
      V(3,2)=-1.0
      V(3,3)=1.0
C**COMPUTE Q MATRIX
      C5=A(1,1)*(1.0+WB*T)
      C5=(1.0-C5)/(WB*WB)
      C5=C2*C2*C5
      Q(1,1)=C3*C3
      Q(2,2)=C5*C5
      Q(2,1)=C3*C5
      Q(1,2)=Q(2,1)
      Q(3,3)=B(3)*B(3)*QSQ
C**COMPUTE R MATRIX
      R(1,1)=VAR1
      R(2,2)=VAR2
      R(3,3)=VAR3
C**COMPUTE IDENTITY MATRIX
      DO 405 I=1,JJ
405   ONE(I,I)=1.0
      REWIND 9
C**SET P(N)=V
      DO 1 J=1,JJ
      DO 1 K=1,JJ
1     P(J,K)=V(J,K)
```

```
      MM=N+1
      M=N+2
      CALL MXTRN(A,ATP,JJ,JJ)
      DO 29 K=1,MM
      K2=M-K
C     COMPUTE BTP
      CALL MXMUL(B,P,BTP,1,JJ,JJ)
C     COMPUTE BTPB
      CALL MXMUL(BTP,B,BTBIV,1,JJ,1)
      BTBIV=1./(BTBIV+S)
C     COMPUTE BTPA
      CALL MXMUL(BTP,A,X1,1,JJ,JJ)
C**COMPUTE G(K)=DEL(K)
      DO 4 L=1,JJ
      DEL(K2,L)=BTBIV*X1(L)
4     Y(L)=DEL(K2,L)
C     COMPUTE BDEL(K)
      CALL MXMUL(B,Y,BDEL,JJ,1,JJ)
C     COMPUTE A-BDEL(K)
      CALL MXADD(A,BDEL,AHAT,JJ,JJ,-1)
C     COMPUTE ATP
      CALL MXMUL(ATP,P,BDEL,JJ,JJ,JJ)
C**COMPUTE P(K+1)
      CALL MXMUL(BDEL,AHAT,BTP,JJ,JJ,JJ)
      CALL MXADD(V,BTP,P,JJ,JJ,1)
29    CONTINUE
C**SET P(0)=Q
      DO 16 I=1,JJ
      DO 16 J=1,JJ
16    P(I,J)=Q(I,J)
      DO 800 K=1,MM
C     COMPUTE P+R
      CALL MXADD(P,R,BDEL,JJ,JJ,1)
C     COMPUTE (P+R) INVERSE
      CALL MTXEQ(BDEL,BTP,ONE,JJ,JJ)
C**COMPUTE K(K+1)
      CALL MXMUL(P,BTP,CAY,JJ,JJ,JJ)
C     COMPUTE I-K
      CALL MXADD(ONE,CAY,BDEL,JJ,JJ,-1)
C     COMPUTE (I-K)P
      CALL MXMUL(BDEL,P,D,JJ,JJ,JJ)
C     COMPUTE A(I-K)P
      CALL MXMUL(A,D,BTP,JJ,JJ,JJ)
C     COMPUTE A(I-K)PAT
      CALL MXMUL(BTP,ATP,BDEL,JJ,JJ,JJ)
C**COMPUTE P(K+1)
      CALL MXADD(BDEL,Q,P,JJ,JJ,1)
      DO 950 I=1,JJ
950   Y(I)=DEL(K2,I)
      CALL MXMUL(B,Y,BDEL,JJ,1,JJ)
      CALL MXADD(A,BDEL,AHAT,JJ,JJ,-1)
      CALL MXADD(ONE,CAY,D,JJ,JJ,-1)
      CALL MXMUL(D,AHAT,BDEL,JJ,JJ,JJ)
      WRITE(9)((BDEL(I,J),J=1,JJ),I=1,JJ)
800   WRITE(9)((CAY(I,J),J=1,JJ),I=1,JJ)
      REWIND 9
      REWIND 10
C**GENERATE N SAMPLES OF I,X,E,U
      SIG1=SQRT(VAR1)
      SIG2=SQRT(VAR2)
      SIG3=SQRT(VAR3)
```

```
      RQ=SQRT(QSQ)
C     SET X(0)  X*(0)  U(0)  ZETA(0)
      DO 43 I=1,JJ
      X1A(I)=0.0
43    X1(I)=0.0
      U=0.0
      NN=1
      NM=2
C     COMPUTE AX
80    CALL MXMUL(A,X1A,AX,JJ,JJ,1)
C     COMPUTE BU
      DO 46 I=1,JJ
46    BU(I)=U*B(I)
C     COMPUTE PLANT NOISE VECTOR
      WW=RANDNM(W)
      ZETA(1)=C3*WW
      ZETA(2)=C5*WW
      WW=RANDNM(W)
      ZETA(3)=B(3)*RQ*WW
C     COMPUTE X2A
      DO 47 I=1,JJ
47    X2A(I)=AX(I)+BU(I)+ZETA(I)
C     COMPUTE Y
      WW=RANDNM(W)
      GNU(1)=SIG1*WW
      WW=RANDNM(W)
      GNU(2)=SIG2*WW
      WW=RANDNM(W)
      GNU(3)=SIG3*WW
      CALL MXADD(X2A,GNU,Y,JJ,1,1)
C     COMPUTE E(X/Y)
      READ(9)((ATP(I,J),J=1,JJ),I=1,JJ)
      READ(9)((BTP(I,J),J=1,JJ),I=1,JJ)
      CALL MXMUL(ATP,X1,BU,JJ,JJ,1)
      CALL MXMUL(BTP,Y,X1,JJ,JJ,1)
      CALL MXADD(BU,X1,X2,JJ,1,1)
C     COMPUTE U
      SUM=0.0
      DO 58 I=1,JJ
58    SUM=SUM+DEL(NM,I)*X2(I)
      U=-SUM
      E=X2A(2)-X2A(3)
      WRITE(10)X2A(2),X2A(3),E,U
C     RESET
65    DO 66 I=1,JJ
      X1(I)=X2(I)
66    X1A(I)=X2A(I)
      NN=NN+1
      NM=NN+1
      IF(NN-MM)80,80,81
81    REWIND 10
C**COMPUTE NORMALIZED TRACKING ERROR
      SUM1=0.0
      SUM2=0.0
      SUMSQ1=0.0
      SUMSQ2=0.0
      DO 710 K=1,MM
710   READ(10)DEL(K,1),C2,DEL(K,2),DE
      DO 711 K=1,MM
      SUM1=SUM1+DEL(K,1)
      SUM2=SUM2+DEL(K,2)
```

```
      SUMSQ1=SUMSQ1+DEL(K,1)*DEL(K,1)
711   SUMSQ2=SUMSQ2+DEL(K,2)*DEL(K,2)
      EM=MM
      XMEAN=SUM1/EM
      EMEAN=SUM2/EM
      XVAR=(SUMSQ1/EM)-XMEAN*XMEAN
      EVAR=(SUMSQ2/EM)-EMEAN*EMEAN
      EM=EVAR/XVAR
      WRITE(6,110)EM
      GO TO 150
      END
```

```
$IBFTC MAIN    DECK
C****DISCRETE STOCHASTIC OPTIMAL CONTROL MODEL
C
C          CASE II  SECOND ORDER PLANT  YC=B/S*S
C
C          PURPOSE
C             TO GENERATE A SERIES OF DATA POINTS FOR EACH OF THE
C             FOLLOWING PURSUIT TRACKING LOOP SIGNALS
C                   I(K)  FORCING FUNCTION INPUT
C                   X(K)  PLANT OUTPUT
C                   E(K)=I(K)-X(K)  SYSTEM ERROR
C                   U(K)  CONTROL
C
C          DESCRIPTION OF PARAMETERS
C             T----SAMPLING PERIOD (SEC)
C             WB---TIME CONSTANT OF INPUT NOISE FILTER (RAD/SEC)
C             SIG--STANDARD DEVIATION OF FORCING FUNCTION INPUT
C             BB---PLANT GAIN
C             AA---PLANT TIME CONSTANT
C             S----CONTROL WEIGHTING
C             N----NUMBER OF SAMPLES TO BE GENERATED
C             QSQ--MOTOR NOISE VARIANCE
C             VAR1-INTERMEDIATE NOISE OBSERVATION NOISE VARIANCE
C             VAR2-FORCING FUNCTION INPUT OBSERVATION NOISE VARIANCE
C             VAR3-PLANT OUTPUT OBSERVATION NOISE VARIANCE
C             VAR4-PLANT VELOCITY OBSERVATION NOISE VARIANCE
C
C          REMARKS
C             1) N IS LIMITED TO 5000 OR LESS BY THE DIMENSION STATEMENT
C             2) THE CHARACTERISTICS OF THE PSEUDO WHITE NOISE GENERATOR,
C             RANDNM, ARE AS FOLLOWS..GIVEN A LARGE SAMPLE OF POINTS
C             X(K) GENERATED BY X(K)=RANDNM(W) THEN
C                    MEAN(X)=0.0
C                    VAR(X)=1.0
C                    PSDXX(W)=0.1 WHERE PSDXX(W) IS THE POWER SPECTRAL
C             DENSITY OF X AS A FUNCTION OF FREQUENCY
C                    10LOG(PSDXX(W))=-10  (DB)
C             3) IF A NEW SET OF SAMPLE POINTS IS GENERATED BY
C                    Y(K)=VAR*X(K)=VAR*RANDNM(W)
C             THEN THE STATISTICS OF Y ARE
C                    MEAN(Y)=0.0
C                    VAR(Y)=VAR
C                    PSDYY(W)=VAR*PSDXX(W)=0.1*VAR
C                    10LOG(PSDYY(W))=-10 + 10LOG(VAR)  (DB)
C             4) THE POWER SPECTRAL DENSITY OF THE FORCING FUNCTION INPUT
C             AT W=0 RAD/SEC IS
C                    PSDII(0)=10LOG(4.*SIG*SIG/WB)
C             5) THE POWER SPECTRAL DENSITY LEVELS OF THE WHITE MOTOR AND
C             OBSERVATION NOISE PROCESSES ARE SET AS DESIRED BY CHOOSING
C             THE VARIANCES AS FOLLOWS..
C                    PSDN(W)=NVAR*0.1   WHERE PSDN(W) IS THE DESIRED
C             POWER SPECTRAL DENSITY LEVEL OF THE NOISE PROCESS AND NVAR
C             IS THE REQUIRED VARIANCE OF THE NOISE BEING CONSIDERED
C
      DIMENSION A(4,4),V(4,4),R(4,4),Q(4,4),D(4,4),ATP(4,4),P(4,4),B(4),
     1AHAT(4,4),BDEL(4,4),BTP(4,4),X1(4),ONE(4,4),AX(4),ZETA(4),GNU(4),X
     12(4),X2A(4),X1A(4),BU(4),Y(4),CAY(4,4)
      DIMENSION DEL(4001,4)
101   FORMAT(1HB,5X,2HT=,F10.4,5X,3HWB=,F10.4,5X,4HSIG=,F10.4,5X,2HB=,F1
     10.4,5X,2HS=,E10.3,5X,2HN=,I6)
102   FORMAT(1HB,5X,4HQSQ=,F10.6,5X,5HVAR1=,F10.6,5X,5HVAR2=,F10.6,5X,5H
```

```
     1VAR3=,F10.6,5X,5HVAR4=,F10.6)
107   FORMAT(5F10.6)
109   FORMAT(5F10.6,I10)
110   FORMAT(1HB,5X,26HNORMALIZED TRACKING ERROR=,E10.3)
150   READ(5,107)T,WB,SIG,BB,S
      READ(5,109)QSQ,VAR1,VAR2,VAR3,VAR4,N
      WRITE(6,101)T,WB,SIG,BB,S,N
      WRITE(6,102)QSQ,VAR1,VAR2,VAR3,VAR4
      JJ=4
      DO 41 I=1,JJ
      DO 41 J=1,JJ
      V(I,J)=0.0
      R(I,J)=0.0
      Q(I,J)=0.0
      ONE(I,J)=0.0
41    A(I,J)=0.0
C**COMPUTE A MATRIX AND B VECTOR
      A(1,1)=EXP(-WB*T)
      C2=SQRT(2.*SIG*WB)
      C2=C2*SQRT(SQRT(10.*WB))
      C3=(1.0-A(1,1))/WB
      C3=C2*C3
      C4=C2*T*A(1,1)
      A(2,1)=C4
      A(2,2)=A(1,1)
      A(3,3)=1.0
      A(4,4)=1.0
      A(3,4)=T
      B(1)=0.0
      B(2)=0.0
      B(3)=0.5*BB*T*T
      B(4)=BB*T
C**COMPUTE V MATRIX
      V(2,2)=1.0
      V(2,3)=-1.0
      V(3,2)=-1.0
      V(3,3)=1.0
C**COMPUTE Q MATRIX
      C5=A(1,1)*(1.0+WB*T)
      C5=(1.0-C5)/(WB*WB)
      C5=C2*C2*C5
      Q(1,1)=C3*C3
      Q(2,2)=C5*C5
      Q(2,1)=C3*C5
      Q(1,2)=Q(2,1)
      Q(3,3)=B(3)*B(3)*QSQ
      Q(4,4)=B(4)*B(4)*QSQ
      Q(3,4)=B(3)*B(4)*QSQ
      Q(4,3)=Q(3,4)
C**COMPUTE R MATRIX
      R(1,1)=VAR1
      R(2,2)=VAR2
      R(3,3)=VAR3
      R(4,4)=VAR4
C**COMPUTE IDENTITY MATRIX
      DO 405 I=1,JJ
405   ONE(I,I)=1.0
      REWIND 9
C**SET P(N)=V
      DO 1 J=1,JJ
      DO 1 K=1,JJ
```

```
1       P(J,K)=V(J,K)
        MM=N+1
        M=N+2
        CALL MXTRN(A,ATP,JJ,JJ)
        DO 29 K=1,MM
        K2=M-K
C       COMPUTE BTP
        CALL MXMUL(B,P,BTP,1,JJ,JJ)
C       COMPUTE BTPB
        CALL MXMUL(BTP,B,BTBIV,1,JJ,1)
        BTBIV=1./(BTBIV+S)
C       COMPUTE BTPA
        CALL MXMUL(BTP,A,X1,1,JJ,JJ)
C**COMPUTE G(K)=DEL(K)
        DO 4 L=1,JJ
        DEL(K2,L)=BTBIV*X1(L)
4       Y(L)=DEL(K2,L)
C       COMPUTE BDEL(K)
        CALL MXMUL(B,Y,BDEL,JJ,1,JJ)
C       COMPUTE A-BDEL(K)
        CALL MXADD(A,BDEL,AHAT,JJ,JJ,-1)
C       COMPUTE ATP
        CALL MXMUL(ATP,P,BDEL,JJ,JJ,JJ)
C**COMPUTE P(K+1)
        CALL MXMUL(BDEL,AHAT,BTP,JJ,JJ,JJ)
        CALL MXADD(V,BTP,P,JJ,JJ,1)
29      CONTINUE
C**SET P(0)=Q
        DO 16 I=1,JJ
        DO 16 J=1,JJ
16      P(I,J)=Q(I,J)
        DO 800 K=1,MM
C       COMPUTE P+R
        CALL MXADD(P,R,BDEL,JJ,JJ,1)
C       COMPUTE (P+R) INVERSE
        CALL MTXEQ(BDEL,BTP,ONE,JJ,JJ)
C**COMPUTE K(K+1)
        CALL MXMUL(P,BTP,CAY,JJ,JJ,JJ)
C       COMPUTE I-K
        CALL MXADD(ONE,CAY,BDEL,JJ,JJ,-1)
C       COMPUTE (I-K)P
        CALL MXMUL(BDEL,P,D,JJ,JJ,JJ)
C       COMPUTE A(I-K)P
        CALL MXMUL(A,D,BTP,JJ,JJ,JJ)
C       COMPUTE A(I-K)PAT
        CALL MXMUL(BTP,ATP,BDEL,JJ,JJ,JJ)
C**COMPUTE P(K+1)
        CALL MXADD(BDEL,Q,P,JJ,JJ,1)
        DO 950 I=1,JJ
950     Y(I)=DEL(K2,I)
        CALL MXMUL(B,Y,BDEL,JJ,1,JJ)
        CALL MXADD(A,BDEL,AHAT,JJ,JJ,-1)
        CALL MXADD(ONE,CAY,D,JJ,JJ,-1)
        CALL MXMUL(D,AHAT,BDEL,JJ,JJ,JJ)
        WRITE(9)((BDEL(I,J),J=1,JJ),I=1,JJ)
800     WRITE(9)((CAY(I,J),J=1,JJ),I=1,JJ)
        REWIND 9
        REWIND 10
C**GENERATE N SAMPLES OF I,X,E,U
        SIG1=SQRT(VAR1)
        SIG2=SQRT(VAR2)
```

```
      SIG3=SQRT(VAR3)
      SIG4=SQRT(VAR4)
      RQ=SQRT(QSQ)
C     SET X(0)  X*(0)  U(0)  ZETA(0)
      DO 43 I=1,JJ
      X1A(I)=0.0
43    X1(I)=0.0
      U=0.0
      NN=1
      NM=2
C     COMPUTE AX
80    CALL MXMUL(A,X1A,AX,JJ,JJ,1)
C     COMPUTE BU
      DO 46 I=1,JJ
46    BU(I)=U*B(I)
C     COMPUTE PLANT NOISE VECTOR
      WW=RANDNM(W)
      ZETA(1)=C3*WW
      ZETA(2)=C5*WW
      WW=RANDNM(W)
      ZETA(3)=B(3)*RQ*WW
      ZETA(4)=B(4)*RQ*WW
C     COMPUTE X2A
      DO 47 I=1,JJ
47    X2A(I)=AX(I)+BU(I)+ZETA(I)
C     COMPUTE Y
      WW=RANDNM(W)
      GNU(1)=SIG1*WW
      WW=RANDNM(W)
      GNU(2)=SIG2*WW
      WW=RANDNM(W)
      GNU(3)=SIG3*WW
      WW=RANDNM(W)
      GNU(4)=SIG4*WW
      CALL MXADD(X2A,GNU,Y,JJ,1,1)
C     COMPUTE E(X/Y)
      READ(9)((ATP(I,J),J=1,JJ),I=1,JJ)
      READ(9)((BTP(I,J),J=1,JJ),I=1,JJ)
      CALL MXMUL(ATP,X1,BU,JJ,JJ,1)
      CALL MXMUL(BTP,Y,X1,JJ,JJ,1)
      CALL MXADD(BU,X1,X2,JJ,1,1)
C     COMPUTE U
      SUM=0.0
      DO 58 I=1,JJ
58    SUM=SUM+DEL(NM,I)*X2(I)
      U=-SUM
      E=X2A(2)-X2A(3)
      WRITE(10)X2A(2),X2A(3),E,U
C     RESET
65    DO 66 I=1,JJ
      X1(I)=X2(I)
66    X1A(I)=X2A(I)
      NN=NN+1
      NM=NN+1
      IF(NN-MM)80,80,81
81    REWIND 10
C**COMPUTE NORMALIZED TRACKING ERROR
      SUM1=0.0
      SUM2=0.0
      SUMSQ1=0.0
      SUMSQ2=0.0
```

```
      DO 910 K=1,MM
910   READ(10)DEL(K,1),C2,DEL(K,2),DE
      DO 711 K=1,MM
      SUM1=SUM1+DEL(K,1)
      SUM2=SUM2+DEL(K,2)
      SUMSQ1=SUMSQ1+DEL(K,1)*DEL(K,1)
711   SUMSQ2=SUMSQ2+DEL(K,2)*DEL(K,2)
      EM=MM
      XMEAN=SUM1/EM
      EMEAN=SUM2/EM
      XVAR=(SUMSQ1/EM)-XMEAN*XMEAN
      EVAR=(SUMSQ2/EM)-EMEAN*EMEAN
      EM=EVAR/XVAR
      WRITE(6,110)EM
      GO TO 150
      END
```

APPENDIX III

THE POWER SPECTRAL DENSITY DATA REDUCTION

The power spectral density data reduction program used is based on the presentation in Section VII (Digital Computer Techniques) of Reference 4. The section discusses the digitizing of continuous data and the computation of autocorrelation functions and power spectral densities. The section includes all the formulas required for these calculations and the data reduction program. There is one modification to the Bendat procedure that was implemented in the formulation of the data reduction program used, and this modification will now be discussed in detail.

Bendat (Reference 4:292) recommends that the power spectral densities be calculated only at the M+1 discrete frequencies

$$f = k f_c/M \qquad k = 0, 1, 2, \ldots, M$$

where

$$f_c = \frac{1}{2T} \text{ cycles/sec}$$

$$T = \text{sampling period}$$

This spacing provides M/2 independent spectral density estimates. Spectral estimates at points less than $2f_c/M$ apart are correlated.

Since low frequencies (0-30 rad/sec) are of primary interest in human response work, it is desirable to have the ratio f_c/M as small as possible. As noted by Bendat though, M should be chosen much less than N, the total number of samples, for small uncertainty in estimates of power spectral density. Thus a compromise choice of M is necessary and Bendat recommends that, as a rule of thumb, choose M less than one-tenth the sample size N. This was the rule used in the selection of M for the data reduction, however, a modification was incorporated in the data reduction program.

The modification to Bendat's procedure is to compute the power spectral density estimates at discrete frequency intervals separated by 0.1 rad/sec until $f = f_c/M$ is reached. At this point, the estimates are computed at intervals of f_c/M until $f_{max} = f_c$ is reached. The justification for such a modification is that first, the interval of frequency from 0 to f_c/M is a small fraction of the total frequency interval of interest. For example, if T = 0.1 sec, then $\omega_c = 2\pi f_c = 2\pi/0.2 = 10\pi$ rad/sec, and, if M = 100 (as is used in the data reduction program), then $\omega_c/M = 2\pi f_c/M = 0.1\pi$. Secondly, the modification does not

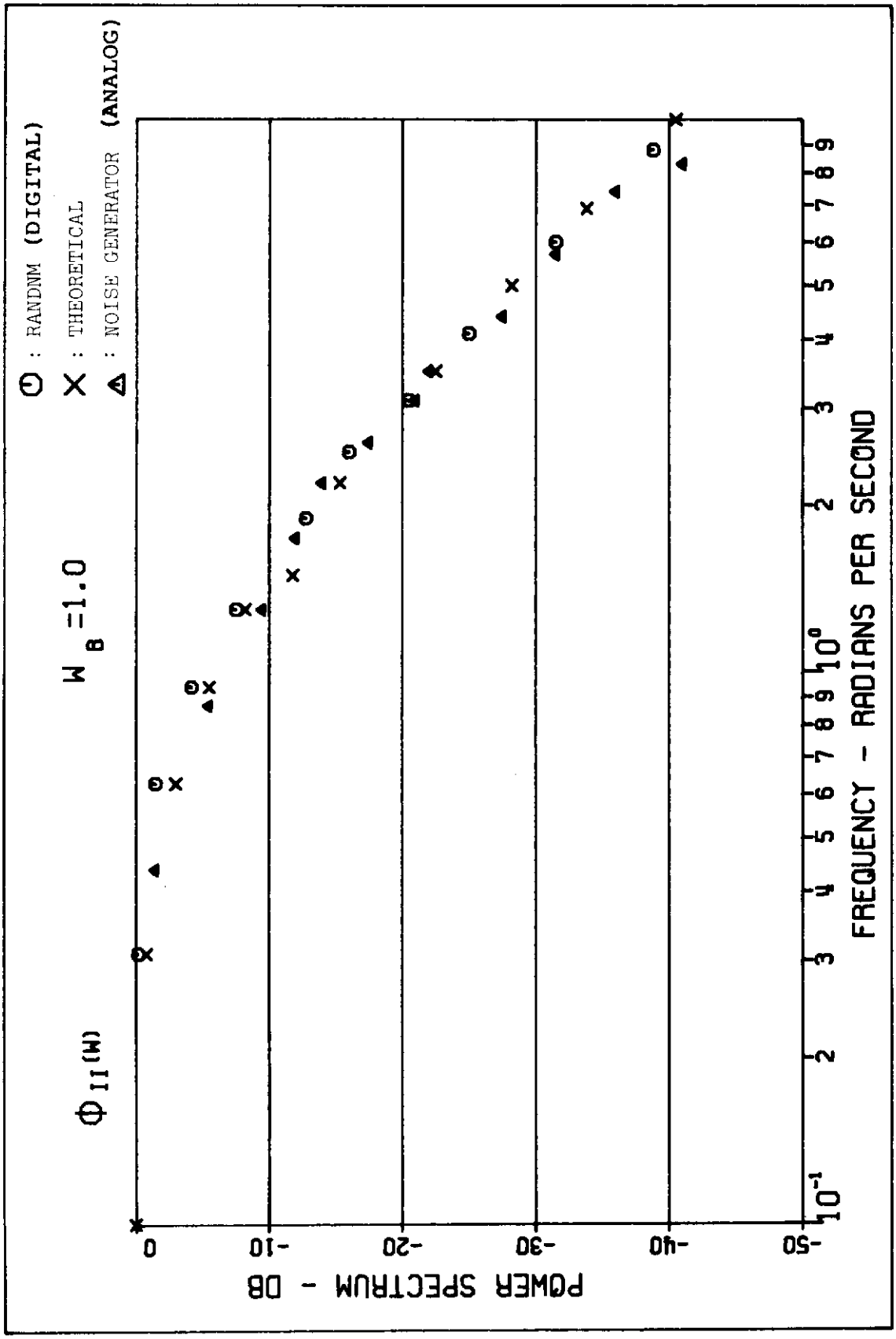

Figure 48. Comparison of Forcing Function Power Spectra

alter the recommended Bendat procedure, it just augments it at the low end of the frequency scale. Thirdly, and finally, when the modification is applied to the computation of known power spectral density shapes, the results fit the known shapes correctly. Specifically, when the power spectral density of the forcing function input is computed with the modification to the data reduction program, the result can be directly compared with the theoretical spectral density

$$\phi_{ii}(\omega) = \frac{k^4}{\omega^4 + 2\omega_B^2\omega^2 + \omega_B^4} \qquad \text{(C-1)}$$

A comparison is shown in Figure 48 for frequencies greater than ω_c/M. Power spectra were obtained for both the simulated noise generated in the digital model simulation and from the experimental forcing function obtained from the noise generator and the analog computer. These spectra are plotted along with the theoretical spectrum obtained from Equation C-1. For frequencies less than ω_c/M, refer to the comparison in Table V.

TABLE V

POWER SPECTRAL DENSITY (DB)

ω(rad/sec)	Theoretical	Digital Simulation	Analog Simulation
0.1	-0.088	0	0
0.2	-0.34	-0.13	-0.2
0.3	-0.75	-0.35	-0.7
0.4	-1.29		-1.2

This modification should not be construed to be universal and should be used only when a priori knowledge of the power spectral shapes confirm the validity of the modified calculations.

BIBLIOGRAPHY

1. Allen, R. W., and H. R. Jex. An Experimental Investigation of Compensatory and Pursuit Tracking Displays with Rate and Acceleration Control Dynamics and a Disturbance Input. NASA Contractor Report 1082. Washington: National Aeronautics and Space Administration. June 1968.

2. Aoki, M. Optimization of Stochastic Systems. New York: Academic Press. 1967.

3. Bekey, G. A. An Investigation of Sampled-Data Models of the Human Operator in a Control System. ASD-TR-62-36. Wright-Patterson AFB, Ohio: Aeronautical Systems Division. May 1962.

4. Bendat, J. S., and A. G. Piersol. Measurement and Analysis of Random Data. New York: John Wiley & Sons. 1966.

5. Bowser, D. K., and G. R. Schubert. Digital Simulation of a Gaussian Random Process Having an Exponential Autocorrelation Function. AFFDL-TR-67-52. Wright-Patterson AFB, Ohio: Air Force Flight Dynamics Laboratory. May 1967.

6. Burchfield, J. D., Elkind, J. I., and D. C. Miller. On the Optimal Behavior of the Human Controller: A Pilot Study Comparing the Human Controller with Optimal Control Models. Rpt 1532. Cambridge, Mass: Bolt-Beranek and Newman Inc. August 1967.

7. Chernikoff, R., et al. "A Comparison of Pursuit and Compensatory Tracking Under Conditions of Aiding and no Aiding." Journal of Experimental Psychology, 49:55-59 (1955).

8. Costello, R. G. "The Surge Model of a Well Trained Human Operator in Simple Manual Control." IEEE Transactions on Man-Machine Systems, MMS-9:2-9 (March 1968.

9. Costello, R. G. and T. J. Higgins. "An Inclusive Classified Bibliography Pertaining to Modeling the Human Operator as an Element in an Automatic Control System." IEEE Transactions on Human Factors in Electronics, HFE-7:174-181 (December 1966).

10. DeRusso, P. M., et al. State Variables for Engineers. New York: John Wiley & Sons. 1966.

11. Elkind, J. I. Characteristics of Simple Manual Control Systems. Rpt 111. Cambridge, Mass: Massachusetts Institute of Technology Lincoln Laboratory. April 1956.

12. Fogel, L. J., and R. A. Moore. Modeling the Human Operator with Finite State Machines. NASA Contractor Report 1112. Washington: National Aeronautics and Space Administration. July 1968.

13. Jex, H. R., et al. A Critical Tracking Task for Man-Machine Research Related to the Operator's Effective Delay Time. NASA Contractor Report 674. Washington: National Aeronautics and Space Administration. January 1967.

14. Kalman, R. E. "A New Approach to Linear Filtering and Prediction Problems." ASME Journal of Basic Engineering, 86:35-45 (March 1960).

BIBLIOGRAPHY (CONTD)

15. Kalman, R. E. "When is a Linear Control System Optimal?" Transactions ASME, Series D, Journal of Basic Engineering, 88:51-60 (March 1964).

16. Kleinman, D. L., et al. "An Optimal Control Model of Human Response, Part I: Theory and Validation." Automatica (May 1970).

17. Kreifeldt, J. G. "A Sampled-Data Pursuit Tracking Model." IEEE Transactions on Human Factors in Electronics, HFE-6:65-73 (September 1965).

18. Levison, W. H., et al. "A Model for Human Controller Remnant." IEEE Transactions on Man-Machine Systems, MMS-10:101-108 (December 1969).

19. McRuer, D. T., et al. Human Pilot Dynamics in Compensatory Systems. AFFDL-TR-65-15. Wright-Patterson AFB, Ohio: Air Force Flight Dynamics Laboratory. July 1965.

20. McRuer, D. T., and H. R. Jex. "A Review of Quasi-Linear Pilot Models." IEEE Transactions on Human Factors in Electronics, HFE-8:231-249 (September 1967).

21. McRuer, D. T., et al. New Approaches to Human Pilot/Vehicle Dynamic Analysis. AFFDL-TR-67-150. Wright-Patterson AFB, Ohio: Air Force Flight Dynamics Laboratory. February 1968.

22. McRuer, D. T., and E. S. Krendel. Dynamic Response of Human Operators. WADC-TR-56-524. Wright-Patterson AFB, Ohio: Wright Air Development Center. October 1957.

23. Marsaglia, G., et al. "A Fast Procedure for Generating Normal Random Variables." Communications of the ACM, 7:4-10 (January 1964).

24. Meditch, J. S. Stochastic Optimal Linear Estimation and Control. New York: McGraw-Hill Book Co. Inc. 1969.

25. Meier, L. Combined Optimum Control and Estimation Theory. NASA Contractor Report 426. Washington: National Aeronautics and Space Administration. April 1966.

26. Meier, L., et al. "Optimal Control of Measurement Subsystems." Preprints of Joint Automatic Control Conference: 527-537 (June 1967).

27. Papoulis, A. Probability, Random Variables, and Stochastic Processes. New York: McGraw-Hill Book Co. Inc. 1965.

28. Ragazzini, J. R., and G. F. Franklin. Sampled-Data Control Systems. New York: McGraw-Hill Book Co. Inc. 1958.

29. Reid, L. D. The Measurement of Human Pilot Dynamics in a Pursuit-Plus-Disturbance Tracking Task. UTIAS Rpt 138. Toronto: University of Toronto Institute for Aerospace Studies. April 1969.

30. Roig, R. W. "A Comparison Between Human Operator and Optimum Linear Controller RMS Error Performance." IRE Transactions on Human Factors in Electronics, 3:18-22 (March 1962).

BIBLIOGRAPHY (CONTD)

31. Schwartz, R. J., and B. Friedland. Linear Systems. New York: McGraw-Hill Book Co. Inc. 1965.

32. Smith, G. M. An Investigation into Some Aspects of the Human Operator Describing Function While Controlling a Single Degree of Freedom. Ph.D. Thesis. University of Toronto Institute of Aerospace Studies.

33. Wasicko, R. J., et al. Human Pilot Dynamic Response in Single-Loop Systems with Compensatory and Pursuit Displays. AFFDL-TR-66-137. Wright-Patterson AFB, Ohio: Air Force Flight Dynamics Laboratory. December 1966.

34. Zadeh, L. A., and C. A. Desoer. Linear System Theory. New York: McGraw-Hill Book Co. Inc. 1963.

UNCLASSIFIED

Security Classification

DOCUMENT CONTROL DATA - R & D

(Security classification of title, body of abstract and indexing annotation must be entered when the overall report is classified)

1. ORIGINATING ACTIVITY (Corporate author) Air Force Flight Dynamics Laboratory Wright-Patterson Air Force Base, Ohio 45433	2a. REPORT SECURITY CLASSIFICATION UNCLASSIFIED 2b. GROUP N/A

3. REPORT TITLE

A DISCRETE, STOCHASTIC, OPTIMAL CONTROL MODEL OF THE HUMAN OPERATOR IN A CLOSED-LOOP TRACKING TASK

4. DESCRIPTIVE NOTES (Type of report and inclusive dates)

Final Report Oct 1968 - Mar 1970

5. AUTHOR(S) (First name, middle initial, last name)

Harvey M. Paskin, Major, USAF

6. REPORT DATE	7a. TOTAL NO. OF PAGES	7b. NO. OF REFS
November 1970	121	34

8a. CONTRACT OR GRANT NO.	9a. ORIGINATOR'S REPORT NUMBER(S)
b. PROJECT NO. 8219	AFFDL-TR-70-129
c. Task No. 821910	9b. OTHER REPORT NO(S) (Any other numbers that may be assigned this report)
d. Work Unit 006	

10. DISTRIBUTION STATEMENT

This document has been approved for public release and sale; its distribution is unlimited.

11. SUPPLEMENTARY NOTES	12. SPONSORING MILITARY ACTIVITY
	Air Force Flight Dynamics Laboratory Wright-Patterson AFB, Ohio 45433

13. ABSTRACT

A discrete stochastic optimal control model of the human operator is developed for the single-loop compensatory and pursuit tracking situations. The model generates signals corresponding to those in the physical closed-loop tracking situation. There is one primary model parameter which is varied to match model-experimental normalized tracking error at a bandwidth of ω_B = 1.0 rad/sec for an input which approximates a rectangular spectra. With this parameter fixed, the model then predicts normalized tracking error and power spectra of control loop signals across a range of input bandwidths of 0.5 to 2.0 rad/sec. The model is applied to simple first- and second-order controlled elements in both compensatory and pursuit display situations.

A comparison between model and experimental normalized tracking error and power spectral density data confirms the model capability of matching and predicting operator performance with sufficient correlation to warrant its application as a tool in manual vehicular control system design. Furthermore, the success of the model substantially confirms the hypothesis that the human operator behaves in some optimal manner when performing in a closed-loop tracking task.

DD FORM 1 NOV 65 1473

UNCLASSIFIED

Security Classification

14. KEY WORDS	LINK A		LINK B		LINK C	
	ROLE	WT	ROLE	WT	ROLE	WT
Compensatory Tracking						
Pursuit Tracking						
Discrete, Stochastic, Optimal Control						
Digital Simulation						